## LIST OF TABLES

Table 1. Marina Puerto Real deployments.

Table 2. May 23 - June 14, 2000 S4 flow statistics without rotation.

Table 3. May 23-28, 2000 RCM9 flow statistics without rotation.

## LIST OF FIGURES

Figure 1. Location map showing mooring locations and deployment dates in yymmdd format. From NOAA Chart 25667. Note that other objects in the chart may be offset from their true GPS position.

Figure 2. Time series of the observed tide (SBE26) and of the predicted tide at Playa de Fajardo. Elevation data calculated from raw pressure data. Tide predicted with *Tide and Currents* software from Nautical Software, Inc.

Figure 3. Observed tide, predicted tide, and meridional component time series.

Figure 4. Raw U (east-west) time series.

Figure 5. Raw V (north-south) time series.

Figure 6. Raw current speed time series.

Figure 7. Raw current direction time series.

Figure 8. Observed tide and V time series.

Figure 9. Progressive vector diagrams. Markers every twelve hours.

Figure 10. Current transport rose. The length of each vector represents the percentage of the total transport that lies in any given 15° bin Each radial divisions indicates 10% of the total transport.

Figure 11. Distributions of the mean and variance of the V current component vs. rotation angle of the coordinate axis (counterclockwise).

Figure 12. Blackman-Tuckey correlograms of the V time series.

Figure 13. Muti-Tapper-Method (MTM) spectrum of the RCM9 V time series. The principal harmonic components in the data as well as the 99% confidence interval are indicated.

Figure 14. Muti-Tapper-Method (MTM) spectrum of the S4 V time series. The principal harmonic components in the data as well as the 99% confidence interval are indicated.

Figure 15. Wave auto-spectral density contours showing the evolution of the wave field as function of time and frequency.

Figure 16. Time series of significant wave height (SWH) calculated from both, the wave auto-spectrum (WAS) and the reconstructed wave time series (WTS).

Figure 17. Time series of significant wave period (SWP) calculated from both, the wave auto-spectrum (WAS) and the reconstructed wave time series (WTS).

Figure 18. Wave burst auto-spectra for representative wave climatologies during March 2000. Labels indicate the date and time of the wave burst.

Figure 19. Raw water temperature time series.

Figure 20. Expanded view of the water temperature time series for May 22-25, 2001.

## LIST OF PLATES

Plates 1. Bottom mooring (center of image) with the RCM9 (upright) and SBE26 (horizontal) attached.

Plates 2. Eastward facing view of the deployment sites. Photo taken from the shoreline north of Punta Fajardo (Figure 1); the south end of Isleta Marina appears in the background. The RCM9 and the SBE26 were bottom mounted in the same mooring, as shown in Plate 1, and positioned at a depth of 1.5 m (5 ft), about 100 m to the west (closer to the camera) of the old relict vessel shown in the center of the image. The S4 mooring lies further to the east, between this vessel and Isleta Marina.

Table 2. May 23 - June 14, 2000 S4 flow statistics without rotation.

```
Plot_TS:  S4

010614.s4a

Data Start date:  1 5 23 12 0
  TS Start date:  1 5 23 12 0
    TS End date:  1 6 14 13 0

mag var correction =  12.0000000
axis rotation  =  0

tcn,tavg,tcycle,non:  1.00000000 120.000000 10.0000000 1

Number of S4 points =  3286
First and last S4 speed points =  8.60000038 16.2000008

Cycle-adjusted number of S4 points =  3286

Total # records, days, hours:  3286 22 20
Data end date:  1 6 15 7 30

istrt, iend:  1 3175
TS # of points =  3175

possible bad u points, threshold =  50.0000000 :


possible bad v points, threshold =  50.0000000 :


mean u                =  -2.00775170
mean v                =  15.3613091
mean scalar speed     =  21.1630878
mean vector speed     =  15.4919615
mean dir              =  353
mean temperature      =  29.3671227

u var & std dev =  45.5274773 6.74740505
v var & std dev =  388.935272 19.7214413
s var & std dev =  226.587402 15.0528202
t var & std dev =  6.42944127E-02 0.253563434


Wrote uvar.dat and vvar.dat
max uvar at j =  108
max vvar at j =  18
max umean at j =  97
max vmean at j =  7

Time Series

*******************************************************
```

Table 3. May 23-28, 2000 RCM9 flow statistics without rotation.

```
Plot_TS:  RC

010614.prn

Data Start date:  1 5 23 0 12
  TS Start date:  1 5 23 0 12
    TS End date:  1 5 28 5 32

mag var correction =  12.0000000
axis rotation  =  0

Total # records, days, hours:  377 5 6
Data end date:  1 5 28 5 32

istrt, iend:  1 377
TS # of points =  377

possible bad u points, threshold =  50.0000000 :


possible bad v points, threshold =  50.0000000 :


mean u              =  -1.09984481
mean v              =  2.79009175
mean scalar speed   =  6.80053043
mean vector speed   =  2.99904490
mean dir            =  338
mean temperature    =  29.2764816

u var & std dev =  23.2148991 4.81818438
v var & std dev =  22.3304596 4.72551155
s var & std dev =  8.29241276 2.87965488
t var & std dev =  0.299503386 0.547269046

Time Series
```

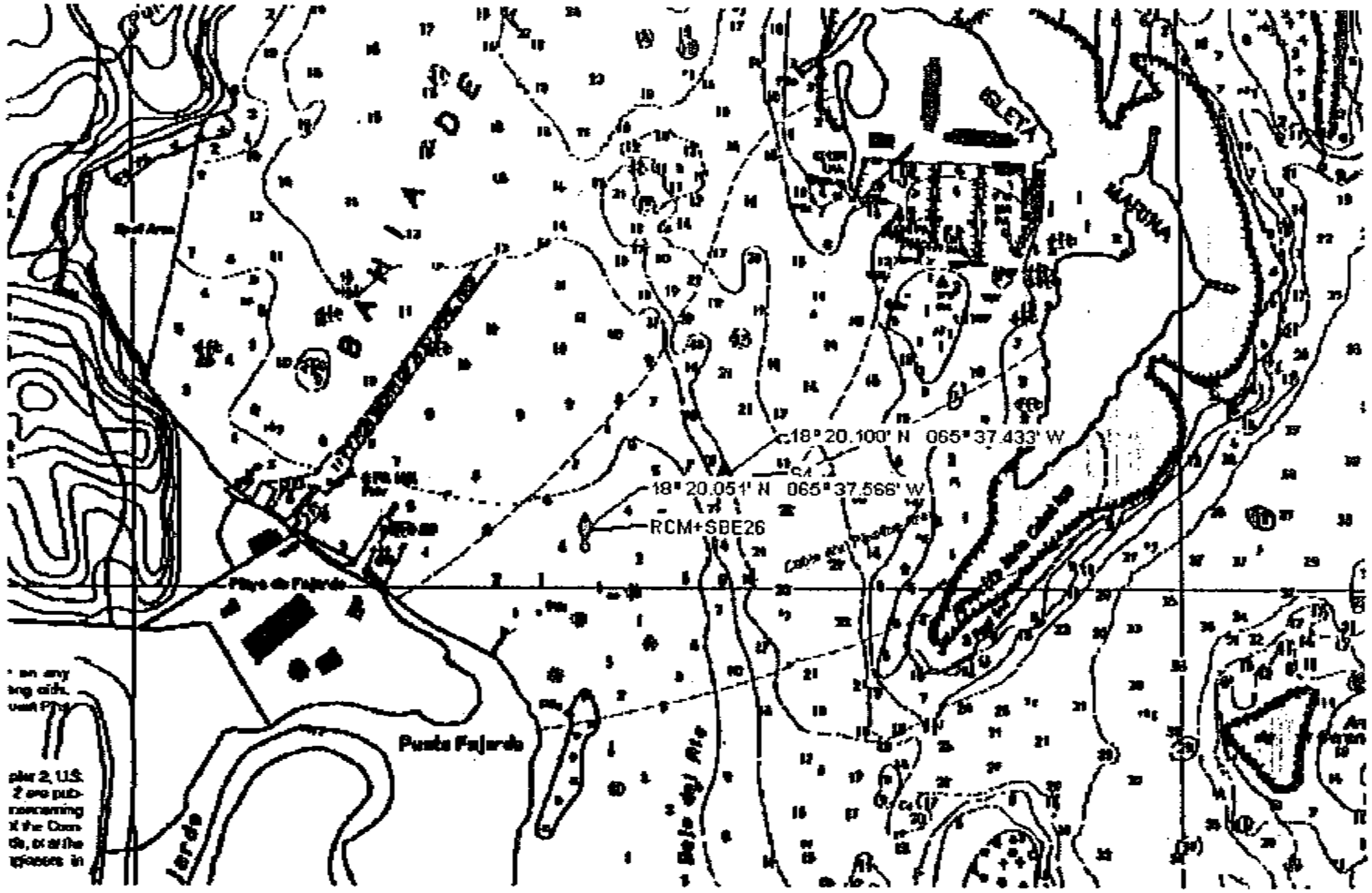
18° 20.100' N 065° 37.433' W
18° 20.051' N 065° 37.566' W
RCM+SBE26
ISLETA
MARINA
Playa de Fajardo
Punta Fajardo

Figure 1.

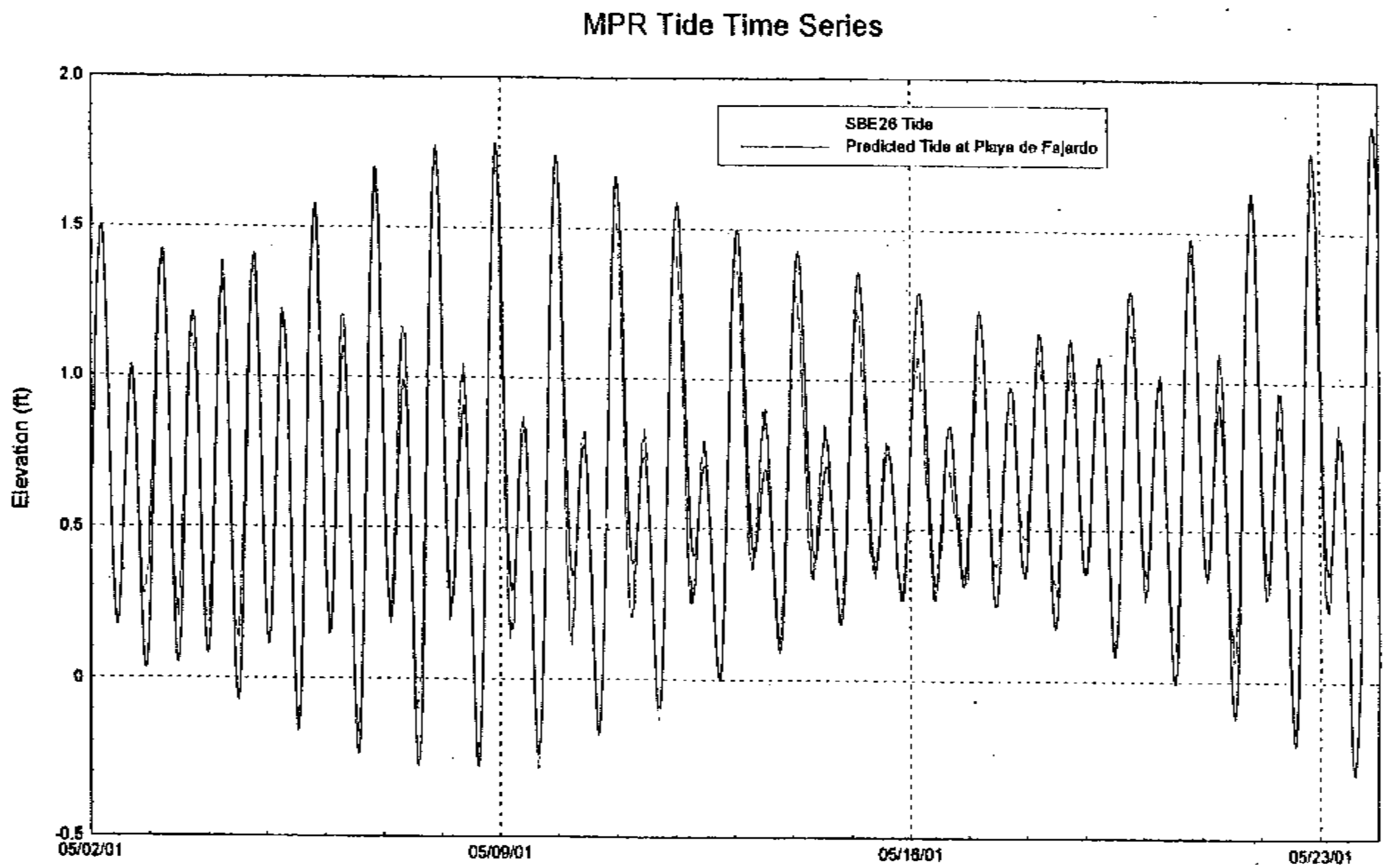
MPR Tide Time Series
SBE26 Tide
Predicted Tide at Playa de Fajardo
Elevation (ft)
2.0
1.5
1.0
0.5
0
-0.5
05/02/01
05/09/01
05/16/01
05/23/01

Figure 2.

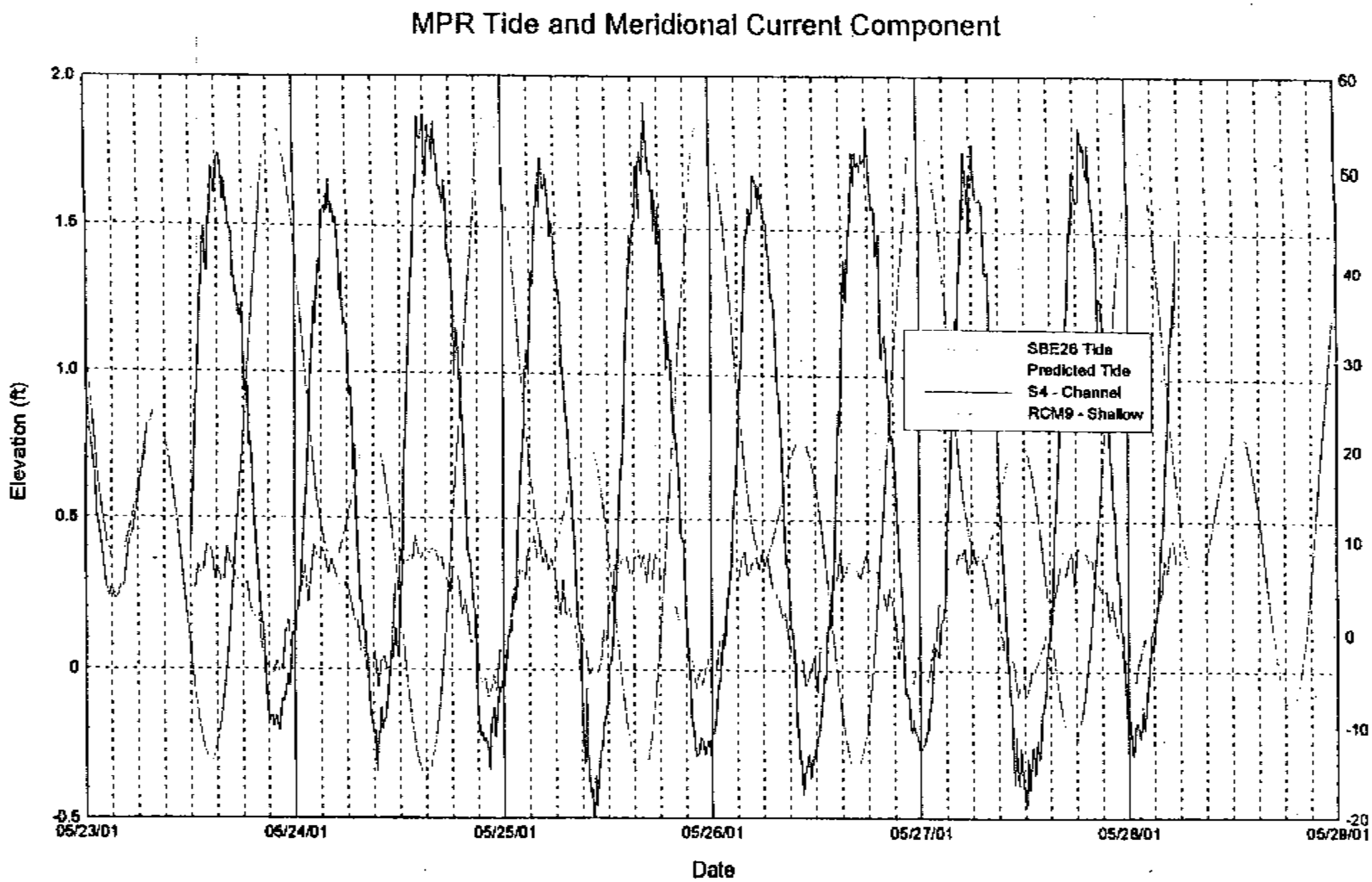
MPR Tide and Meridional Current Component
2.0
1.5
1.0
0.5
0
-0.5
Elevation (ft)
60
50
40
30
20
10
0
-10
-20
V (cm/s)
05/23/01
05/24/01
05/25/01
05/26/01
05/27/01
05/28/01
05/29/01
Date
SBE26 Tide
Predicted Tide
S4 - Channel
RCM9 - Shallow

Figure 3.

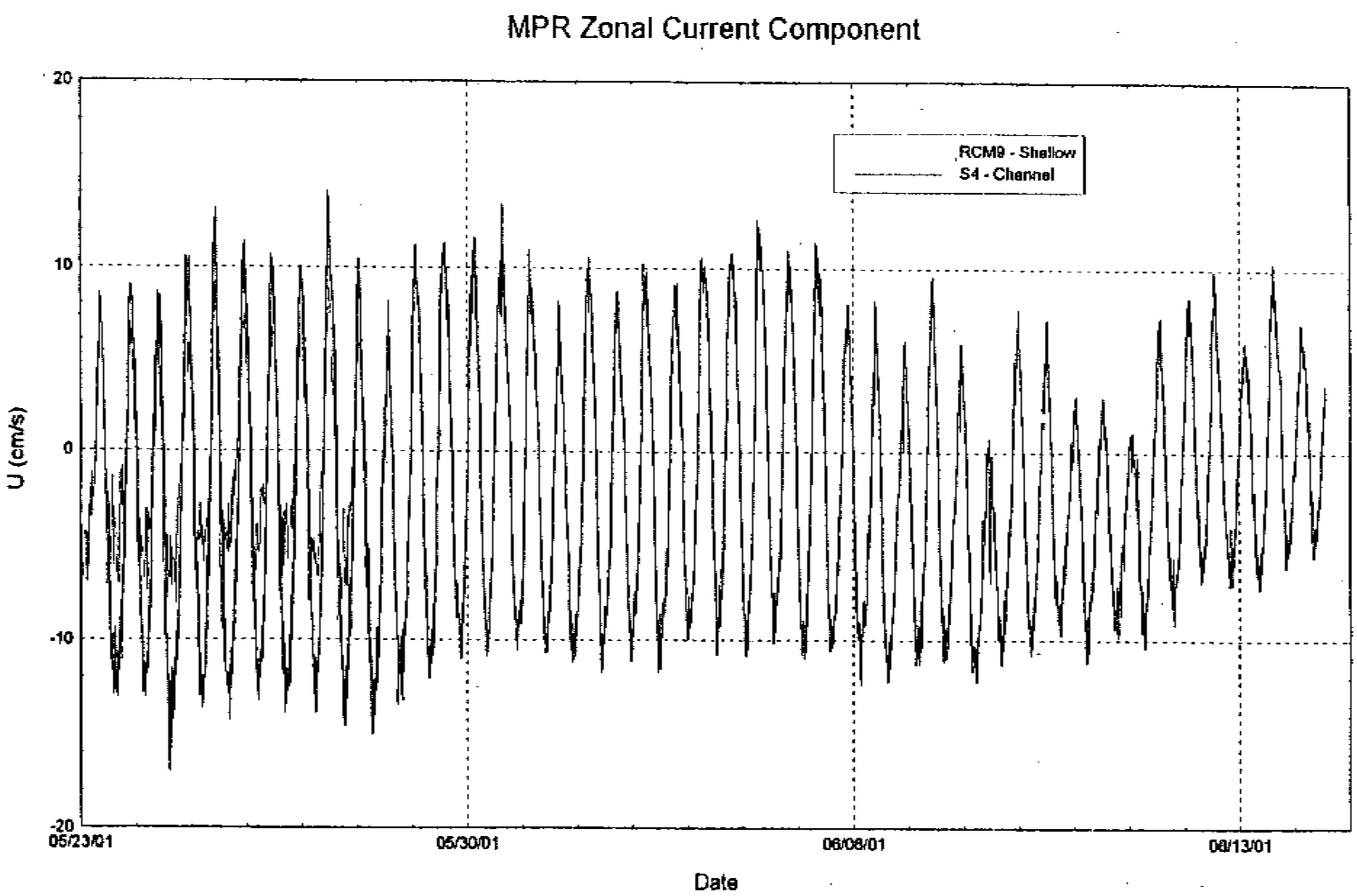
MPR Zonal Current Component
RCM9 - Shallow
S4 - Channel
20
10
0
-10
-20
U (cm/s)
05/23/01
05/30/01
06/06/01
06/13/01
Date

Figure 4.

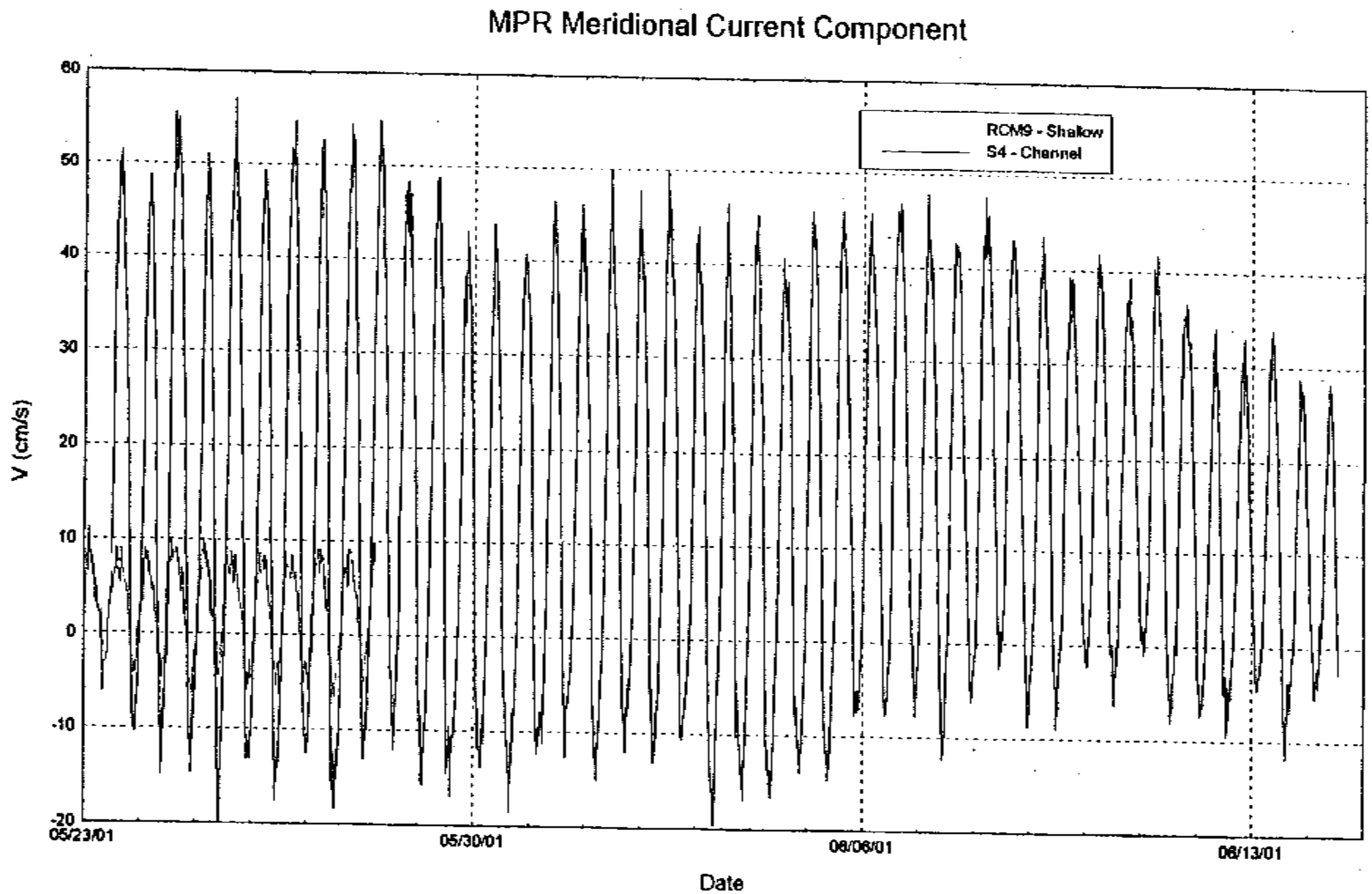
MPR Meridional Current Component
RCM9 - Shallow
S4 - Channel
V (cm/s)
60
50
40
30
20
10
0
-10
-20
05/23/01
05/30/01
06/06/01
06/13/01
Date

Figure 5.

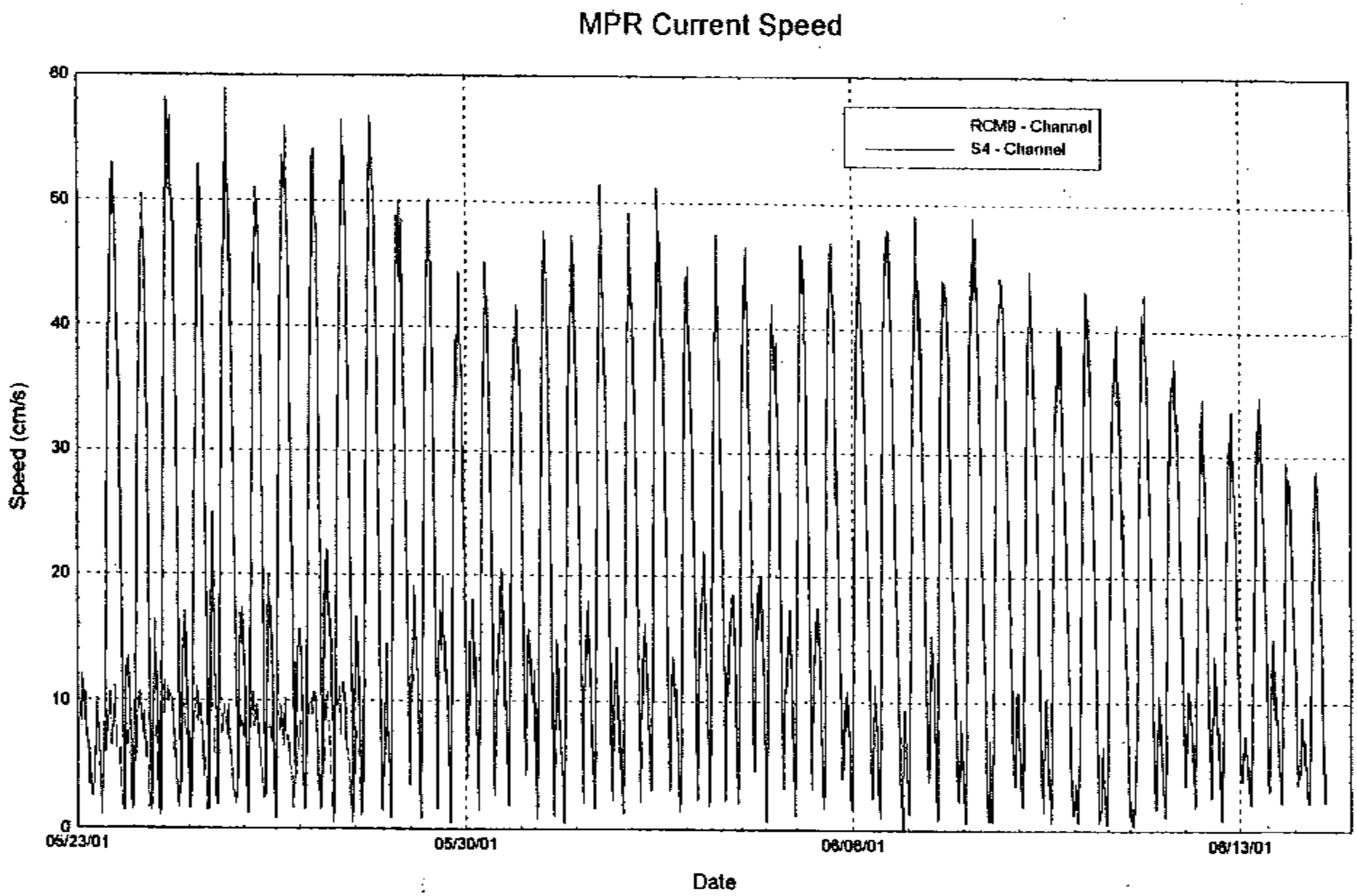
MPR Current Speed
RCM9 - Channel
S4 - Channel
Speed (cm/s)
60
50
40
30
20
10
0
05/23/01
05/30/01
06/06/01
06/13/01
Date

Figure 6.

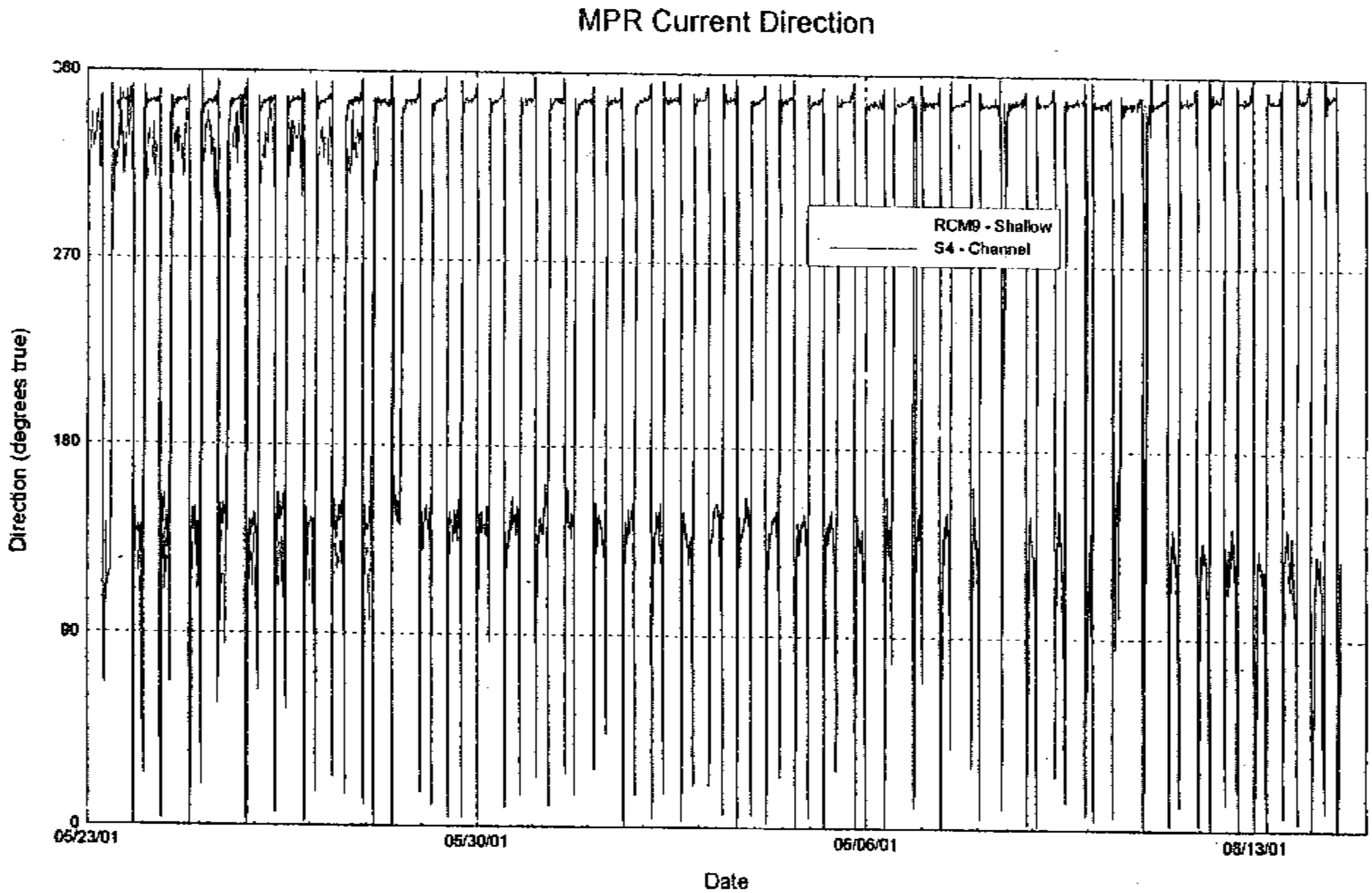
MPR Current Direction
360
270
180
90
0
Direction (degrees true)
05/23/01
05/30/01
06/06/01
06/13/01
Date
RCM9 - Shallow
S4 - Channel

Figure 7.

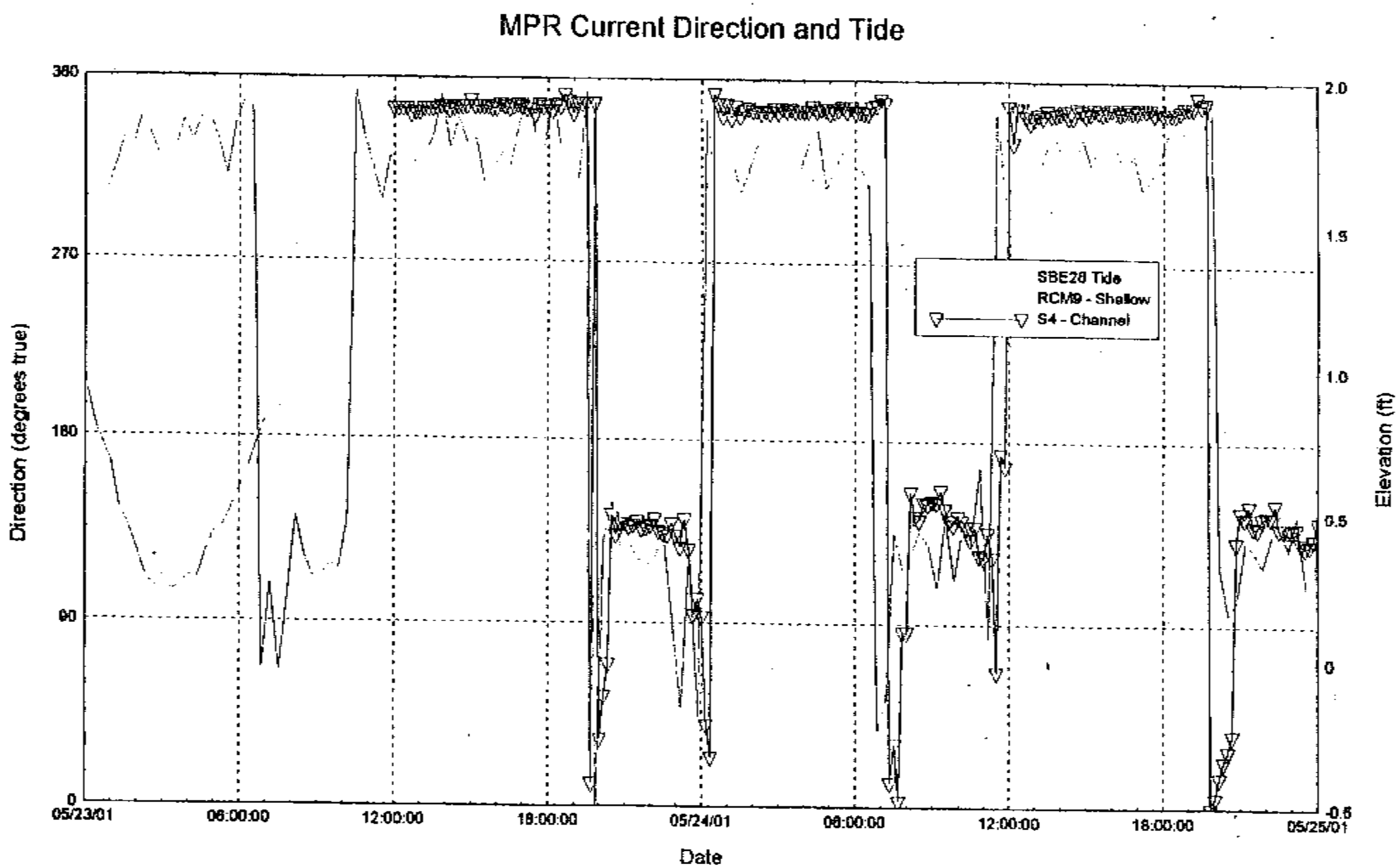
MPR Current Direction and Tide
360
270
180
90
0
2.0
1.5
1.0
0.5
0
-0.5
05/23/01
06:00:00
12:00:00
18:00:00
05/24/01
06:00:00
12:00:00
18:00:00
05/25/01
Date
Direction (degrees true)
Elevation (ft)
SBE28 Tide
RCM9 - Shallow
S4 - Channel

Figure 8.

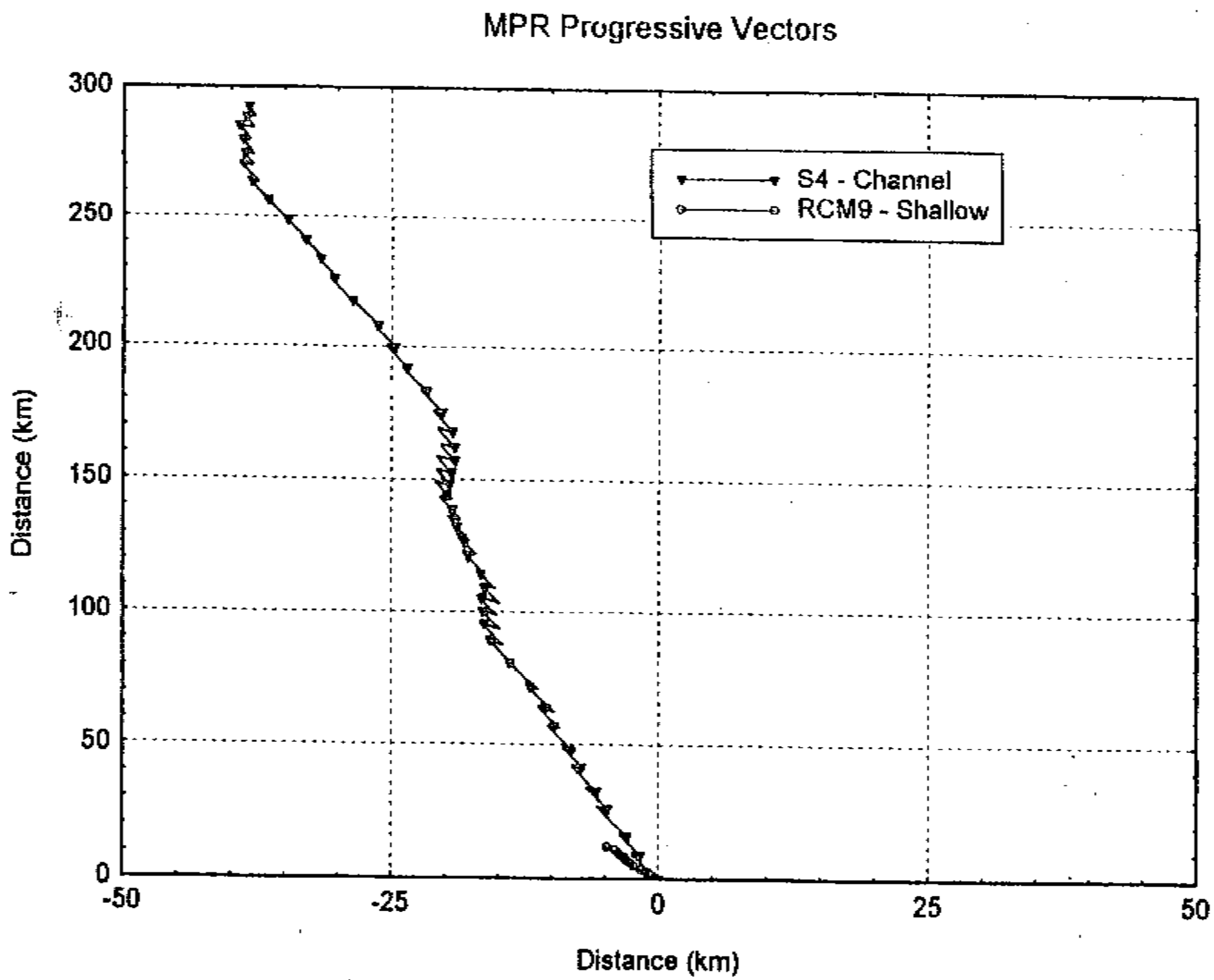
MPR Progressive Vectors
S4 - Channel
RCM9 - Shallow
Distance (km)
Distance (km)
300
250
200
150
100
50
0
-50
-25
0
25
50

Figure 9.

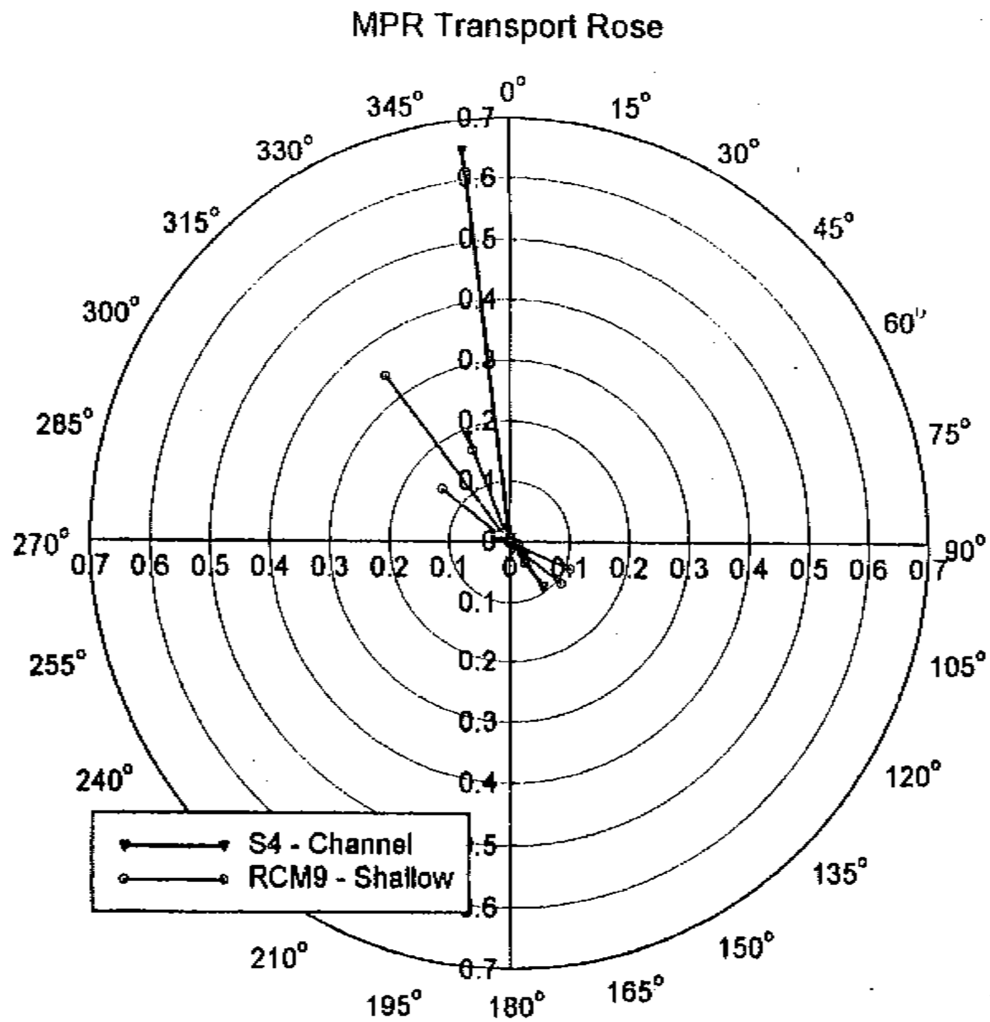
MPR Transport Rose
0°
15°
30°
45°
60°
75°
90°
105°
120°
135°
150°
165°
180°
195°
210°
240°
255°
270°
285°
300°
315°
330°
345°
0.1
0.2
0.3
0.4
0.5
0.6
0.7
S4 - Channel
RCM9 - Shallow

Figure 10.

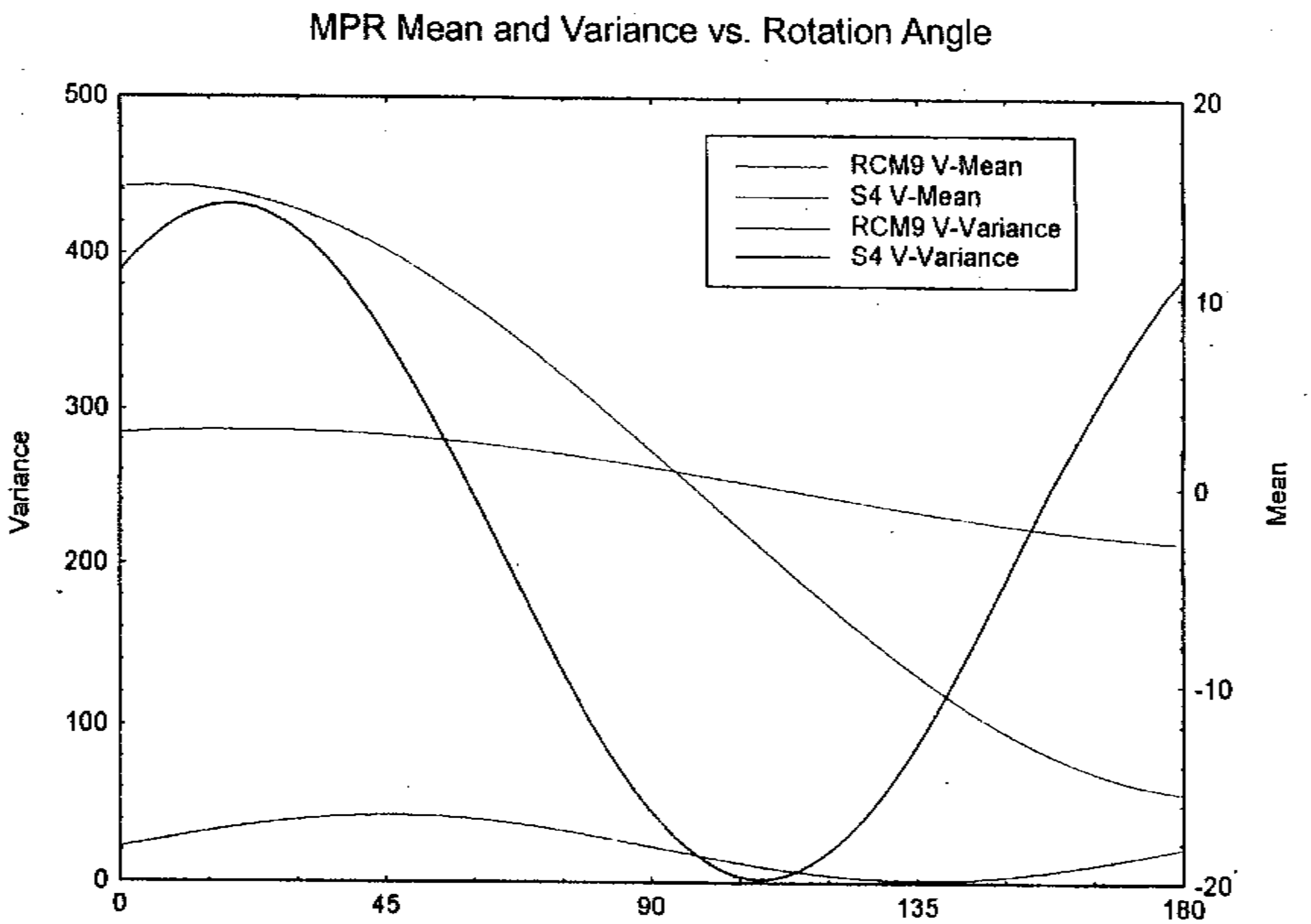
MPR Mean and Variance vs. Rotation Angle
RCM9 V-Mean
S4 V-Mean
RCM9 V-Variance
S4 V-Variance
Variance
Mean
500
400
300
200
100
0
20
10
0
-10
-20
0
45
90
135
180

Figure 11.

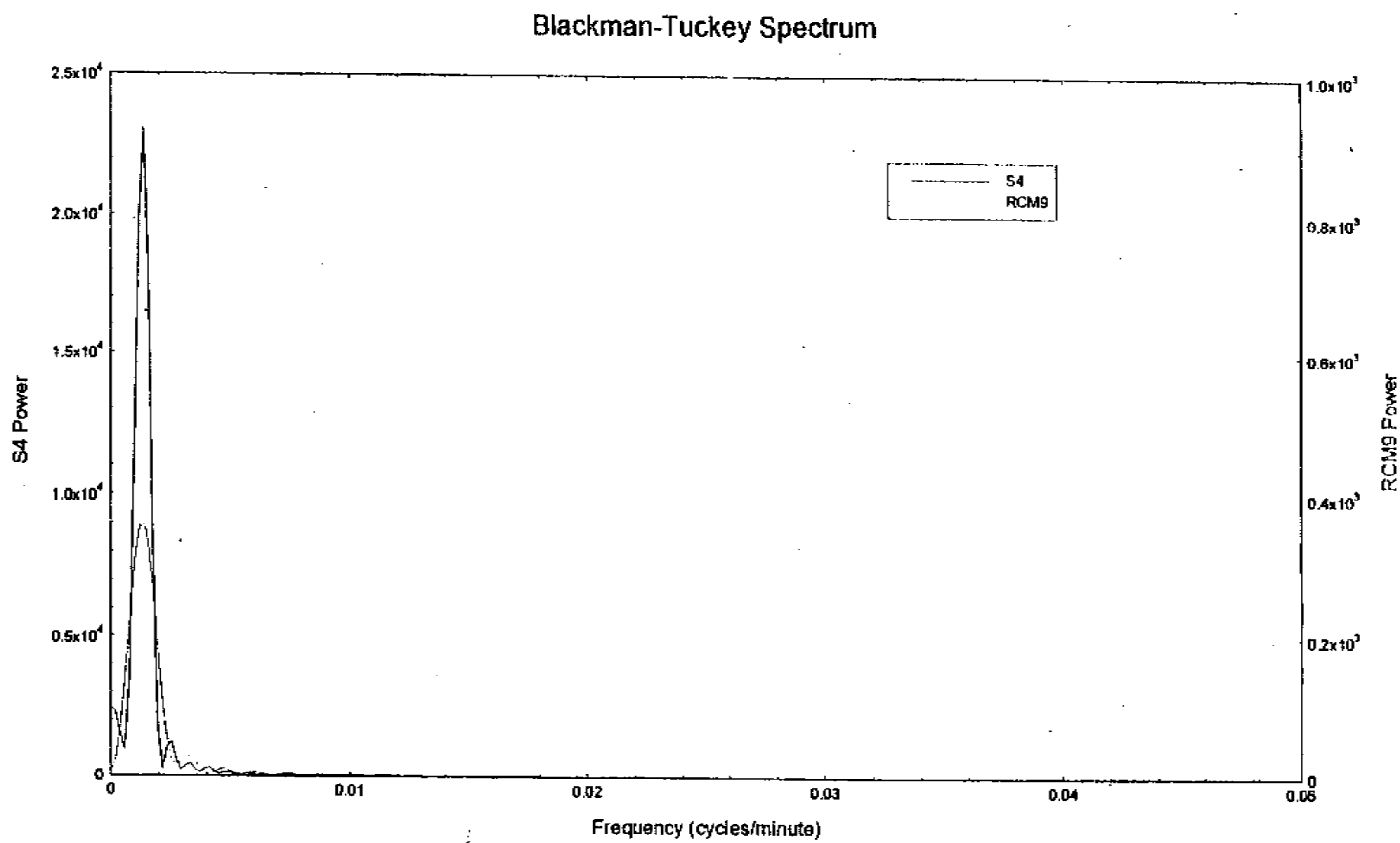
Blackman-Tuckey Spectrum
S4
RCM9
S4 Power
RCM9 Power
Frequency (cycles/minute)
2.5x10^4
2.0x10^4
1.5x10^4
1.0x10^4
0.5x10^4
0
1.0x10^3
0.8x10^3
0.6x10^3
0.4x10^3
0.2x10^3
0.01
0.02
0.03
0.04
0.05

Figure 12.

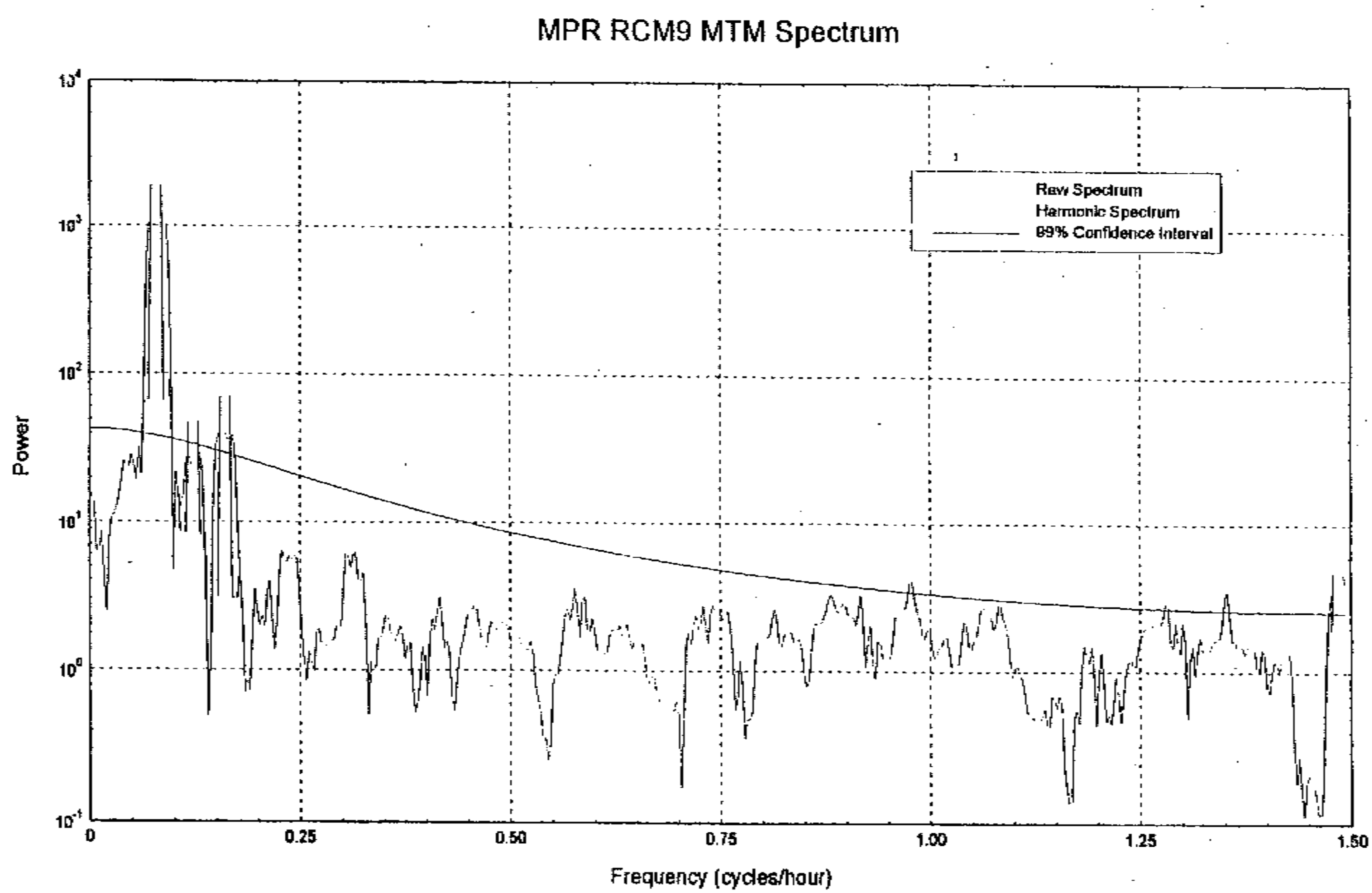
MPR RCM9 MTM Spectrum
Raw Spectrum
Harmonic Spectrum
99% Confidence Interval
Power
$10^4$
$10^3$
$10^2$
$10^1$
$10^0$
$10^{-1}$
0
0.25
0.50
0.75
1.00
1.25
1.50
Frequency (cycles/hour)

Figure 13.

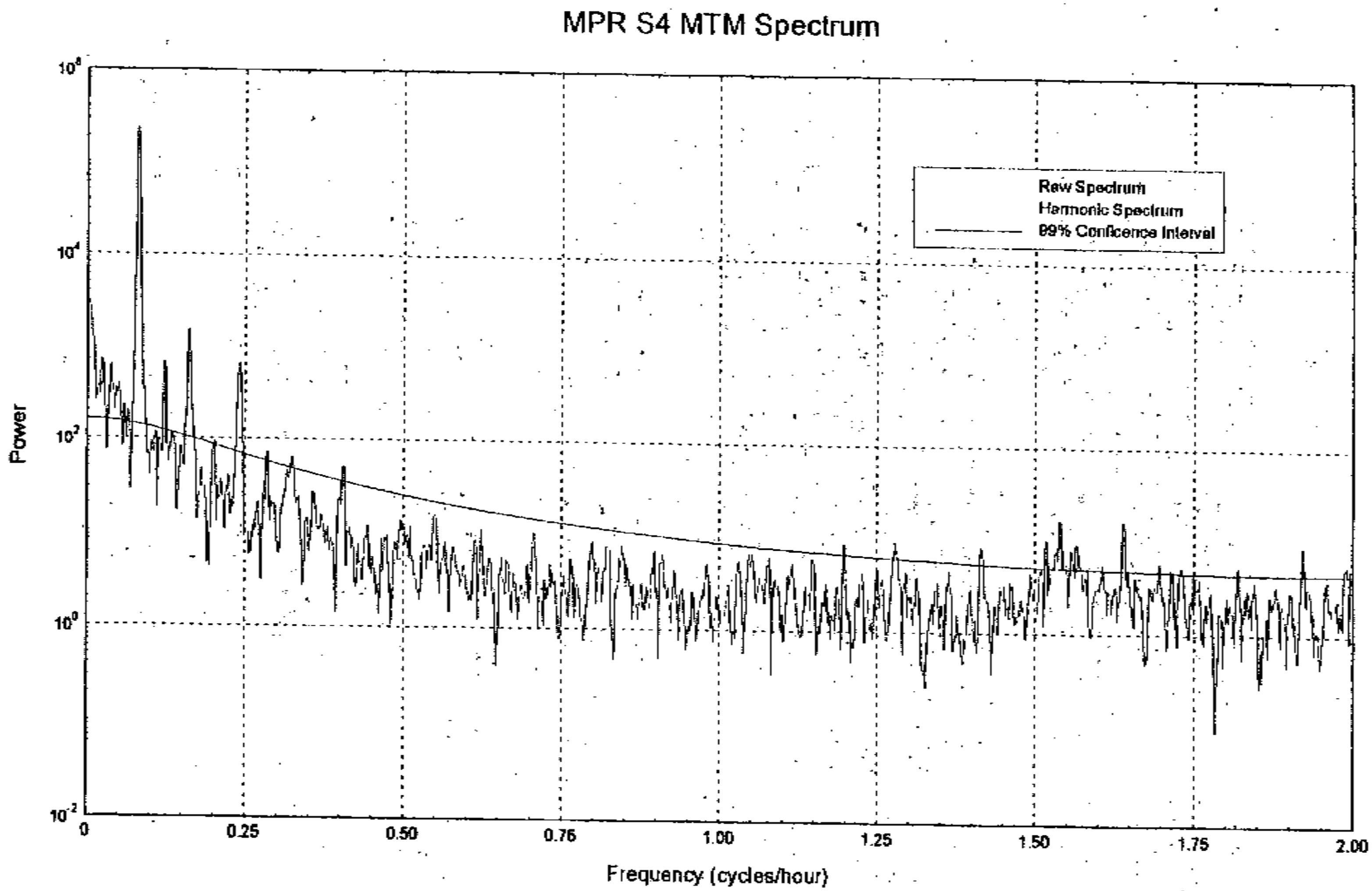
MPR S4 MTM Spectrum
Raw Spectrum
Harmonic Spectrum
99% Conficence Interval
Power
10^6
10^4
10^2
10^0
10^-2
0
0.25
0.50
0.75
1.00
1.25
1.50
1.75
2.00
Frequency (cycles/hour)

Figure 14.

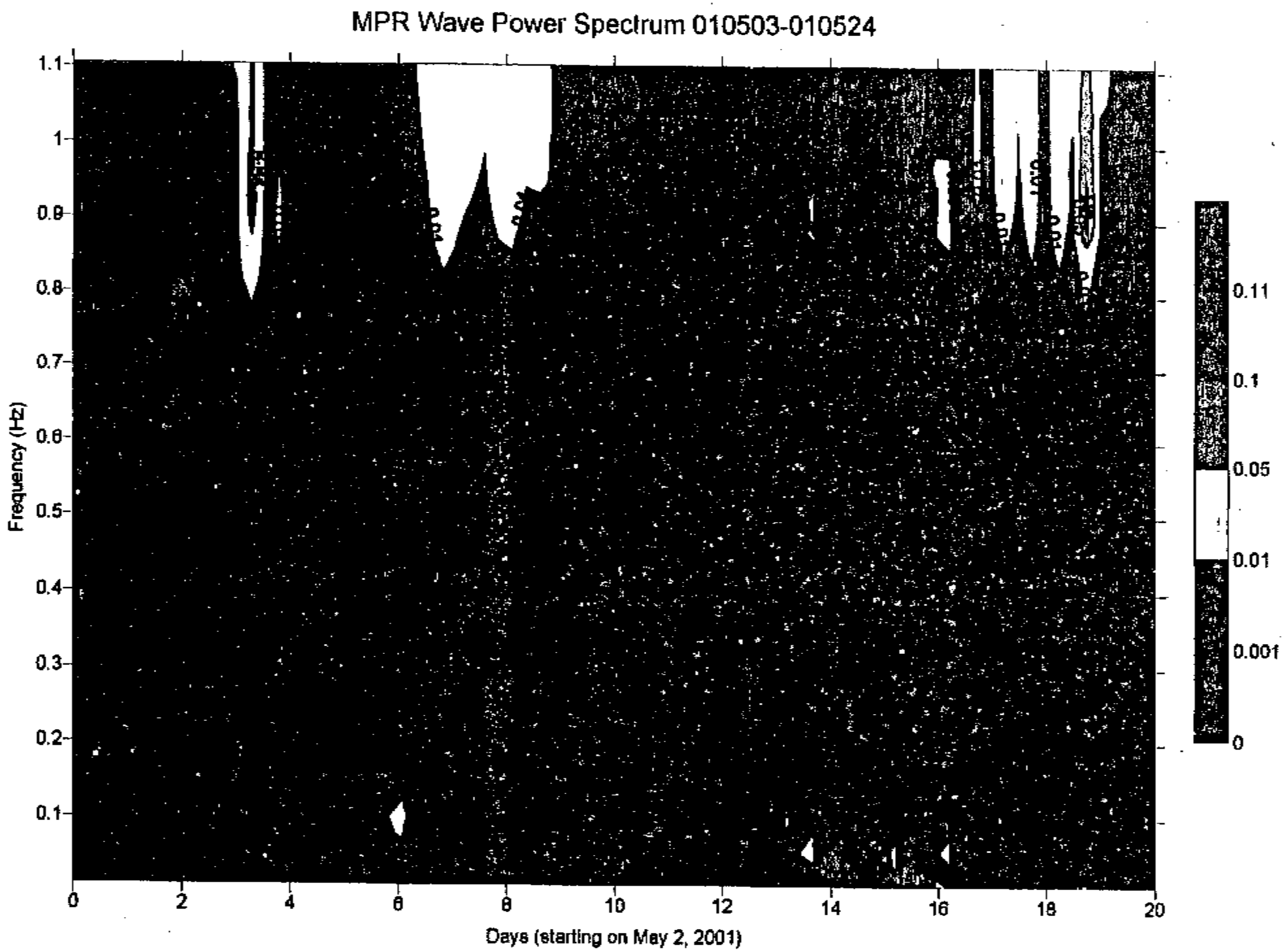
MPR Wave Power Spectrum 010503-010524
Frequency (Hz)
1.1
1
0.9
0.8
0.7
0.6
0.5
0.4
0.3
0.2
0.1
0
2
4
6
8
10
12
14
16
18
20
Days (starting on May 2, 2001)
0.11
0.1
0.05
0.01
0.001
0

Figure 15.

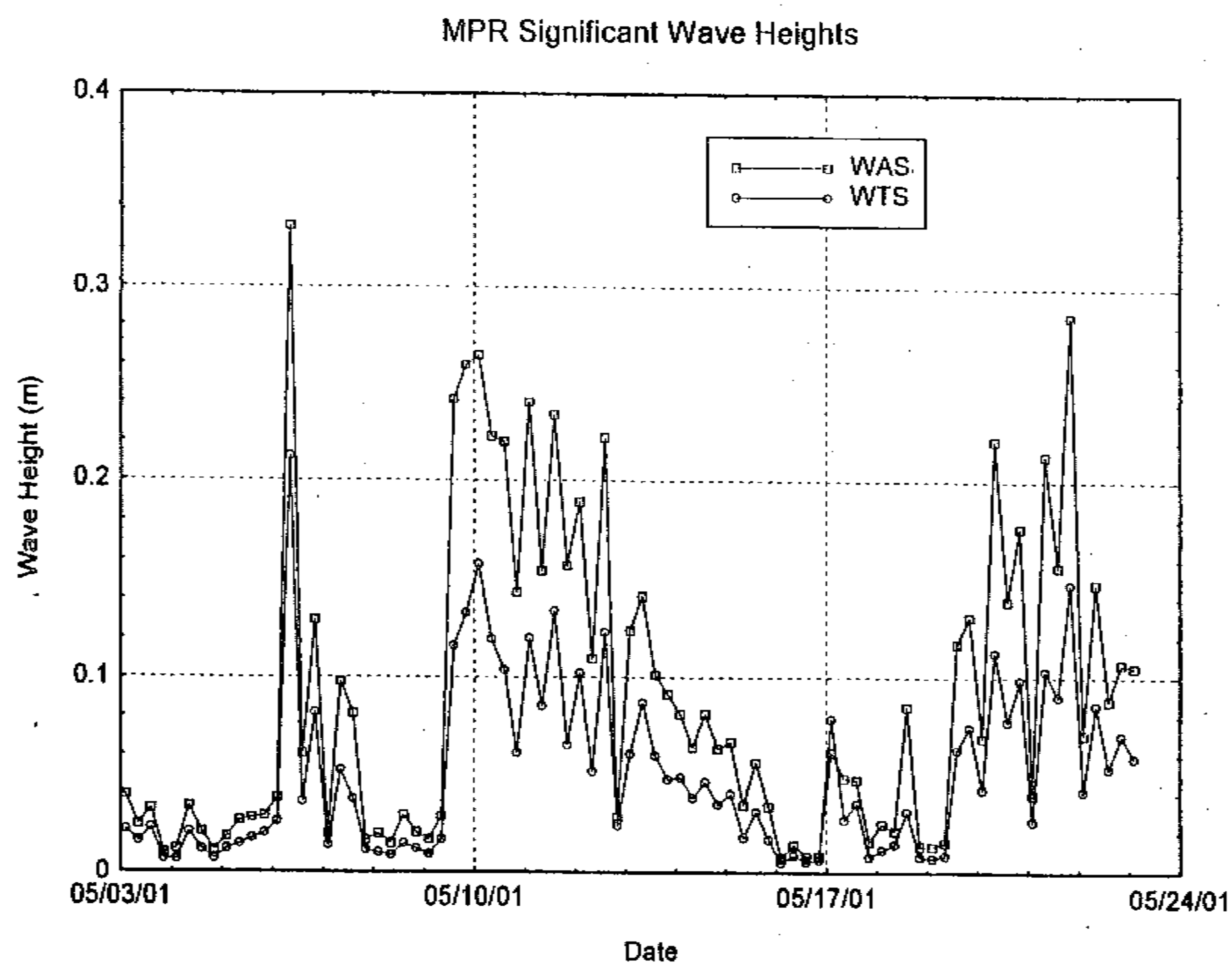

MPR Significant Wave Heights
WAS
WTS
0.4
0.3
0.2
0.1
0
Wave Height (m)
05/03/01
05/10/01
05/17/01
05/24/01
Date


Figure 16.

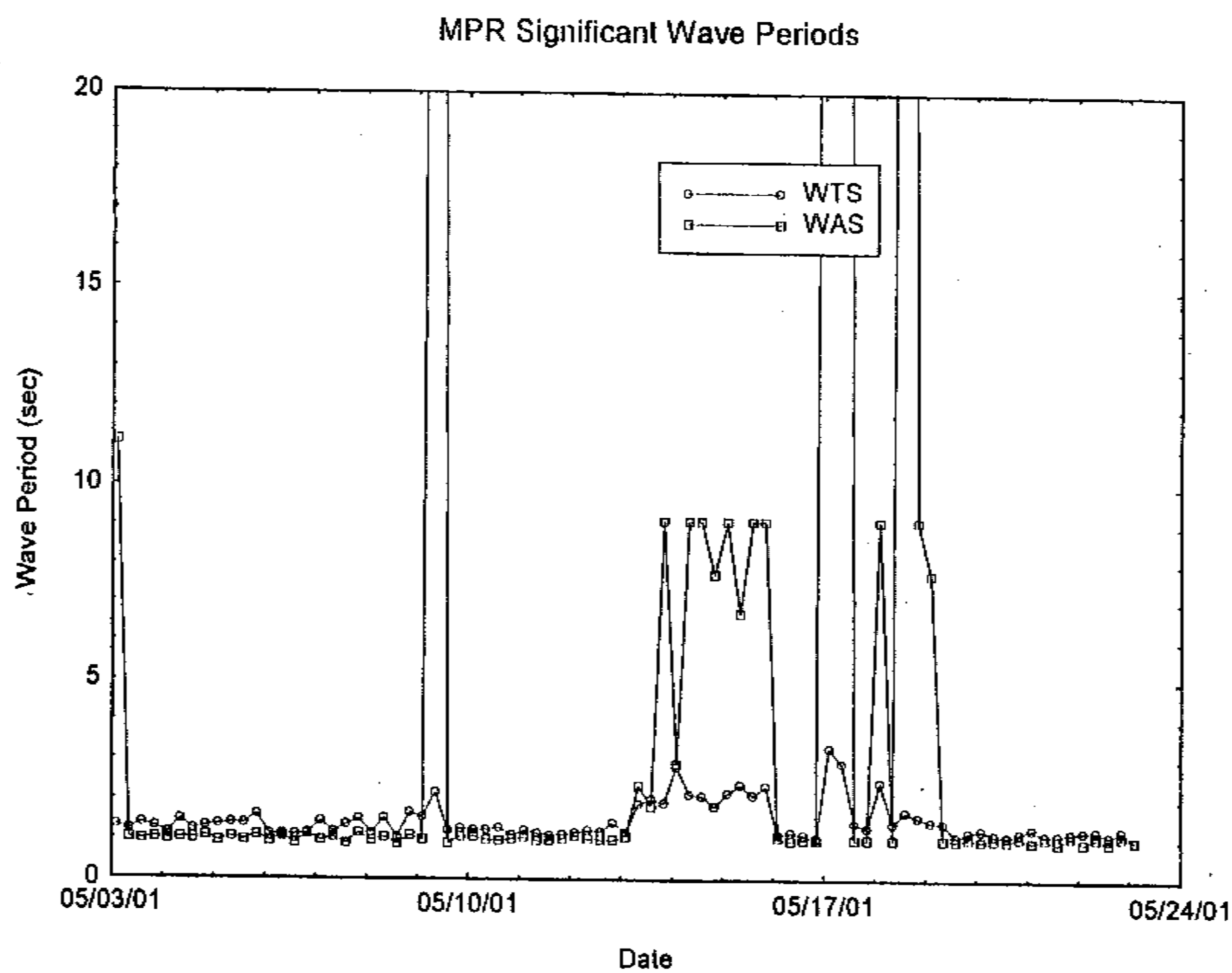
MPR Significant Wave Periods
WTS
WAS
Wave Period (sec)
20
15
10
5
0
05/03/01
05/10/01
05/17/01
05/24/01
Date

Figure 17.

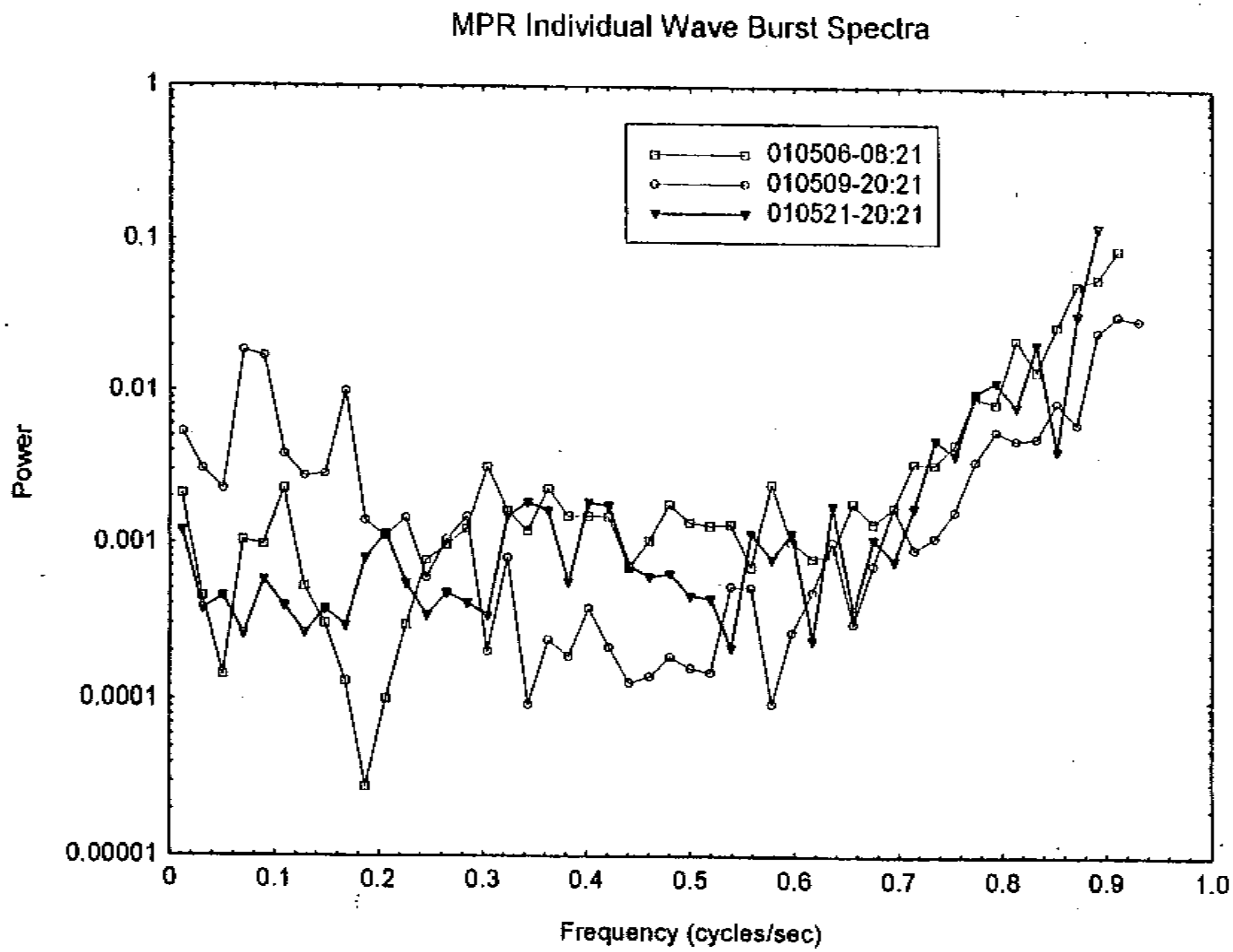
MPR Individual Wave Burst Spectra
010506-08:21
010509-20:21
010521-20:21
Power
1
0.1
0.01
0.001
0.0001
0.00001
0
0.1
0.2
0.3
0.4
0.5
0.6
0.7
0.8
0.9
1.0
Frequency (cycles/sec)

Figure 18.

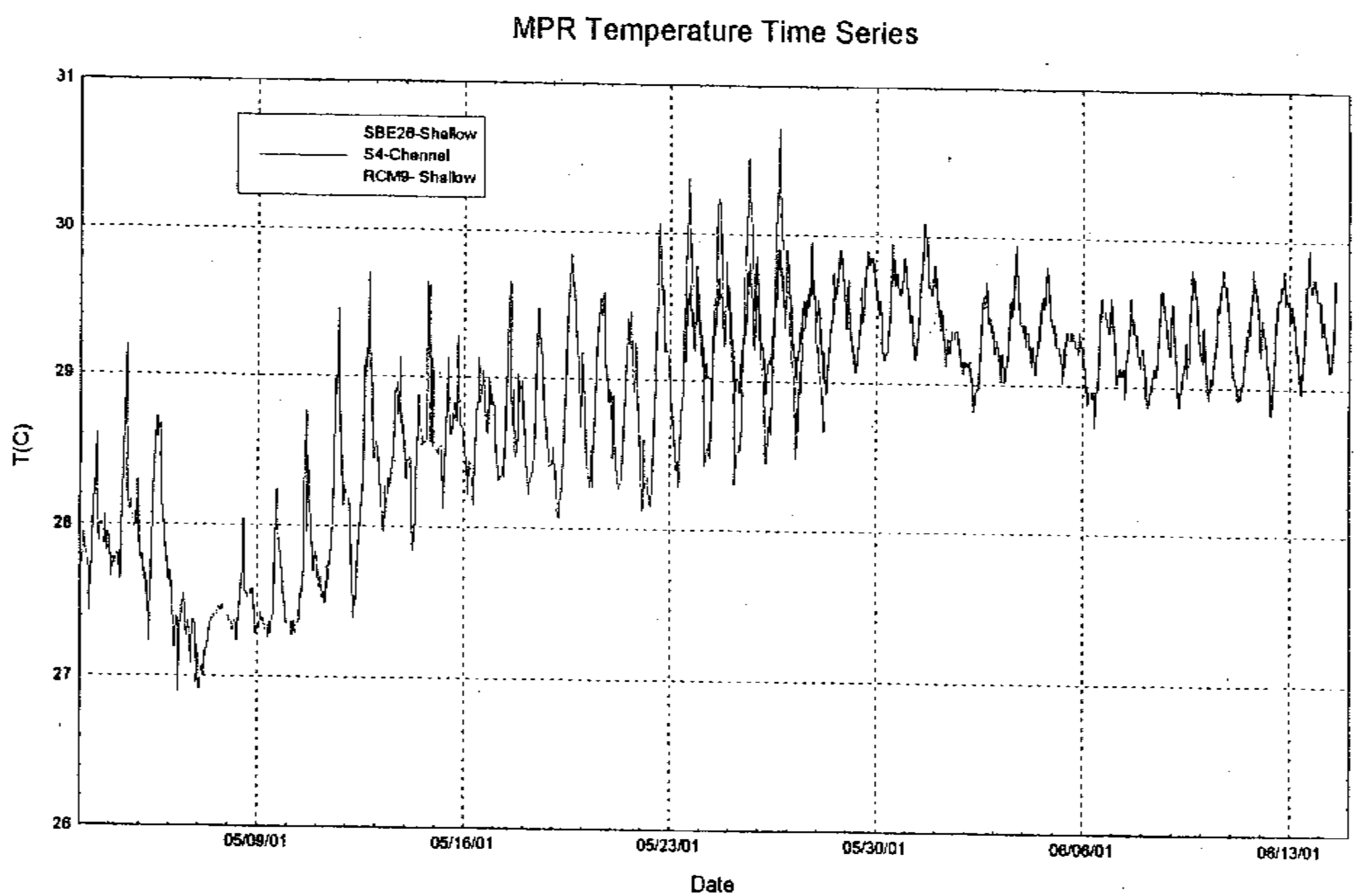
MPR Temperature Time Series
SBE28-Shallow
S4-Chennel
RCM9- Shallow
T(C)
31
30
29
28
27
26
05/09/01
05/16/01
05/23/01
05/30/01
06/06/01
06/13/01
Date

Figure 19.

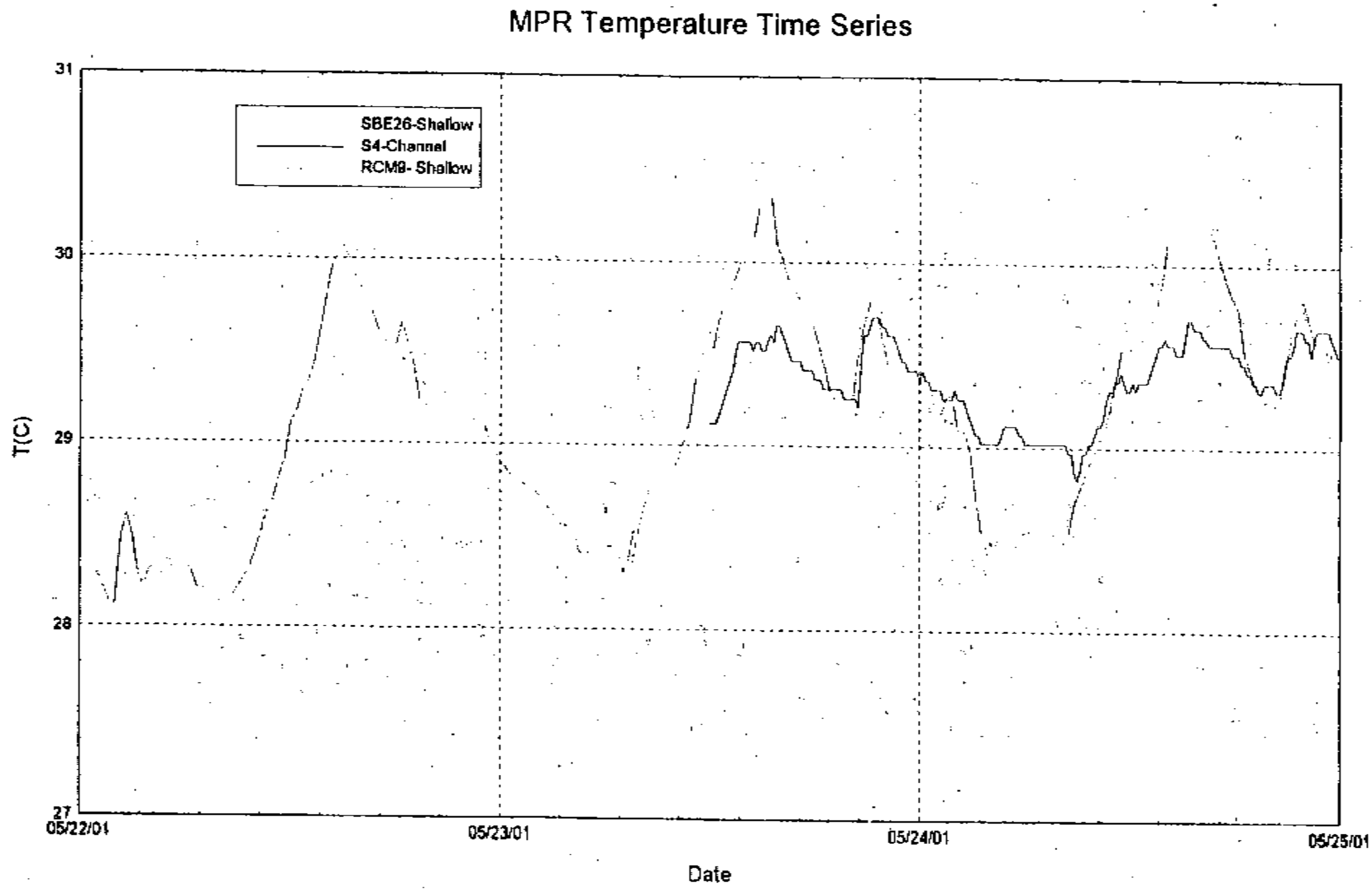

MPR Temperature Time Series
SBE26-Shallow
S4-Channel
RCM9- Shallow
31
30
29
28
27
T(C)
05/22/01
05/23/01
05/24/01
05/25/01
Date


Figure 20.

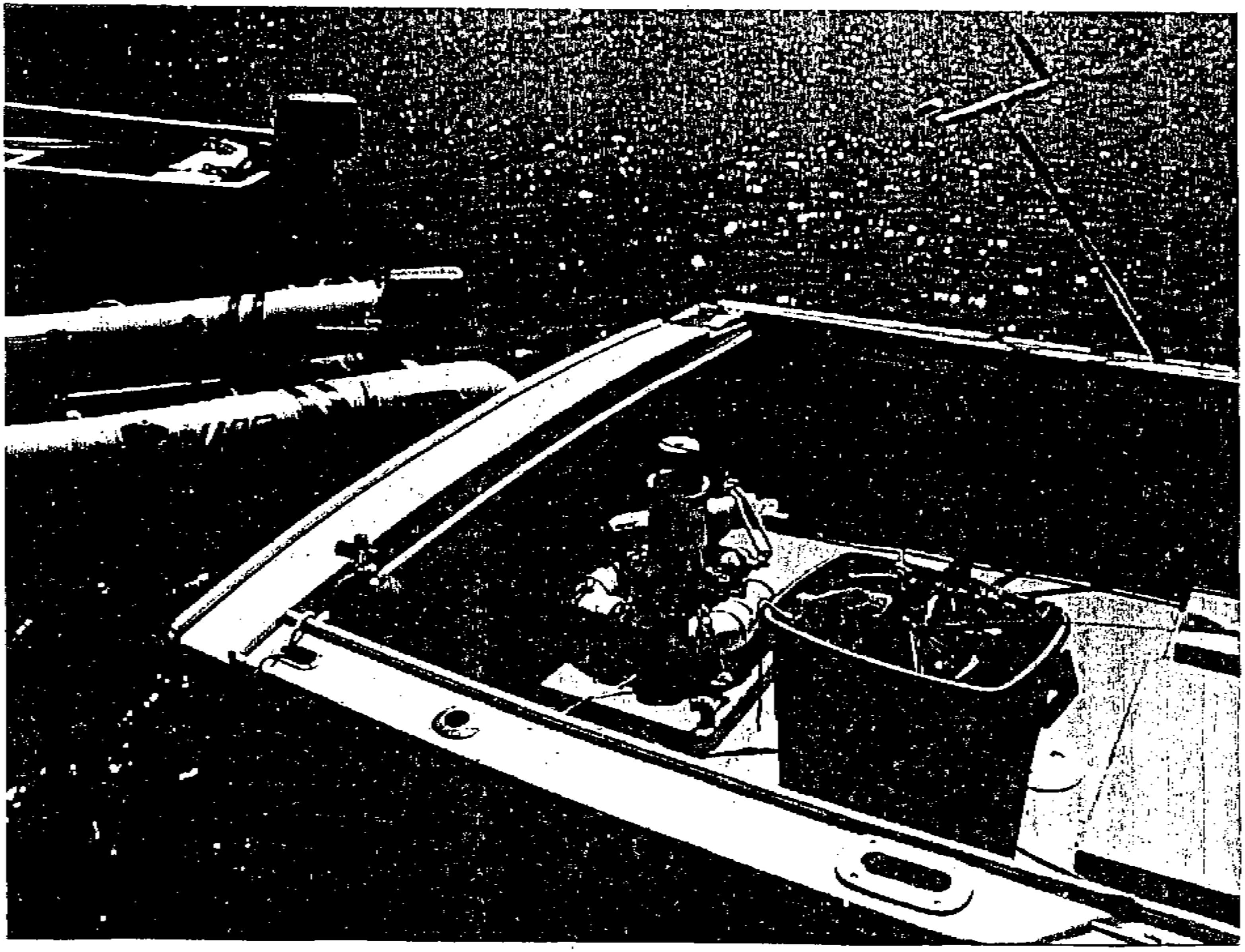

Plate 1.

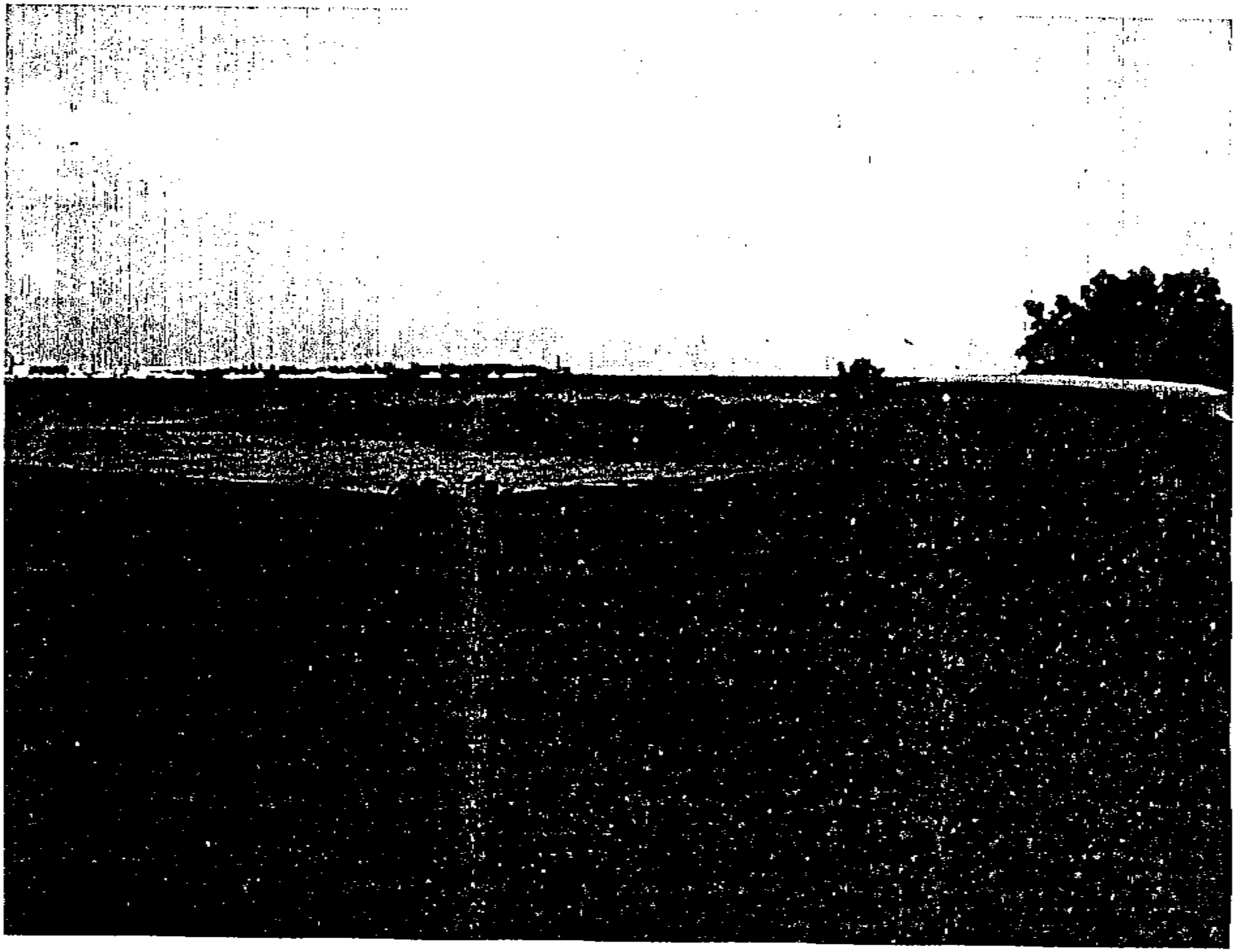

Plate 2.

# InterOcean systems, inc.

*The Leader in Ocean Technology - Since 1946*

Home | Products | Contact Us

# S4 Current Meter Family

**Current Measurement and Much More!**

- **Currents**
- **Waves**
- **Tides**
- **CTD**
- **Water Quality**

- **Immediate Data Access**
- **True Vector Averaging**
- **Low Threshold (0.03 cm/sec)**
- **Excellent Wave Zone Performance**

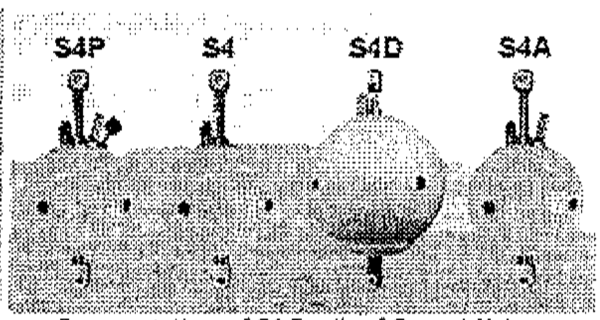


Representatives of S4 Family of Current Meters

# S4 Current Meter Family

## General Description

The **S4 Current Meter** family is a continuing evolution of a series of related products that are continuously upgraded using the latest devices and techniques in microprocessor based instrumentation.

The S4 families of instruments measure Current Speed, Direction, Wave, Tide, CTD, Turbidity, and Water Quality parameters.

The S4 Current Meter is a truly unique instrument for water current sensing. The instrument itself is the self-contained current measuring sensor, enclosing all necessary solid-state electronics for acquiring, processing and outputting data.


A shallow water mooring device used in San Francisco Bay

The S4 is designed to measure the true magnitude and direction of horizontal current motion in any water environment. The voltage is sensed by the two pairs of titanium electrodes located symmetrically on the equator of the sensor. The data obtained is then stored in non-volatile solid-state memory.

The simple spherical shape of the S4 is a contributing factor in the excellent rejection of vertical components of water movement, providing significant improvements in measuring currents in the wave zone. Also, because of its low threshold and low noise level, the S4 is the current meter of choice for low current regimes.

The unique grooved surface of the S4 housing produces stable hydrodynamic characteristics that ensure exceptional linearity and stability. This new hydrodynamic design, in which the instrument body itself is the source of current measurement, is a technological breakthrough. The S4 has withstood rigorous performance testing, and has produced excellent and stable data in the field.

The internal flux-gate compass provides heading information, which is used to reference the current direction to magnetic North. For fixed installations, the S4 may be operated in an X-Y orthogonal mode whereby the current vector can be referenced to the instrument housing.

Adaptive sampling, user programmability, optional sensors and expandable memory permit highly selective data collection and /or longer deployment intervals.

# SEAGAUGE Wave & Tide Recorder

## *SBE 26*

Click the icon to download the SBE 26 manual.


- Standard Quartzonix pressure sensor
- Optional Digiquartz® pressure sensor
- Up to 8 Mb solid-state memory
- RS-232 direct data upload
- Accurate temperature sensor
- Optional conductivity sensor
- Powerful software included
- All plastic/titanium construction
- Operates with alkaline D batteries

DESCRIPTION

The SBE 26 combines Sea-Bird's reliable semiconductor-memory electronics, stable time base, precision thermometer, and quartz-crystal pressure sensor to provide wave and tide recording of unprecedented resolution and accuracy, along with high-quality temperature information. A second input connector for a conductivity sensor is also standard.

The SBE 26 (shown above) is being secured in its optional mounting fixture. After installation at a mooring site, the fixture allows removal and precise repositioning by a diver. Tools are not required, and there are no loose parts to misplace.

The SBE 26 continuously integrates pressure samples to obtain water level measurements unaffected by wave action, and also independently burst-samples pressure at rates up to 4 Hz for wave amplitude calculation. Water level integration and wave burst sampling intervals and durations are programmable. The large memory permits frequent water level recording and highly detailed wave characterization. For example, with an 8M byte memory, a 120-day deployment could include water level measurements every 15 minutes and 20 minute 2 Hz wave-burst samples 8 times a day.

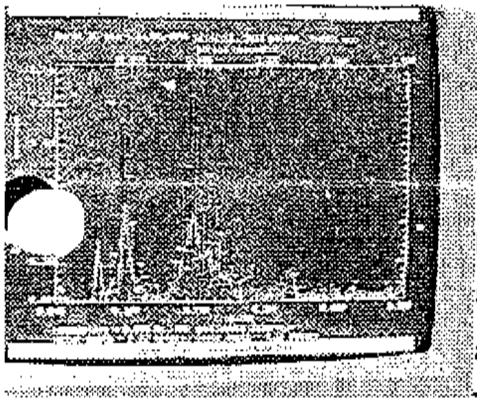

The SBE 26 includes *SEASOFT© for Waves*, a comprehensive package of programs including deployment planning, instrument set-up, data retrieval, plotting, auto-spectrum, time series analysis, and statistics reporting.

The data example, shown at right, is an auto-spectrum plot of surface wind waves obtained from one burst sample of 1024 pressure measurements. The error bars correspond to 90% confidence intervals.

Using SEASOFT for Waves and an IBM PC-compatible computer, the recorded data (wave, tide, temperature, and optional conductivity) are uploaded after recovery via an RS-232 interface, without opening the housing. The battery compartment is separated from the electronics by a moisture-proof seal. It contains 9 standard alkaline D-cells and provides 6 months of operation. Longer deployments are possible using lithium batteries.

SENSORS

The standard pressure sensor is a 45 psia Quartzonix temperature-compensated transducer (other ranges, using a Digiquartz sensor, are optional). Temperature is measured with an aged thermistor imbedded in the SEAGAUGE end cap. An SBE 4 conductivity sensor (optional) may be interfaced via the second bulkhead connector and clamped to the SEAGAUGE housing.

PROGRAMMING AND RECORDING

The tide integration time is user-programmable in minute increments over a range of 1 to 30,000 minutes. Temperature data is recorded with each tide integration. Waves are characterized by burst sampling with the number of samples per burst, burst interval, and burst integration time programmed by the user. A tide and temperature measurement consists of 4 bytes (6 bytes with optional conductivity); each sample in a wave burst uses 3 bytes.

SPECIFICATIONS

| | **Temperature (°C)** | **Conductivity (S/m)** *optional* | **Pressure** |
|---|---|---|---|
| **Measurement Range** | -5 to + 35[1] | 0 to 7[1] | 0 to 21 meters (45 psia F.S.) |

| | | | |
|---|---|---|---|
| Accuracy | 0.02 | 0.001 | 0.01% F.S.<br>(3 mm for 45 psia range) |
| Resolution | 0.01 | 0.0001 | *Tide*:<br>0.2 mm (0.008 in.) with<br>1 minute integration;<br>0.01 mm (0.0004 in.) with<br>15 minute integration |
| | | | *Wave*:<br>0.4 mm (0.016 in.) with<br>0.25 second integration;<br>0.1 mm (0.004 in.) with<br>1 second integration |
| Calibration | -1 to +31 | 1.5 - 6 | 0 psia to F.S. Pressure |
| Repeatability | | | 0.005% F.S. (1.5mm) |
| Hysteresis | | | 0.005% F.S. (1.5 mm) |

*[1]Measurements outside the specified calibration ranges will be at reduced accuracy due to extrapolation errors*

Counter time-base:

± 2 ppm stability vs. temperature

(-5 to 35 °C);

± 2 ppm per year aging

Memory:

- 1024K byte CMOS static RAM standard
- 2, 4, or 8 Mb optional
- Back- up battery gives 2 years data retention after main battery is exhausted

Real-time clock:

15 seconds per month stability; battery-backed

Weight, in air:

6.4 kg (14 lbs) with alkaline batteries (mounting fixture weighs 3.6 kg (8 lbs) )


AANDERAA INSTRUMENTS
DATA COLLECTING INSTRUMENTS FOR LAND SEA AND AIR
The RCM 9
A unique
Recording Current Meter
for use in the sea
and in freshwater
featuring the Mark II
DOPPLER CURRENT
SENSOR DCS 3920
Measuring:
Current Speed
Current Direction
Temperature
Conductivity (optional)
Instrument Depth (optional)
Turbidity (optional)
Oxygen (optional)
Stores data internally in the standard Data Storage Unit DSU 2990 or transmits data in real-time via cable.
Features:
- No offset
- Low noise
- Forward pinging algorithm improves accuracy
- Insensitive to fouling
- No moving parts
- Easy installation and handling
- Easy functional verification using an external Test Unit
Specially well suited for:
- Operation in the Wave Zone
- Monitoring Low Current Speeds

# Apéndice 13: Wave Refraction and Sediment Transport

# WAVE REFRACTION AND SEDIMENT TRANSPORT

# MARINA PUERTO REAL, FAJARDO, PUERTO RICO

Prepared for:

**Ecosystems and Associates**
**Port rd. 13, Palmas del Mar**
**Humacao, P.R. 00791**

Prepared by:


MOFFATT & NICHOL
ENGINEERS

1509 West Swann Avenue, Suite 225
Tampa, Florida 33606
813-258-8818

M&N File: 4890

**December 2001**

# EXECUTIVE SUMMARY

This report presents the results of a wave refraction and sediment transport numerical modeling study of the proposed breakwaters at Marina Puerto Real, Puerto Rico. The study addresses the potential impacts of constructing two protective breakwaters for the marina.

The project site is located on east coast of Puerto Rico at Fajardo. The site is in a semi-protected cove with a series of small offshore islands that dissipate the incident wave energy. This reduction in wave energy corresponds to low values of sediment transport along the shoreline of the bay.

The wave climate is predominantly comprised of waves from the east, north, and northeast with average significant heights of approximately 1.5 meters and periods of 6 to 14 seconds. A line of islands to the northeast and an island nearer to shore adjacent to the site provide shelter reducing these wave heights approximately 65-90%.

The presence of the breakwater had little impact on the wave heights and currents modeled. The proposed breakwater resulted in minor increases in the amount of sediment deposition. The potential for increases to the initial rate of sediment deposition in existing shipping regions ranged from an average of 0.1 to 0.7 mm/day. However, because of the conservative nature of the analysis (as presented in Section 7.1) these values represent the worst-case scenario.

Based on the results of the modeling, it is our opinion that the construction of the breakwaters will not have a significant impact on the adjacent properties.

Moffatt & Nichol Engineers (M&N) has been retained to perform a numerical modeling evaluation of the potential wave climate and sediment transport changes resulting from the construction of two protective breakwaters at the proposed Marina Puerto Real in Fajardo, Puerto Rico. The results will be used to guide the design of the structures and basin as well as to support the permitting effort with the United States Army Corps of Engineers (USACE). A conceptual design layout of the breakwaters is shown in Figure 1.1.

## 1.1 Scope

The scope of the study consisted of the following tasks:

- Data Collection and Review,
- Wave Transformation Analysis,
- Hydrodynamic Analysis,
- Sediment Transport Analysis, and
- Summary Report.

## 1.2 Numerical Modeling Approach

The following summarizes the approach used for the numerical modeling:

- Develop representative shoreline orientation, profile, and offshore/nearshore bathymetry,
- Review wave data for direction, period, height, and frequency of occurrence and categorize the applicable wave events by period, direction, and height,
- Transform the wave data from deep water to shallow water conditions at the proposed marina site,
- Establish a finite difference modeling grid based on the dimensions of the area to be modeled and the period (wavelength) of the waves,
- Perform numerical modeling to determine the nearshore wave heights, directions, and radiation stresses for each of the wave categories,
- From the radiation stresses and tides, calculate the resulting nearshore current velocities for each of the wave categories,

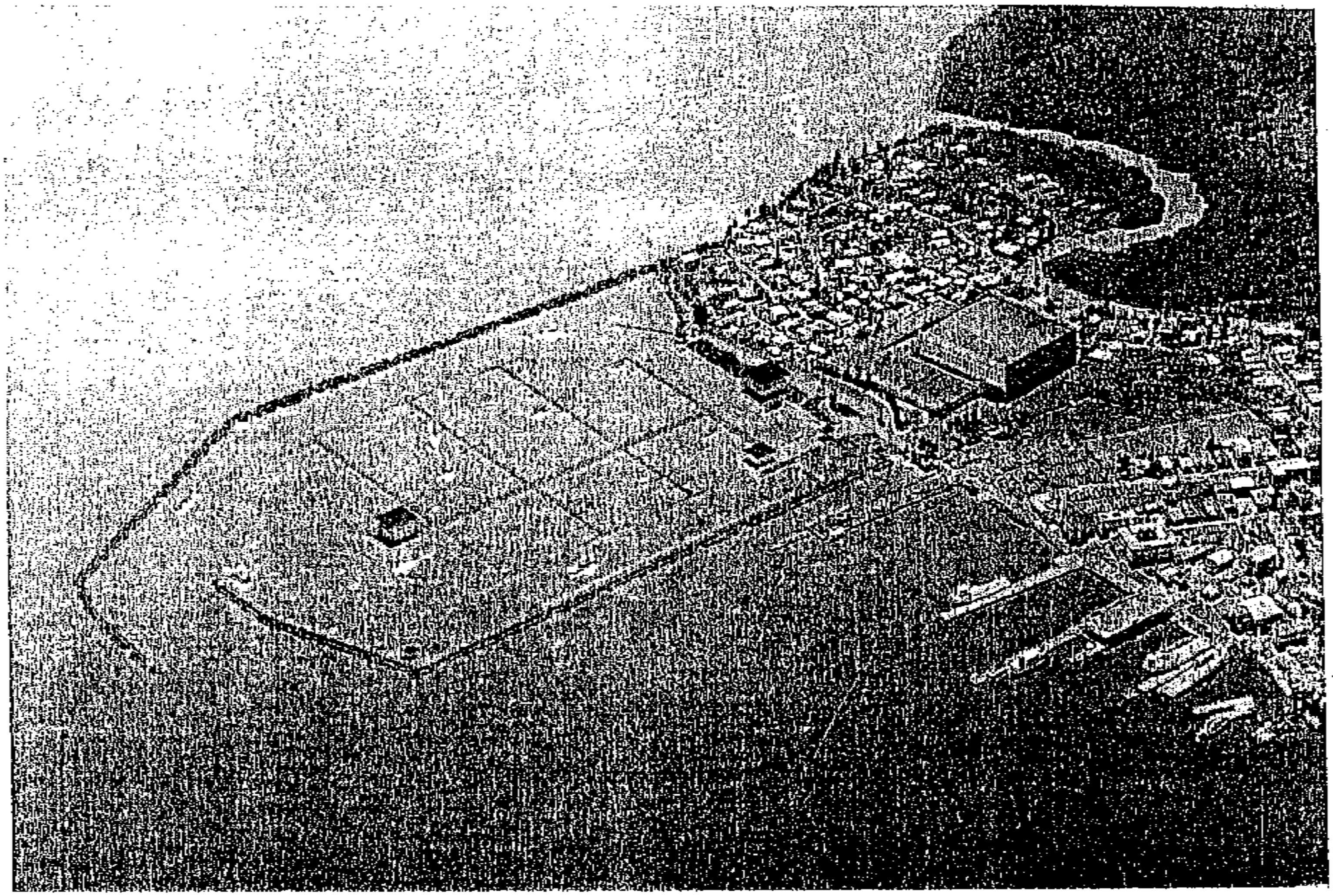

MOFFATT & NICHOL
ENGINEERS

Figure 1.1: Conceptual Design Layout

- From the current velocities, calculate the sediment transport rates for each of the categories and evaluate the potential for changes in sedimentation due to the presence of the proposed breakwaters.

The project site is located on the northeastern coast of Puerto Rico, as shown in Figure 2.1 (approximately 18° 20' Latitude and 65° 38' Longitude). The shoreline orientation is generally northwest to southeast with small wave exposure windows to the northeast and eastsoutheast. There is a USACE wave hindcast station located approximately 94 kilometers (~51 nautical miles) offshore of the site in ~3 kilometers of water. (Refer to Section 3.0, Wave Data, for further details.)

## 2.1 Bathymetric Data

The bathymetry was digitized from available nautical charts (NOAA Chart 25663). The modeling region was divided into two areas as shown in Figure 2.2. A coarser grid (10m × 40m) covering an area of approximately 10 km by 12 km was used to model wave transformations from offshore, past the sheltering islands, to within a kilometer of the proposed marina site. A finer local model grid (1m × 4m) was used to model further wave transformations. Finer resolution of the bathymetry grid near the proposed breakwater site, where the water depths are shallower and wave interaction with the seafloor is increased. provides improved results for wave transformation calculations. The resulting wave and tidally induced currents, which drive the sediment transport processes, were modeled on a uniform grid (4m × 4m) encompassing a 2 km by 2 km area around the proposed marina.

## 2.2 Sediment Characteristics

Sediment samples collected from three borings within the proposed marina (in depths from 2 to 8 feet) were predominantly silt with fine sand. The mean sediment diameter, or $D_{50}$, for each of the sample locations is shown in Table 2.1. The midrange mean sediment diameter, 0.06 mm, was used in the numerical model.

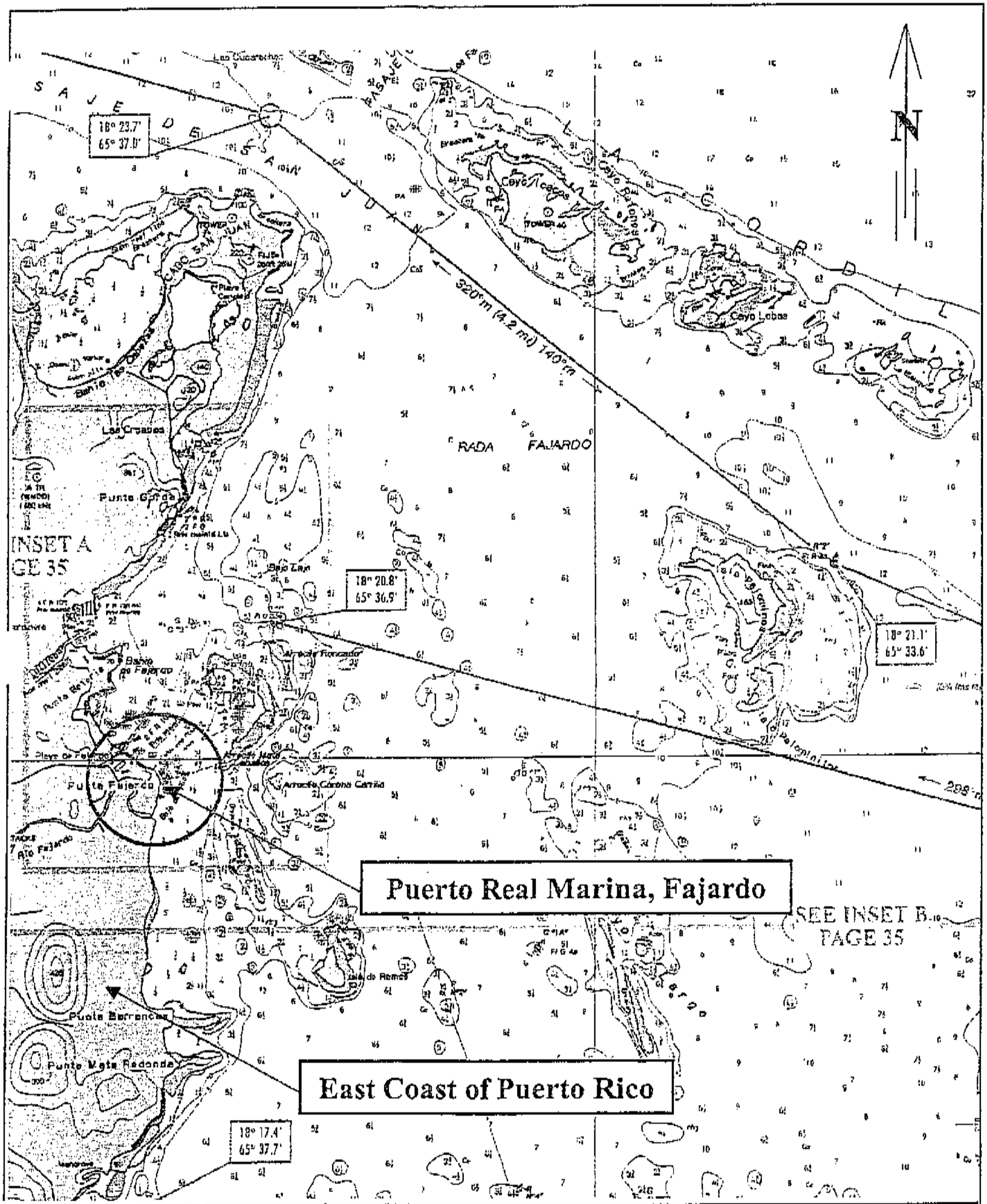


MOFFATT & NICHOL
ENGINEERS

Figure 2.1:Project Site

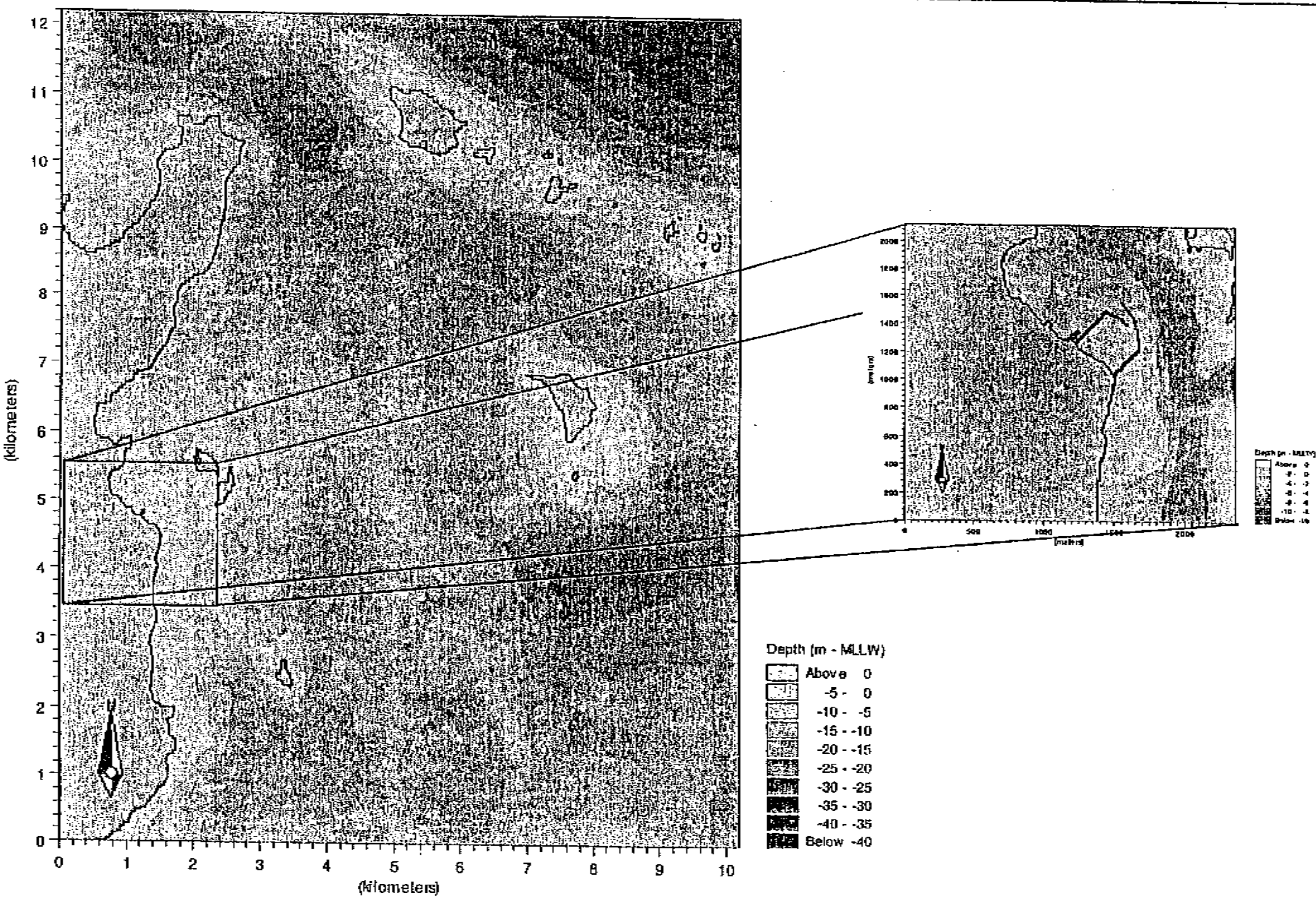


MOFFATT & NICHOL
ENGINEERS

Figure 2.2: Modeled Regions

**Table 2. 1 Sediment Mean Diameter**

| Location | $D_{50}$ |
|---|---|
| 1 | 0.035 mm |
| 2 | 0.105 mm |
| 3 | 0.06 mm |

2.3 Wind

The predominant winds over Puerto Rico are from the east year-round. With the approach of a cold front, the wind shifts to the south then through the southwest and northwest quadrants as the front passes. The stronger winds occur midsummer; spring and autumn typically see lighter winds. Mean wind speeds range from 10 mph (16 kph) to 11 mph (18 kph) in the autumn and from 13 mph (22 kph) to 18 mph (29 kph) in midsummer.

The east wind is the predominant wind direction in the area year-round fluctuating from 4.5 mph (7.2 kph) to 31 mph (50 kph) in the summer. Northeast winds are less frequent during the summer but increase to near the frequency of the east winds in the winter months. The north and southeast winds are more prevalent during the winter months than the summer months. While the north and northwest winds are absent in the summer, they are relatively strong in the winter.

2.3 Tides and Water Levels

The Caribbean coast of Puerto Rico experiences tides classified as mixed diurnal with a small semi-diurnal component resulting in two high and two low tides per day. The tidal current moves south during the flood tide and north during the ebb tide. The maximum (spring) tide occurs during the new moon and summer solstice. The astronomical tidal range fluctuates between 1.6 foot (0.5 meters) Mean Higher High Water (MHHW) and 0.0 feet (0.0 meters) Mean Lower Low Water (MLLW).

The offshore wave data used for this study were records obtained from USACE Wave Information Study (WIS) Puerto Rico station number a1003 located at Latitude 19.0° N and Longitude 65° W. The WIS station is located in approximately 3,000 meters of water. The records include spectrally based significant wave heights, periods, and frequency of occurrence by direction, on a monthly basis covering a hindcast period from 1956 to 1975. The results are verified, where possible, by comparison to National Oceanographic and Atmospheric (NOAA) buoys and wave gages.

The WIS Station information was grouped by the frequency of occurrence of wave height, period, and direction. The wave data was then reviewed to determine the applicability of each of the event groups to the site. Twenty-two wave cases, which represent the relevant wave conditions at the site across three 45-degree bins (predominant wave directions) of WIS data, were selected for analysis.

Table 3.1 presents the initial offshore WIS wave parameters (height, $H_s$, period, $T_p$, and direction of wave approach). The percent occurrence is the weighted amount of the total time associated with each of the wave cases on an annual basis.

**Table 3. 1 Deep Water Wave Transformations**

| Wave Case | Wave Direction | Significant Wave Height, $H_s$ (m) | Peak Wave Period, $T_p$ (s) | Percent Occurrence (%) |
|---|---|---|---|---|
| 1 | N | 1.5 | 8 | 2.7 |
| 2 | N | 1.5 | 10 | 6.2 |
| 3 | N | 1.5 | 12 | 2.3 |
| 4 | N | 1.5 | 14 | 1.0 |
| 5 | N | 2.5 | 10 | 2.7 |
| 6 | N | 2.5 | 12 | 3.3 |
| 7 | N | 2.5 | 14 | 1.2 |
| 8 | N | 3.5 | 14 | 1.0 |
| 9 | NE | 1.5 | 6 | 1.5 |
| 10 | NE | 1.5 | 8 | 8.8 |
| 11 | NE | 1.5 | 10 | 5.4 |
| 12 | NE | 1.5 | 12 | 2.1 |
| 13 | NE | 2.5 | 8 | 1.5 |
| 14 | NE | 2.5 | 10 | 2.3 |
| 15 | NE | 2.5 | 12 | 1.1 |
| 16 | NE | 2.5 | 14 | 1.6 |
| 17 | E | 1.5 | 6 | 16.7 |
| 18 | E | 1.5 | 8 | 20.4 |
| 19 | E | 1.5 | 10 | 5.0 |
| 20 | E | 2.5 | 8 | 4.8 |
| 21 | E | 2.5 | 10 | 2.0 |
| 22 | E | 2.5 | 12 | 0.4 |
| 23 | Assumed calm (no waves) – tidal currents only | | | 6.0 |

These 22 wave cases represent the input wave conditions for the numerical modeling analysis. The wave events were applied a constant surface elevation equal to 0.24 meters (Mean Tide Level) for all wave cases.

The numerical modeling package used for this analysis was the MIKE series developed and maintained by the Danish Hydraulic Institute (DHI). The three MIKE21 modules used in this study were the Nearshore Spectral Wind-Wave Module, the Hydrodynamics Module, and the Sediment Transport Module.

## 4.1 MIKE21 Overview

MIKE21 is a two-dimensional finite difference model system. One of the model's unique features is the fact that wave-induced currents can be solved for and included in hydrodynamic, water quality, and sediment transport solutions

## 4.2 Finite Difference Grids

The models within MIKE21 require that the beach system be represented by a grid of nodal points defined by coordinates in the horizontal plane and water depth. The two most important aspects in the definition of a finite difference grid are: (1) determining the level of detail (grid spacing in X and Y between adjacent nodes) necessary to adequately represent the region to be modeled and (2) determining the extent or coverage of the grid. The level of detail required for the grid can be forced by the complexity of the bathymetry or the spacing required for the solution stability of different models.

There are several factors that influence the spatial extent of the grid. First, it is desirable to extend the grid to areas which are sufficiently distant from the proposed areas of change so as to be unaffected by that change. Second, the outer regions of the grid must be located along boundaries where conditions can be reasonably described to a computer model. Two model grids were used in the wave transformation analysis. A grid modeling the offshore region having a 10 meter grid spacing in cross shore direction (X direction) and a 40 meter grid spacing in the longshore direction (Y direction) was used to model a 10 kilometer by 12 kilometer region. A more refined grid of 1 meter by 4 meter grid spacing extending approximately 2,000 meters along shore and 1,750 meters offshore to the nearest island was used for analysis of the nearshore region around the proposed breakwater site as illustrated in Figure 4.1. For each of the 22 wave cases, the offshore wave conditions were input at the

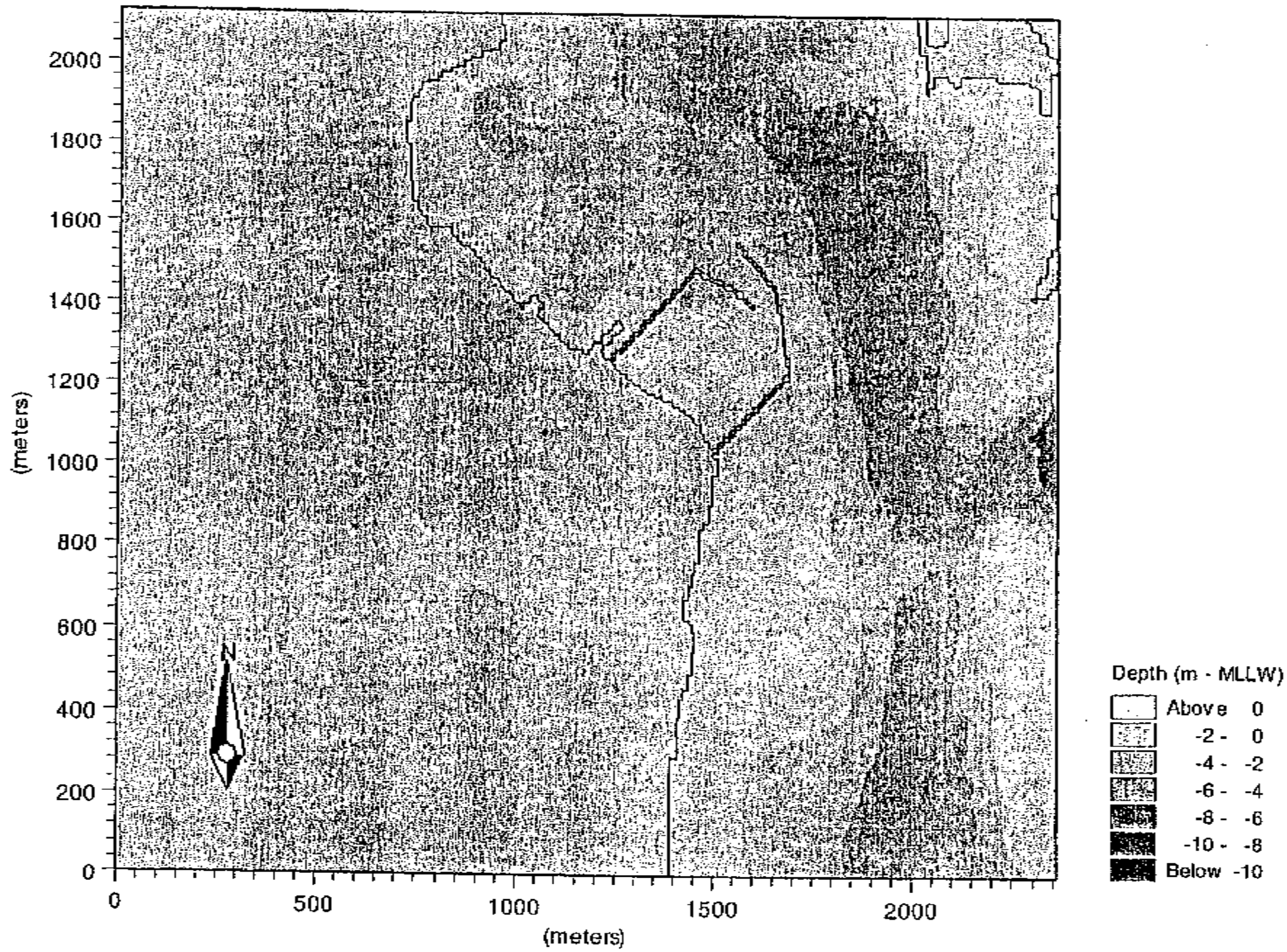


MOFFATT & NICHOL
ENGINEERS

Figure 4.1: Model Site Bathymetry with Proposed Breakwater

boundary of the larger offshore grid and the wave transformations calculated. Calculated wave conditions from the larger grid model were used as the input wave conditions for the smaller nearshore model area. The nearshore model was run for all wave conditions under existing conditions and then again with the proposed breakwater included (44 total model runs). In this manner, the sheltering from the waves due to the northeast chain of islands was accounted for by the larger model grid, and the transformation of the waves by the nearshore bathymetry and the addition of the breakwater was analyzed using the higher resolution nearshore grid.

## 4.3 Modeling Approach

Offshore wave data was transformed to the proposed marina site. The transformed wave climate and tides were then used to calculate the local currents, which together with the waves produce sediment motion. Finally, the potential sedimentation rates were computed, and the differences in deposition between the modeled existing conditions and the modeled conditions with the proposed breakwater were assessed in the existing shipping areas. The overall approach used is summarized in Figure 4.2.

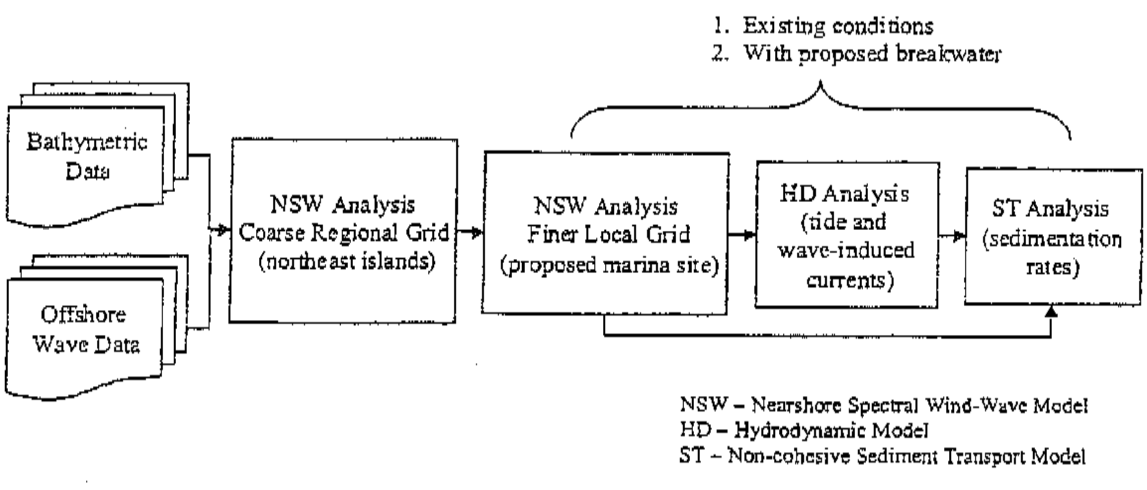


Figure 4.2 Modeling Approach Used.

"The Near-shore Spectral Wind-Wave Model (MIKE21 NSW) describes the propagation, growth, and decay of short-period and short-crested waves in nearshore areas. The model takes into account the effects of refraction and shoaling with regards to varying depth, local wind generation, and energy dissipation due to bottom friction and wave breaking. The model also takes into account the effect of wave-current interaction.

The basic output from the model is integral wave parameters such as the significant wave height, the mean wave period, the mean wave direction, the directional standard deviation, and the radiation stresses. In addition, spectral output data in the form of the distribution of wave energy with direction at a number of user-selected points can also be obtained." (Danish Hydraulic Institute, MIKE21 Nearshore Spectral Wind-Wave Module - User Guide and Reference Manual).

The wave conditions presented in Table 3.1 were applied to the NSW model. A constant water level of 0.24 meters, corresponding to the mean tidal level, was used for the wave transformation model. Local winds were approximated using a uniform wind speed based on the offshore wave height. The wind speed was calculated using the methods outlined in the Shore Protection Manual (US Army Corps of Engineers, 1984) and are given in Table 5.1. The wind was applied to the model in the same direction as the corresponding offshore waves.

**Table 5.1 Applied Wind Speeds**

| Wave Height (m) | Wind Speed (m/s) |
|---|---|
| 1.5 | 7 |
| 2.5 | 8.5 |
| 3.5 | 10 |

The output of the NSW model consists of various parameters. The computed wave height and period at each node was reported as well as the wave radiation stresses, which were later used by the hydrodynamic module to account for wave-induced currents.

Figures 5.1 to 5.66 illustrate the wave transformation for the offshore area and the nearshore region with and without the proposed breakwater. The arrows in the figures indicate the mean direction of the wave travel and the colored contours the wave heights. Figures 5.1 through 5.14 illustrate the offshore wave cases from the east and northeast and Figures 5.15 through 5.22 the wave cases from the north. The figures clearly show the sheltering provided by the islands and the considerable reduction of the offshore wave heights prior to arriving at the study site. Figures 5.23 to 5.44 show the wave cases under existing conditions at the proposed marina site while Figures 5.45 to 5.66 show the same wave cases with the proposed breakwater. Relatively little difference can be seen in the overall wave heights and patterns between the two.

## 5.1 Wave Discussion

As expected, the results show greater wave heights seaward of the chain of northeast islands with much lower wave heights to the lee of the islands. The islands shelter the site greatly reducing the wave energy transmitted to the nearshore region. The island nearer to the shore provides still further protection from offshore waves. As can be seen from the model results, the marina site is sheltered from waves by land to the north and islands to the east and northeast, which are the main wave directions. The islands and bathymetric features reduce the wave heights thereby limiting the wave energy at the proposed marina site.

The proposed breakwaters appear to have minimal effect on the surrounding wave climate outside of its confines. It typically results in wave height reductions of less than 5 cm (compared to existing conditions) within its shadow zone of a couple hundred meters. Figure 5.67 illustrates this effect for the most frequent wave case (offshore waves from the east with a wave height of 1.5 m and a period of 8 s).

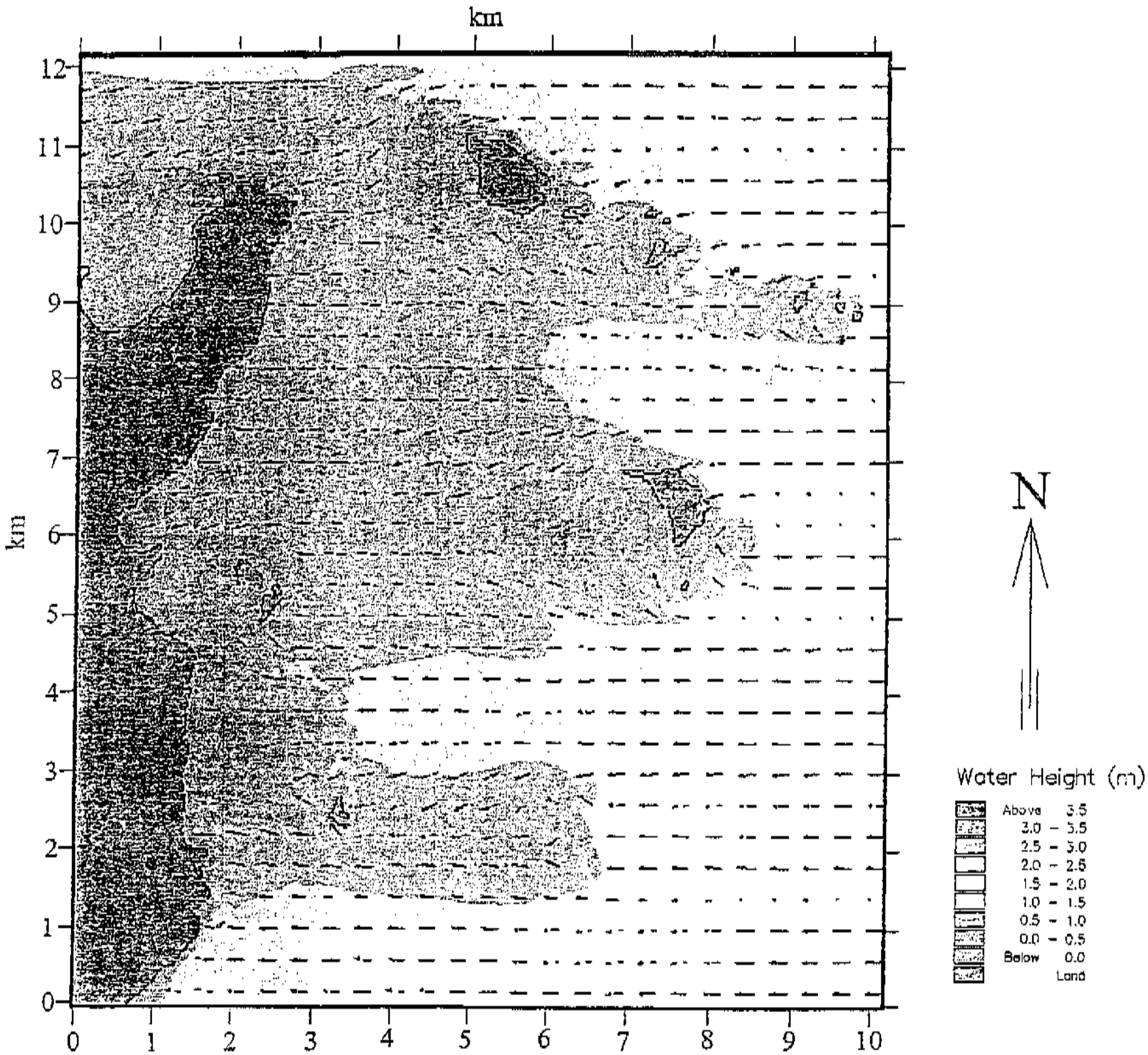


MOFFATT & NICHOL
ENGINEERS

Figure 5.1:
NSW Results
1.5 m East Wave - 6 Sec

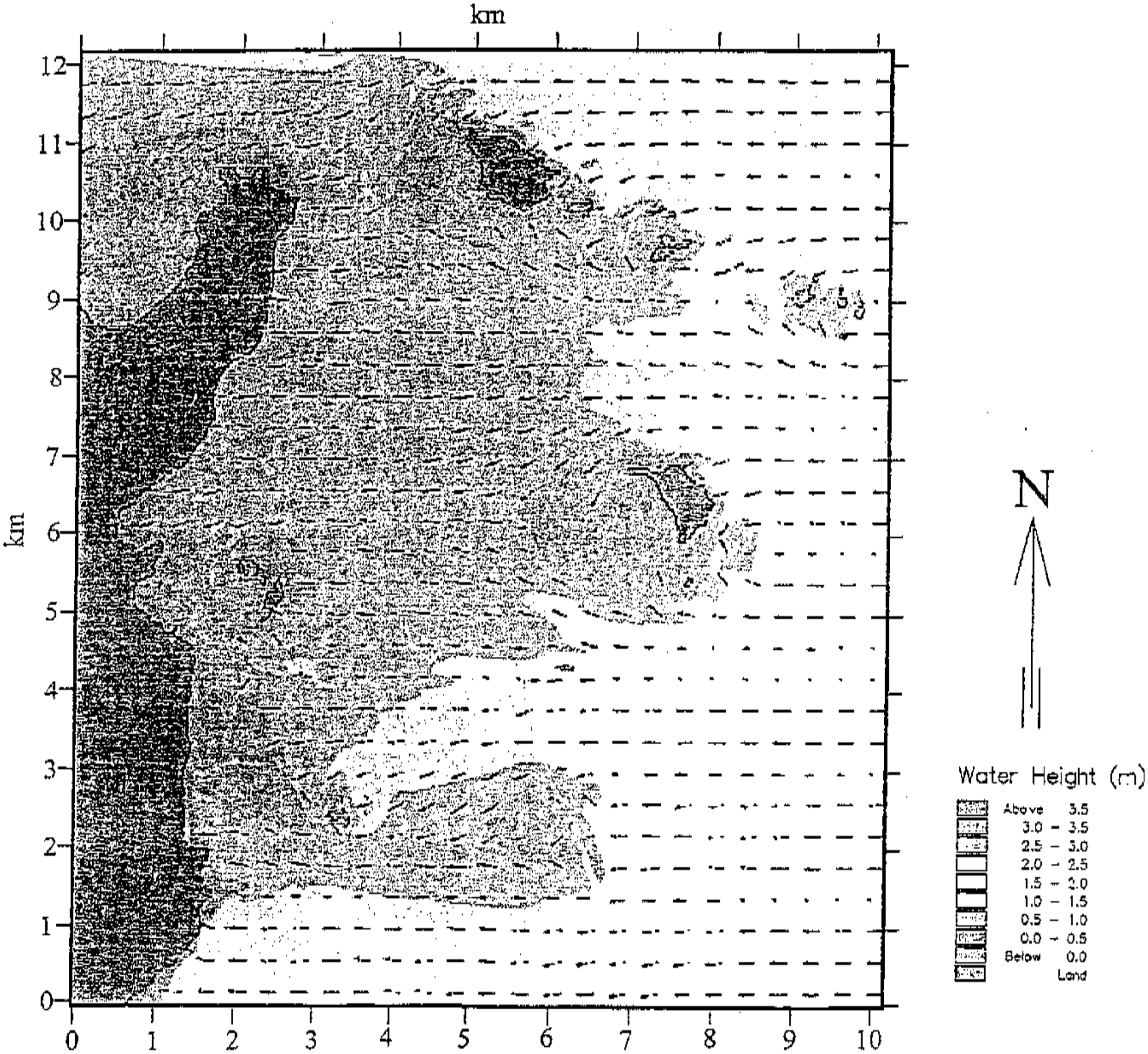


MOFFATT & NICHOL
ENGINEERS

Figure 5.2:
NSW Results
1.5 m East Wave - 8 Sec

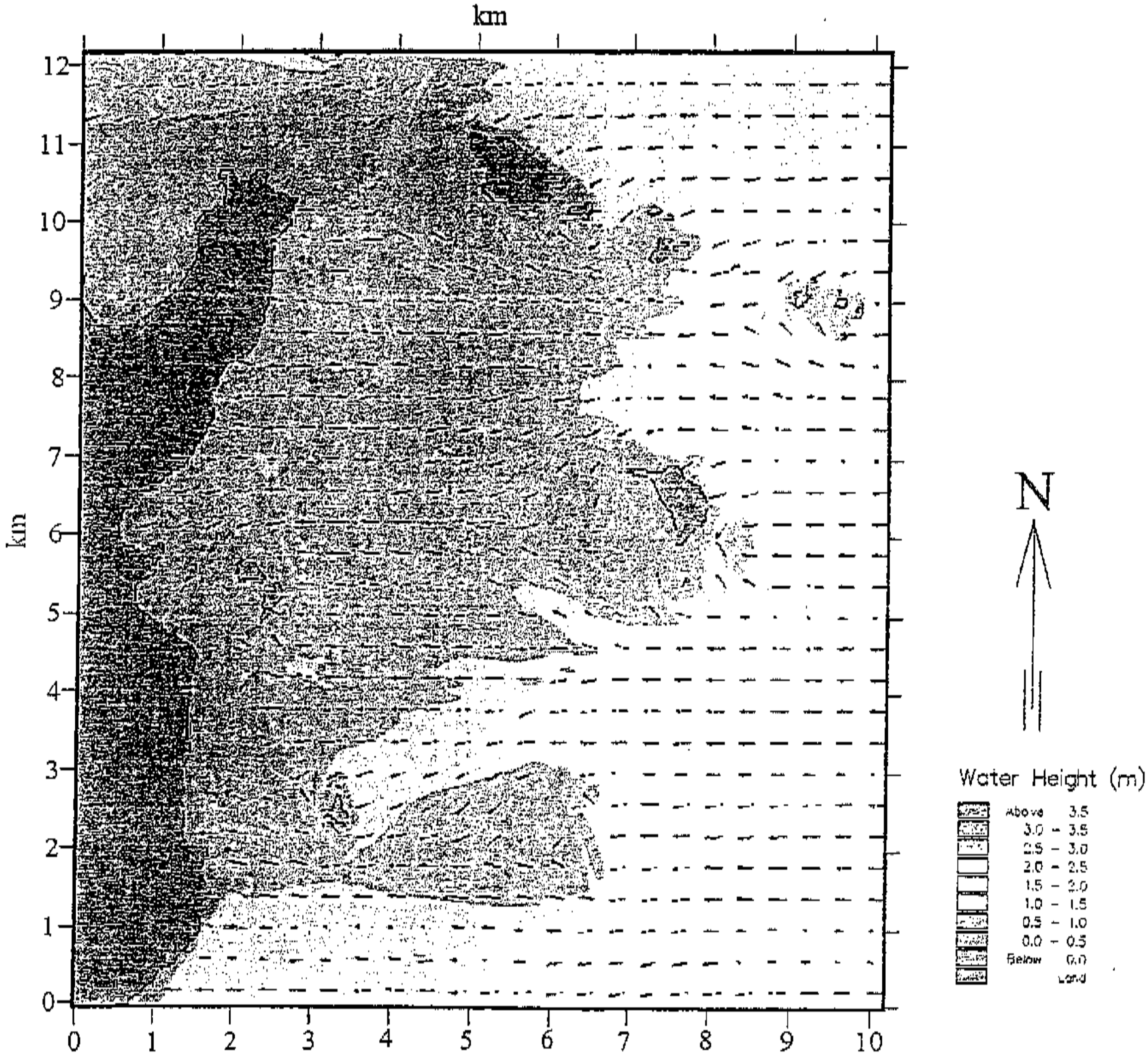


MOFFATT & NICHOL ENGINEERS

Figure 5.3:
NSW Results
1.5 m East Wave - 10 Sec

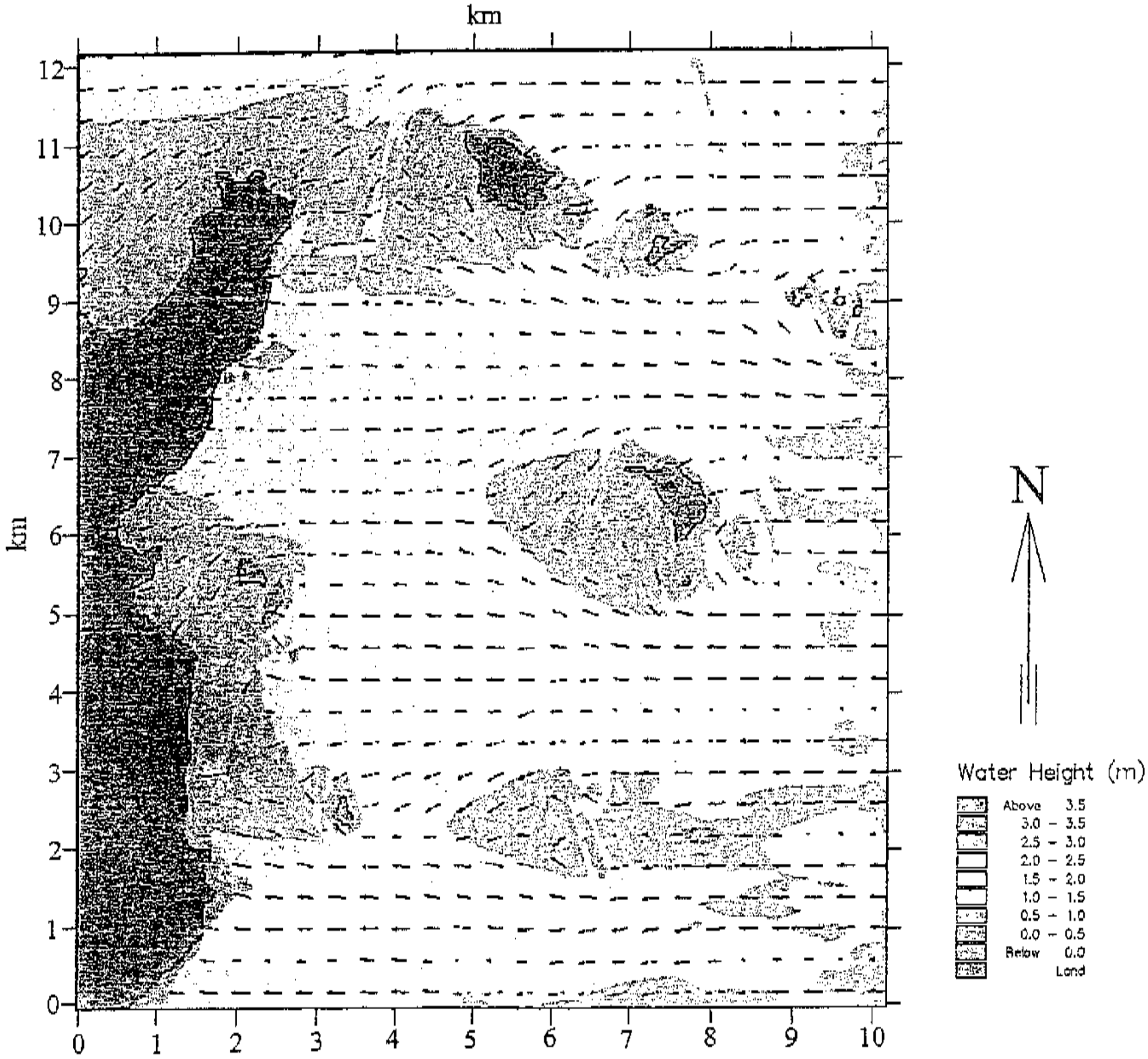


MOFFATT & NICHOL
E N G I N E E R S

Figure 5.4:
NSW Results
2.5 m East Wave - 8 Sec

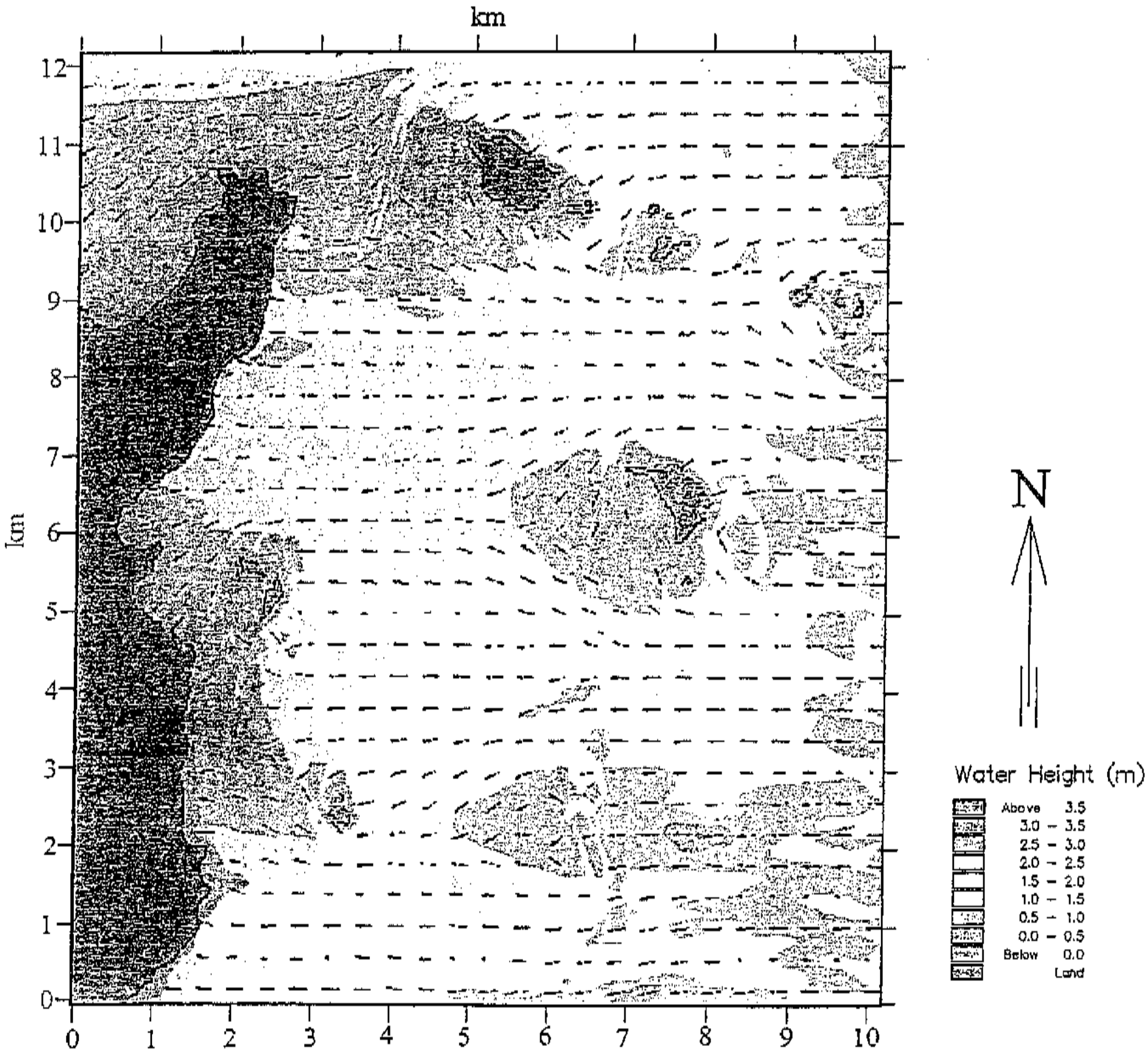


MOFFATT & NICHOL
E N G I N E E R S

Figure 5.5:
NSW Results
2.5 m East Wave - 10 Sec

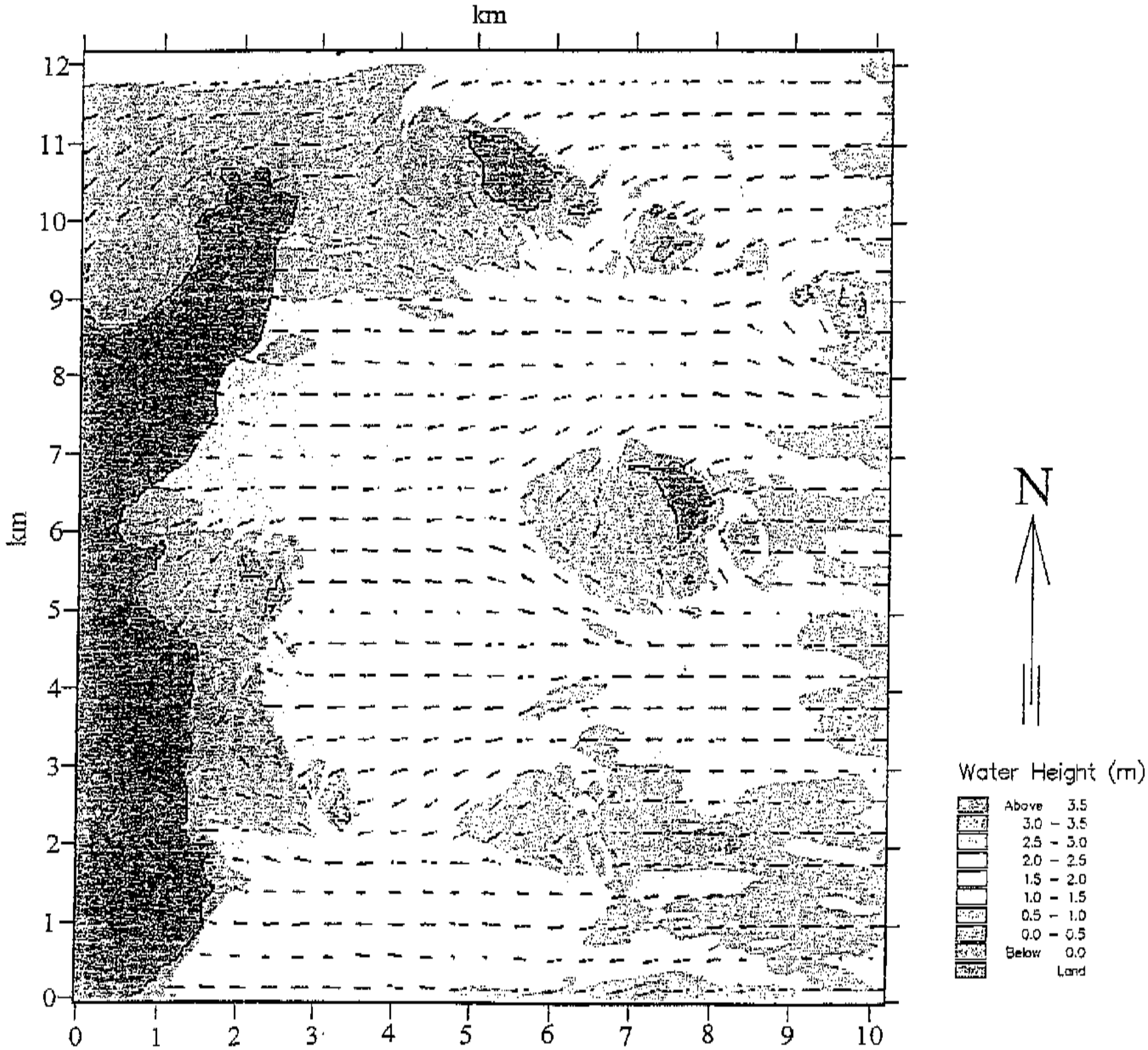


MOFFATT & NICHOL ENGINEERS

Figure 5.6:
NSW Results
2.5 m East Wave - 12 Sec

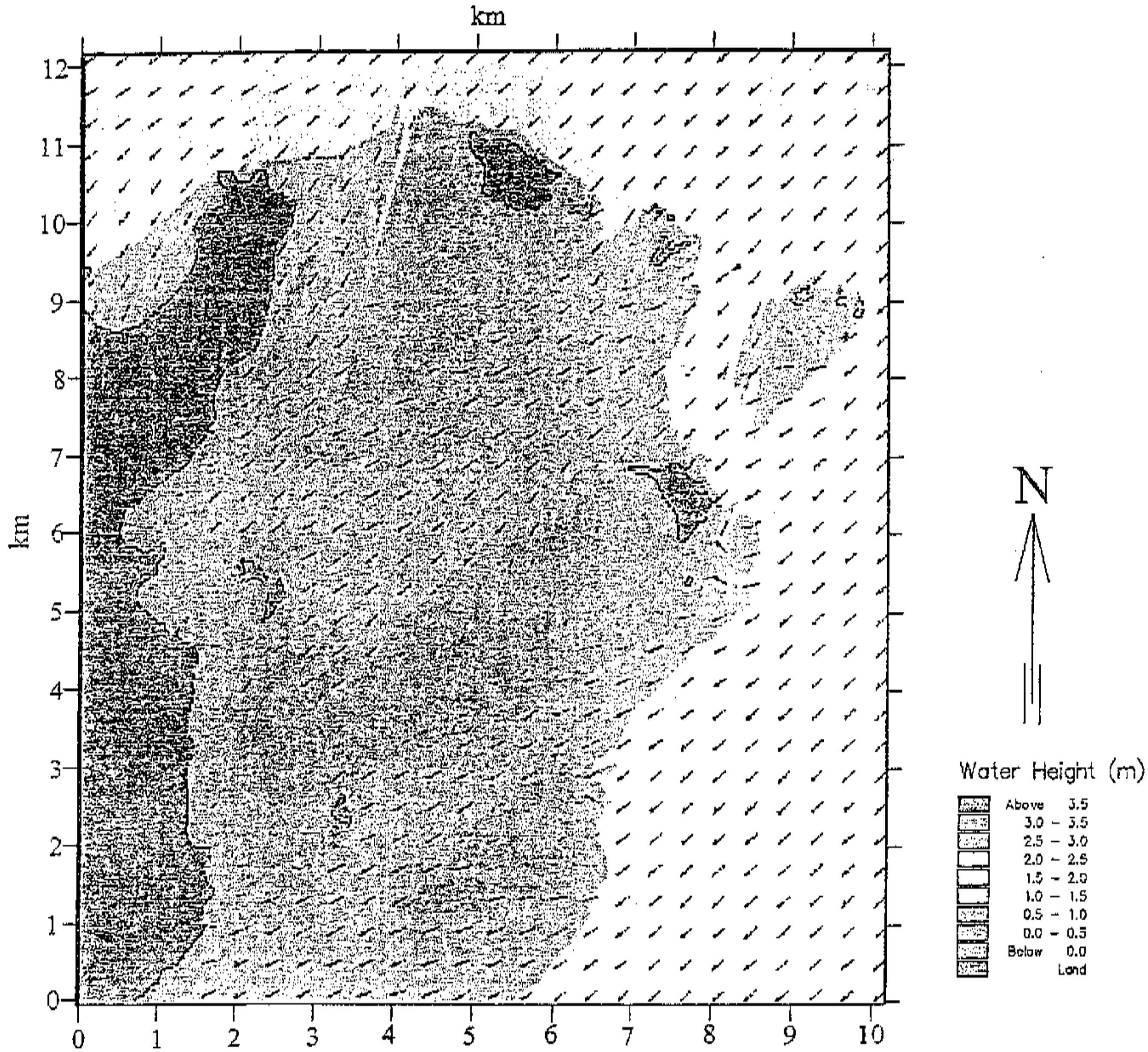


MOFFATT & NICHOL
ENGINEERS

Figure 5.7:
NSW Results
1.5 m NE Wave - 6 Sec

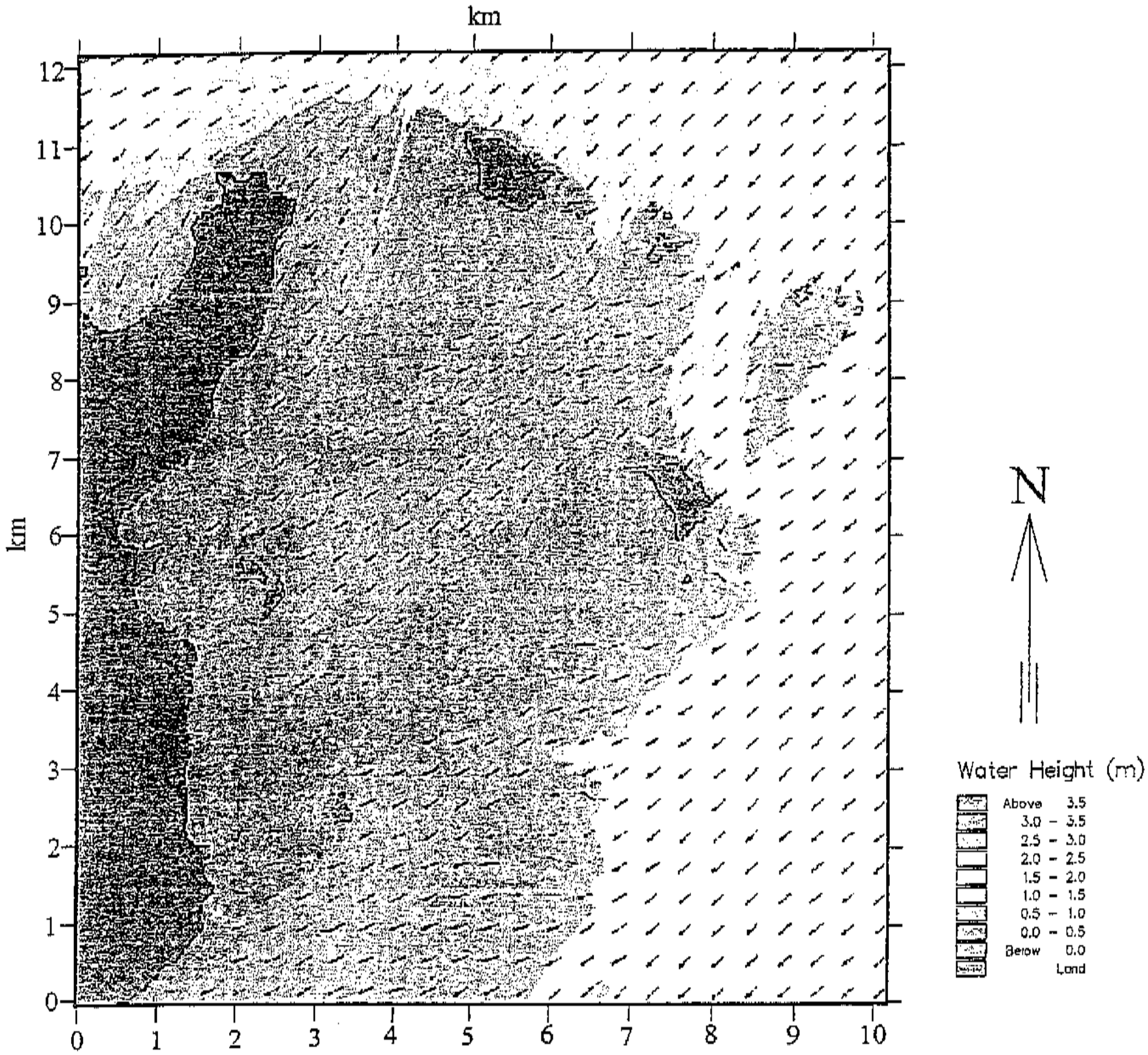


MOFFATT & NICHOL
ENGINEERS

Figure 5.8:
NSW Results
1.5 m NE Wave - 8 Sec

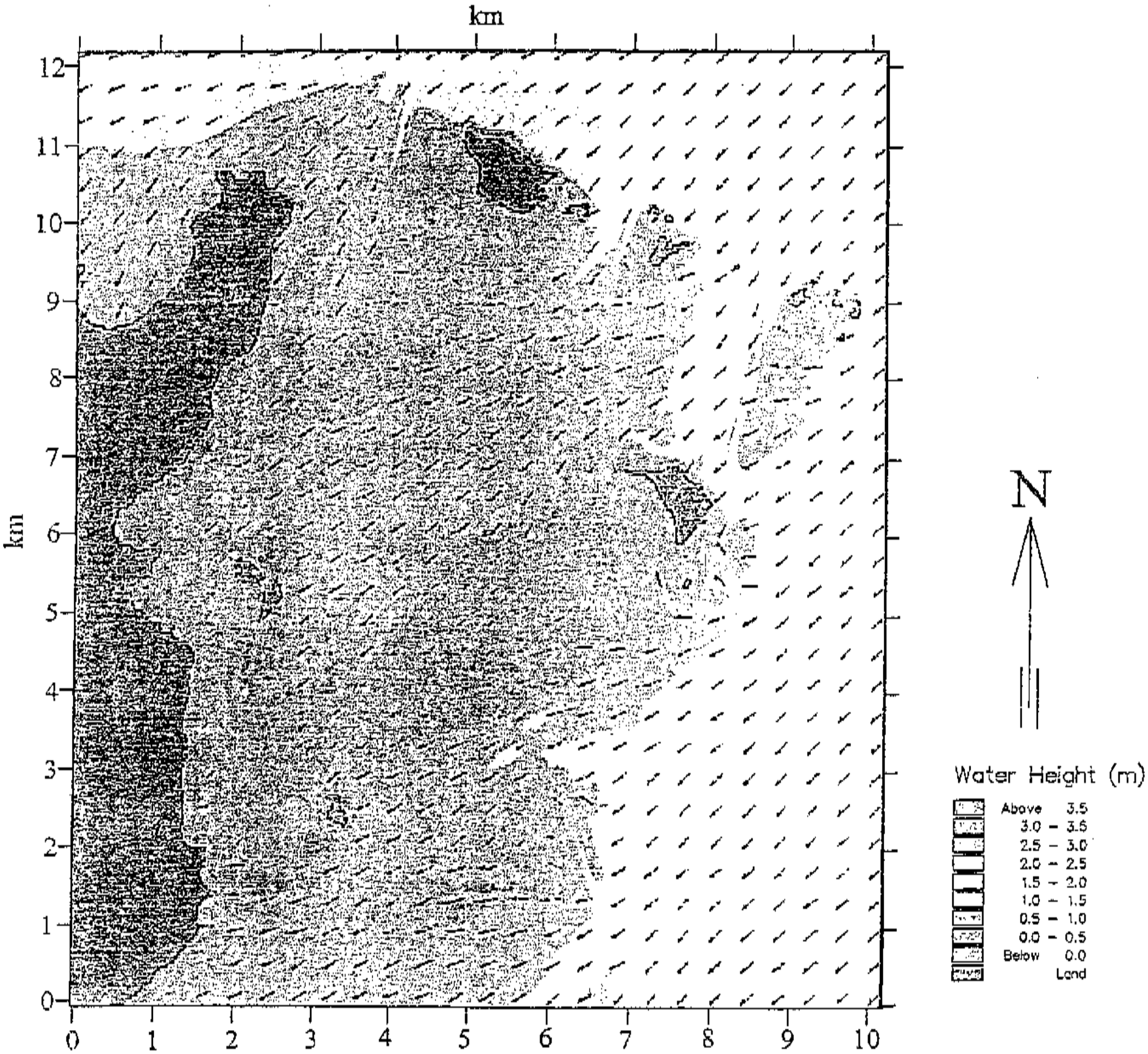


MOFFATT & NICHOL ENGINEERS

Figure 5.9:
NSW Results
1.5 m NE Wave - 10 Sec

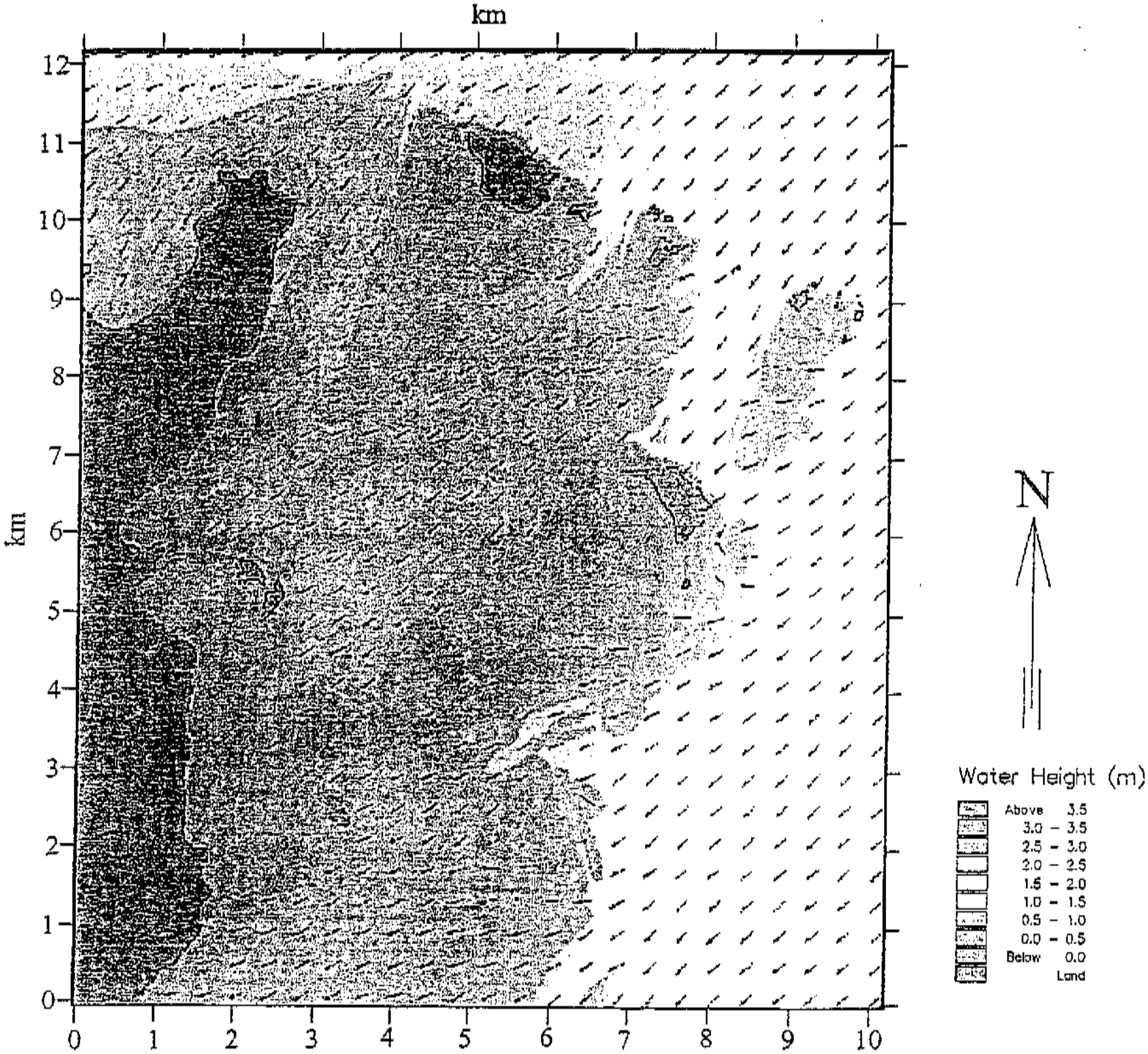


MOFFATT & NICHOL
E N G I N E E R S

Figure 5.10:
NSW Results
1.5 m NE Wave - 12 Sec

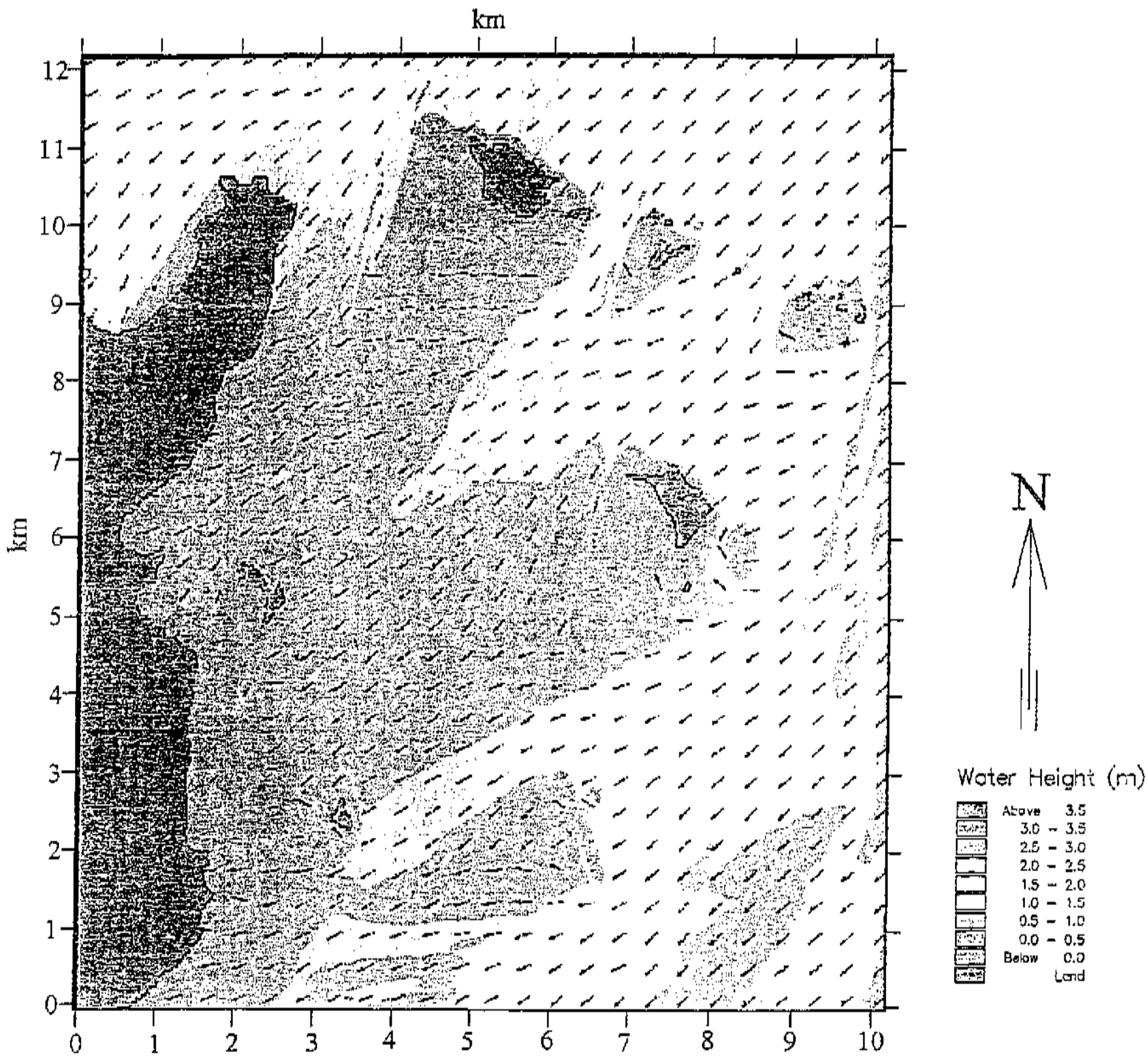


MOFFATT & NICHOL
E N G I N E E R S

Figure 5.11:
NSW Results
2.5 m NE Wave - 8 Sec

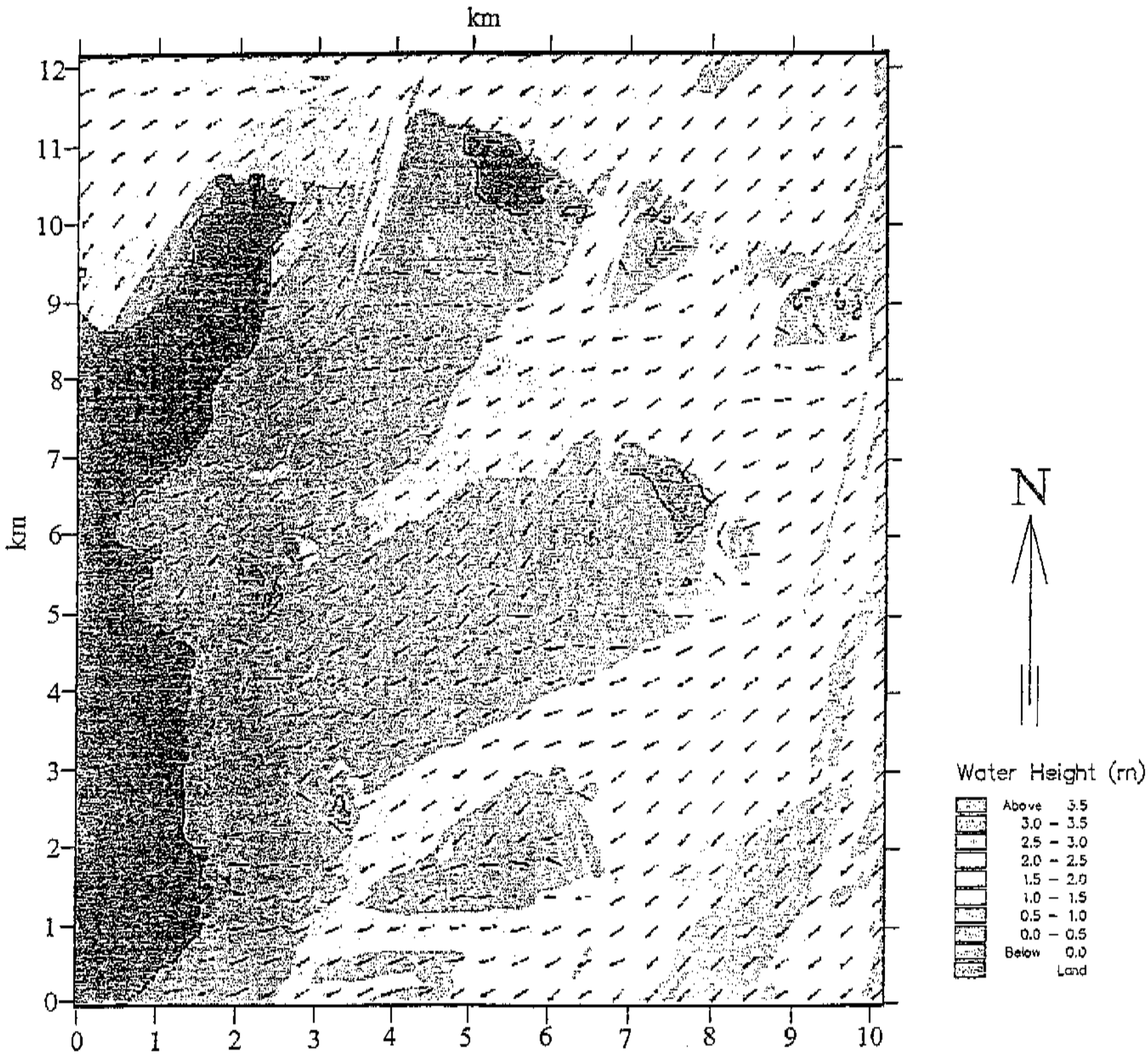


MOFFATT & NICHOL
ENGINEERS

Figure 5.12:
NSW Results
2.5 m NE Wave - 10 Sec

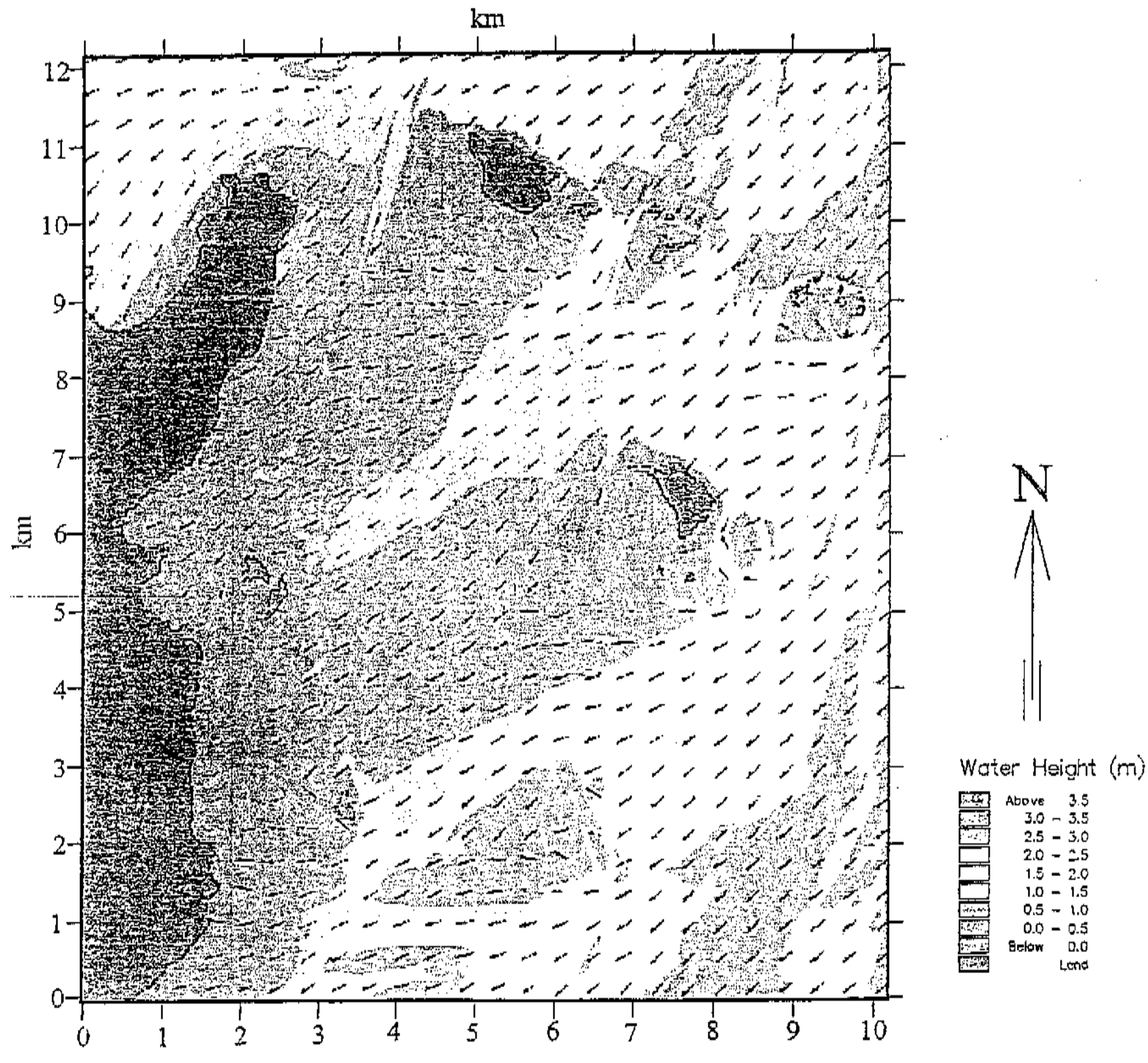


MOFFATT & NICHOL
ENGINEERS

Figure 5.13:
NSW Results
2.5 m NE Wave -12 Sec

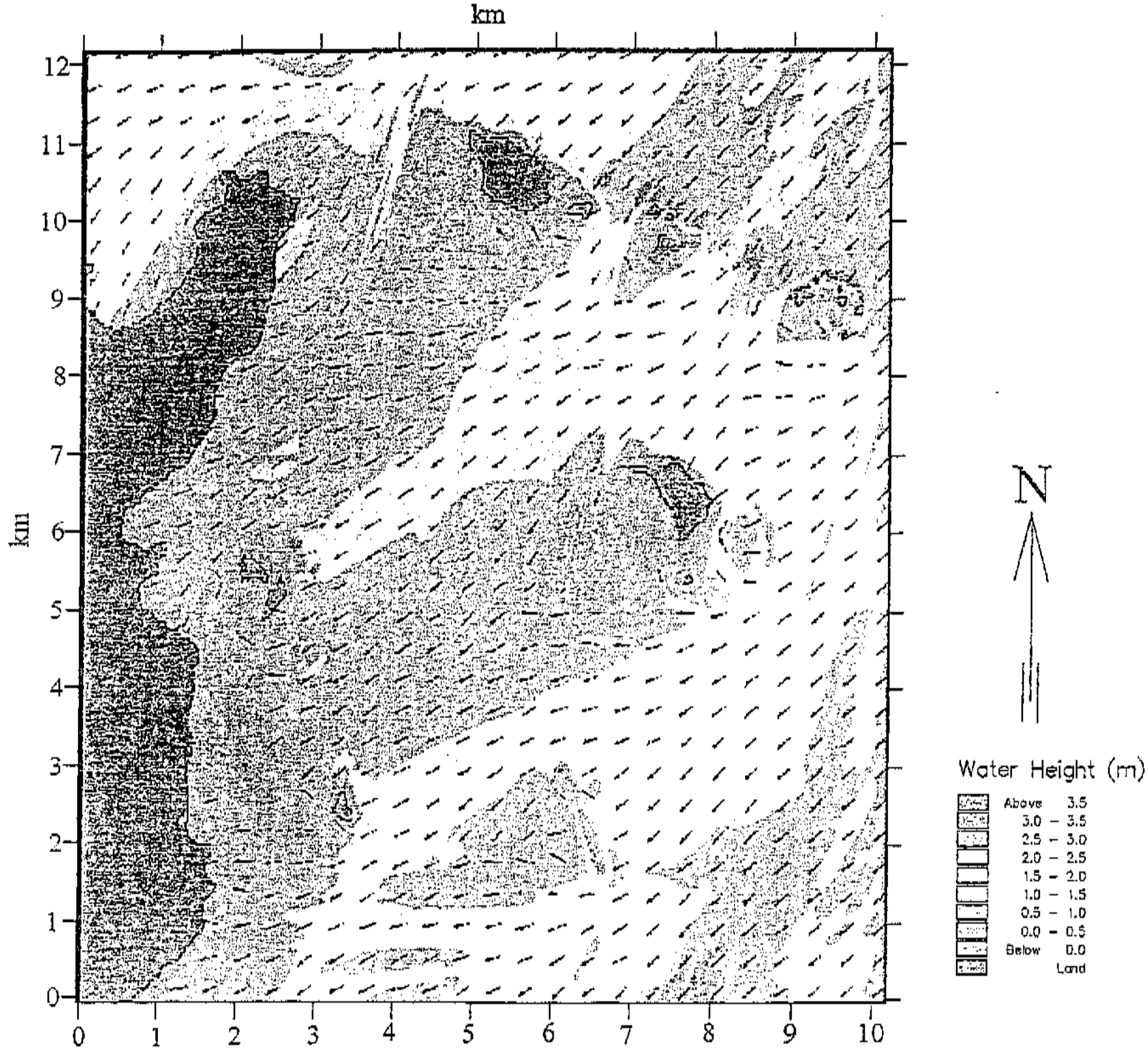


MOFFATT & NICHOL
E N G I N E E R S

Figure 5.14:
NSW Results
1.5 m NE Wave - 14 Sec

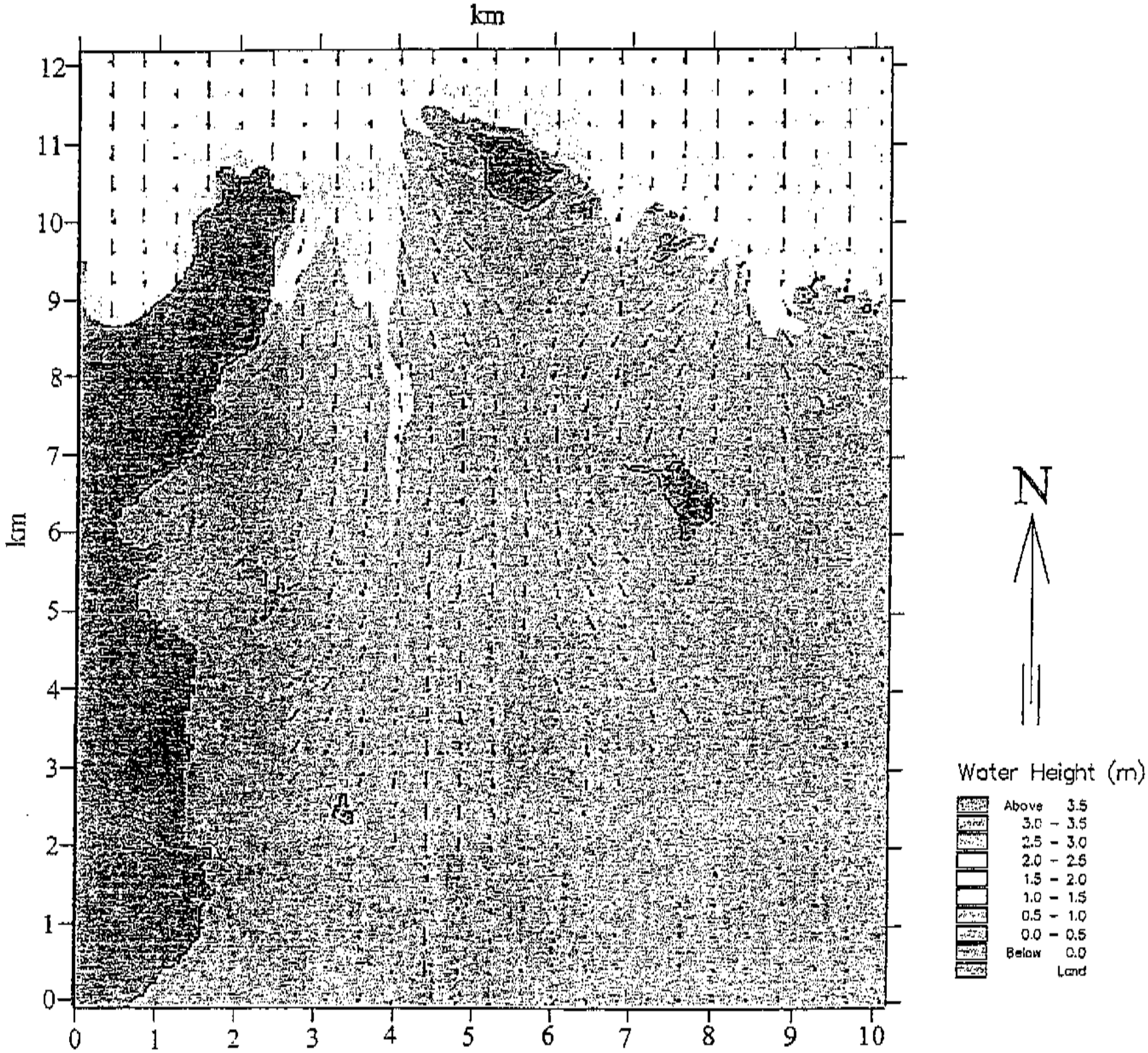


MOFFATT & NICHOL ENGINEERS

Figure 5.15:
NSW Results
1.5 m North Wave - 8 Sec

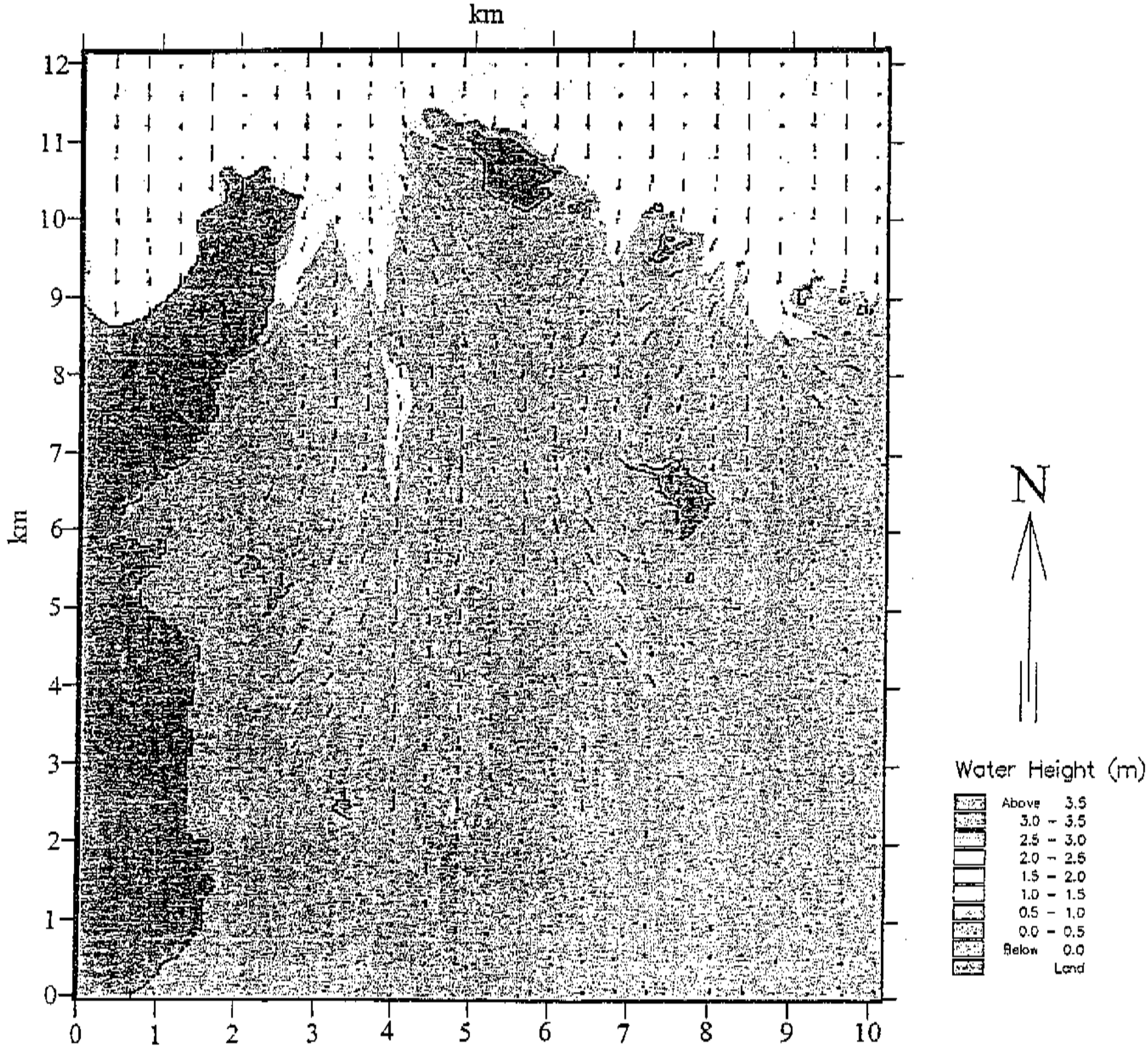


MOFFATT & NICHOL
ENGINEERS

Figure 5.16:
NSW Results
1.5 m North Wave - 10 Sec

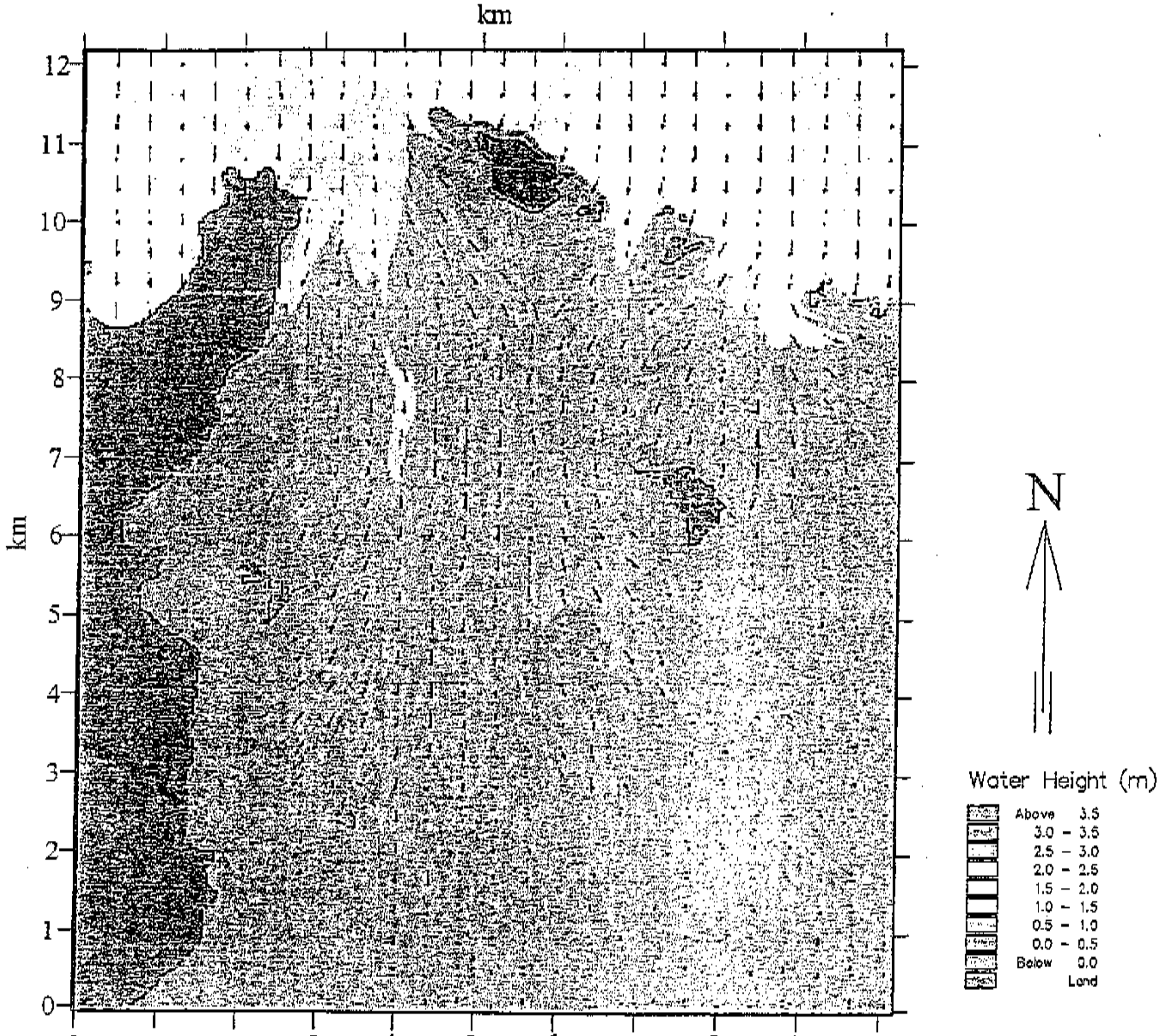


MOFFATT & NICHOL
ENGINEERS

Figure 5.17:
NSW Results
1.5 m North Wave - 12 Sec

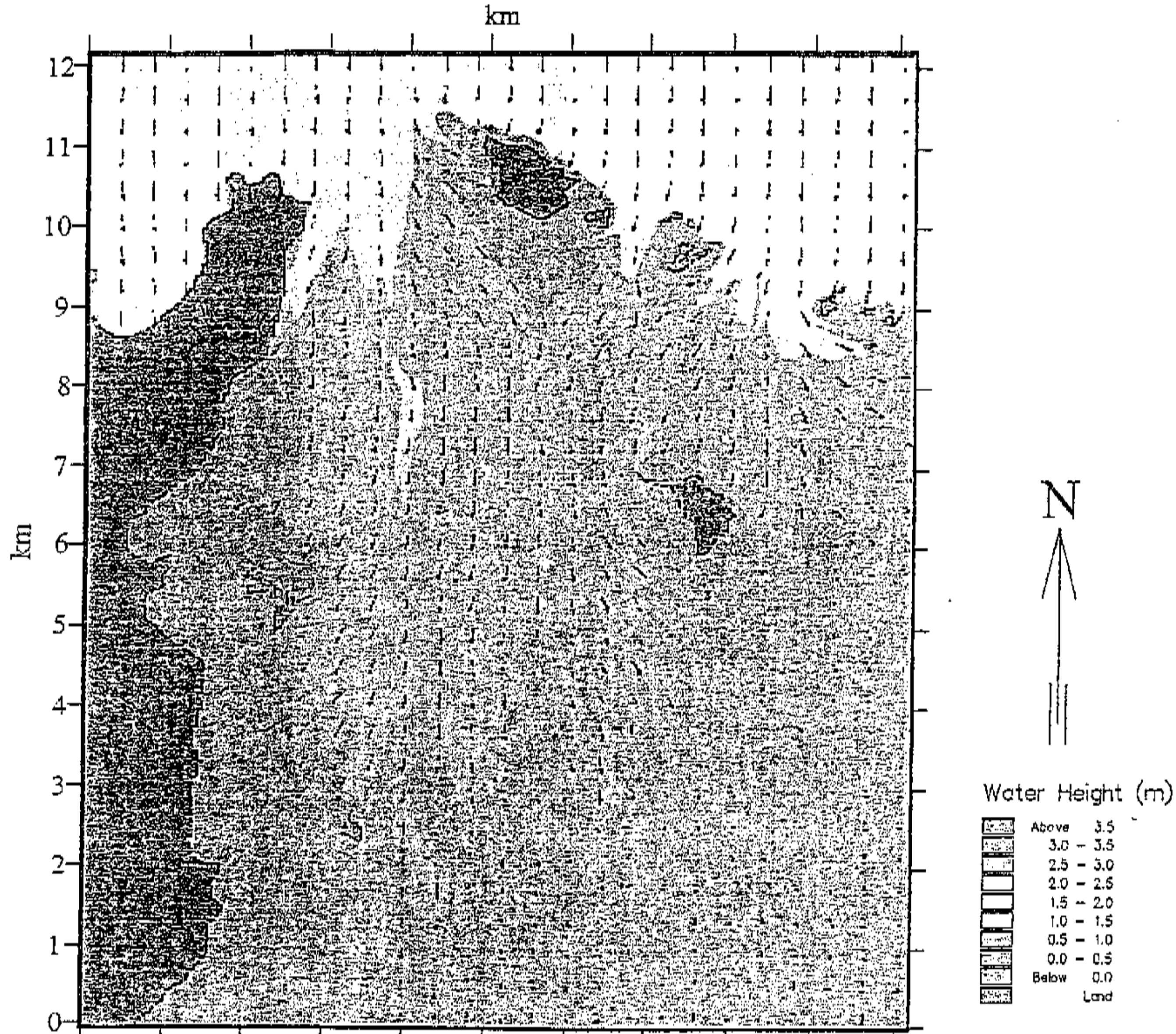


MOFFATT & NICHOL
ENGINEERS

Figure 5.18
NSW Results
1.5 m North Wave - 14 Sec

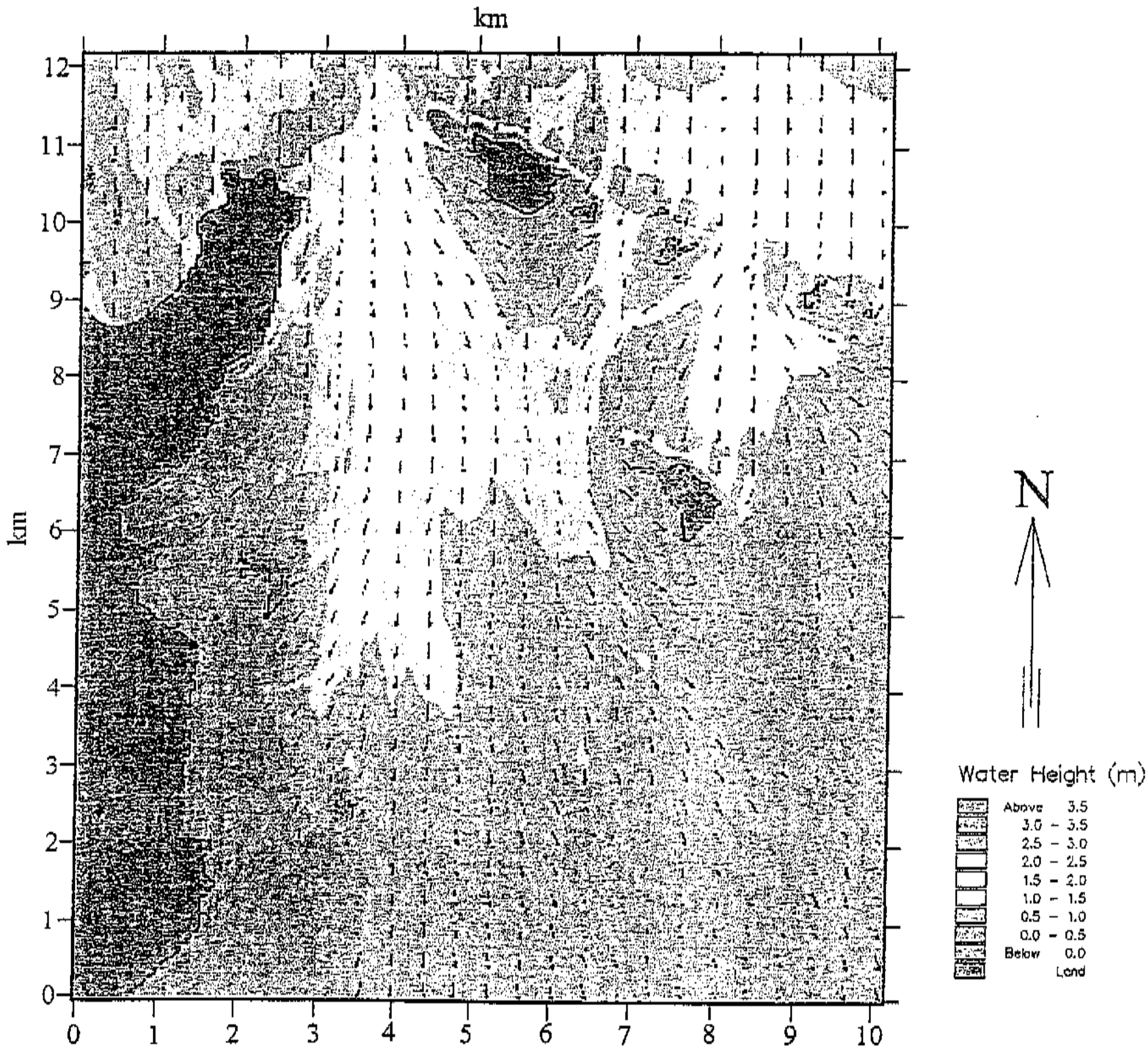


MOFFATT & NICHOL
ENGINEERS

Figure 5.19:
NSW Results
2.5 m North Wave - 10 Sec

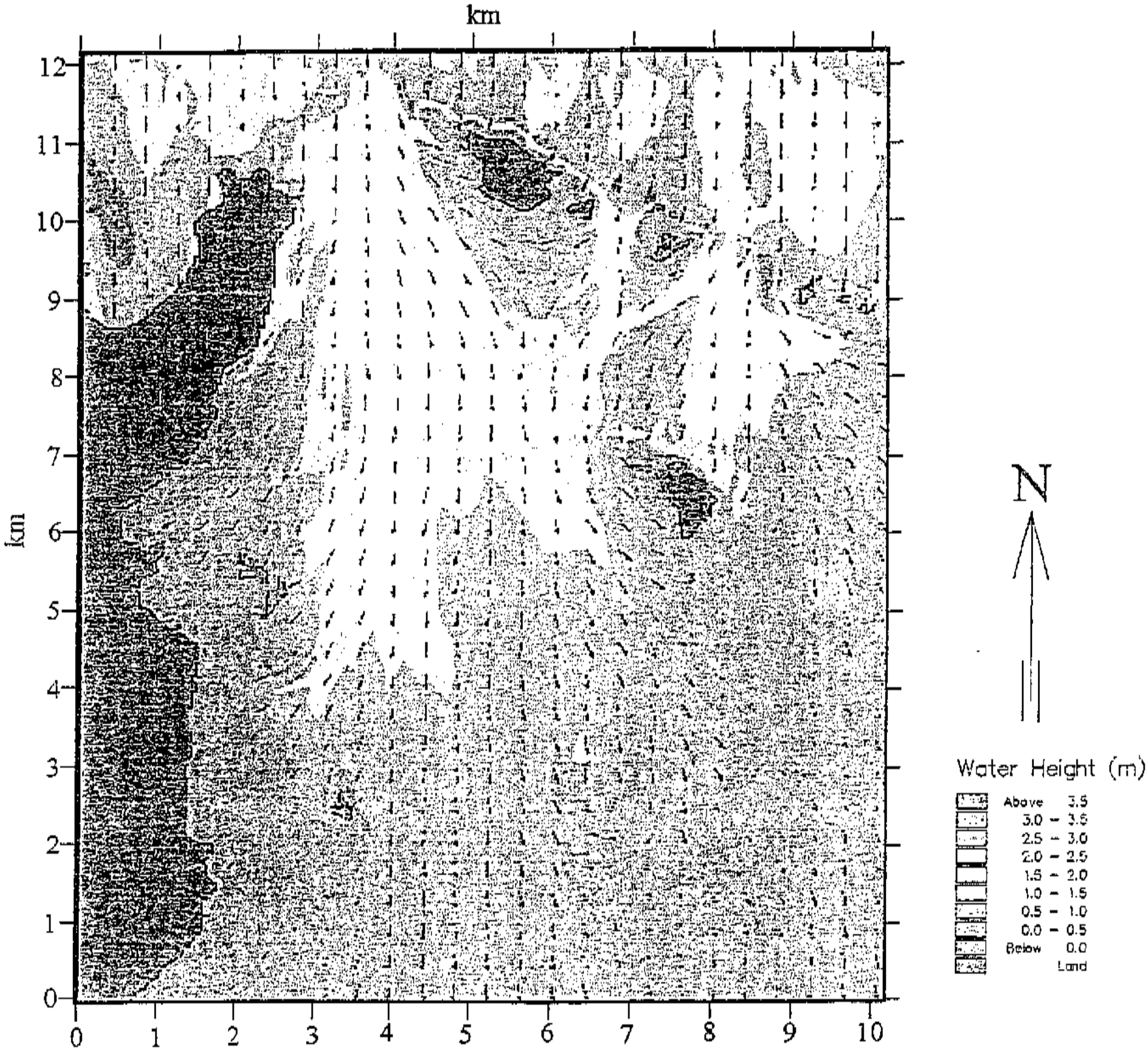


MOFFATT & NICHOL ENGINEERS

Figure 5.20:
NSW Results
2.5 m North Wave - 12 Sec

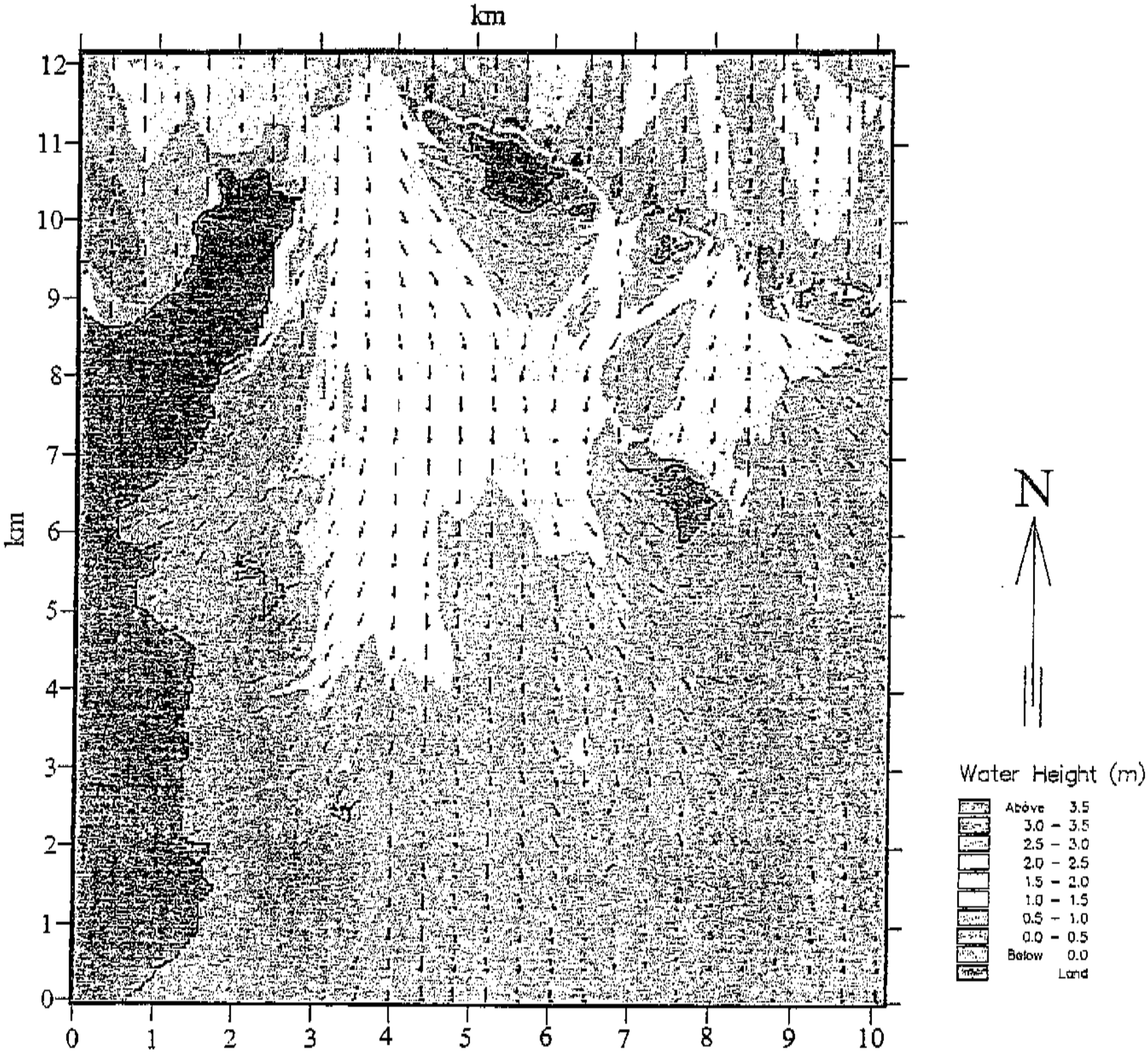


MOFFATT & NICHOL
ENGINEERS

Figure 5.21:
NSW Results
2.5 m North Wave - 14 Sec

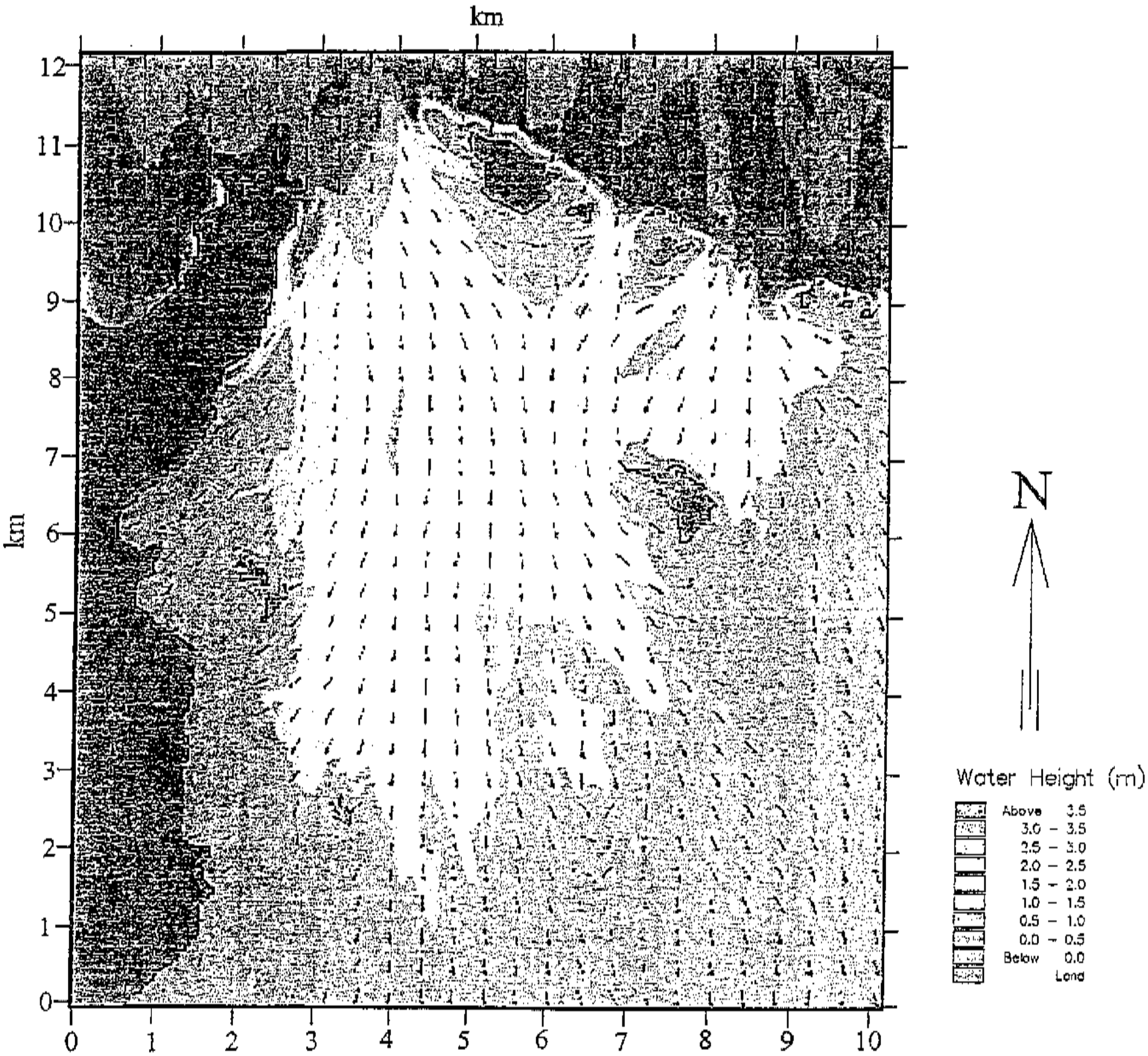


MOFFATT & NICHOL
ENGINEERS

Figure 5.22:
NSW Results
3.5 m North Wave - 14 Sec

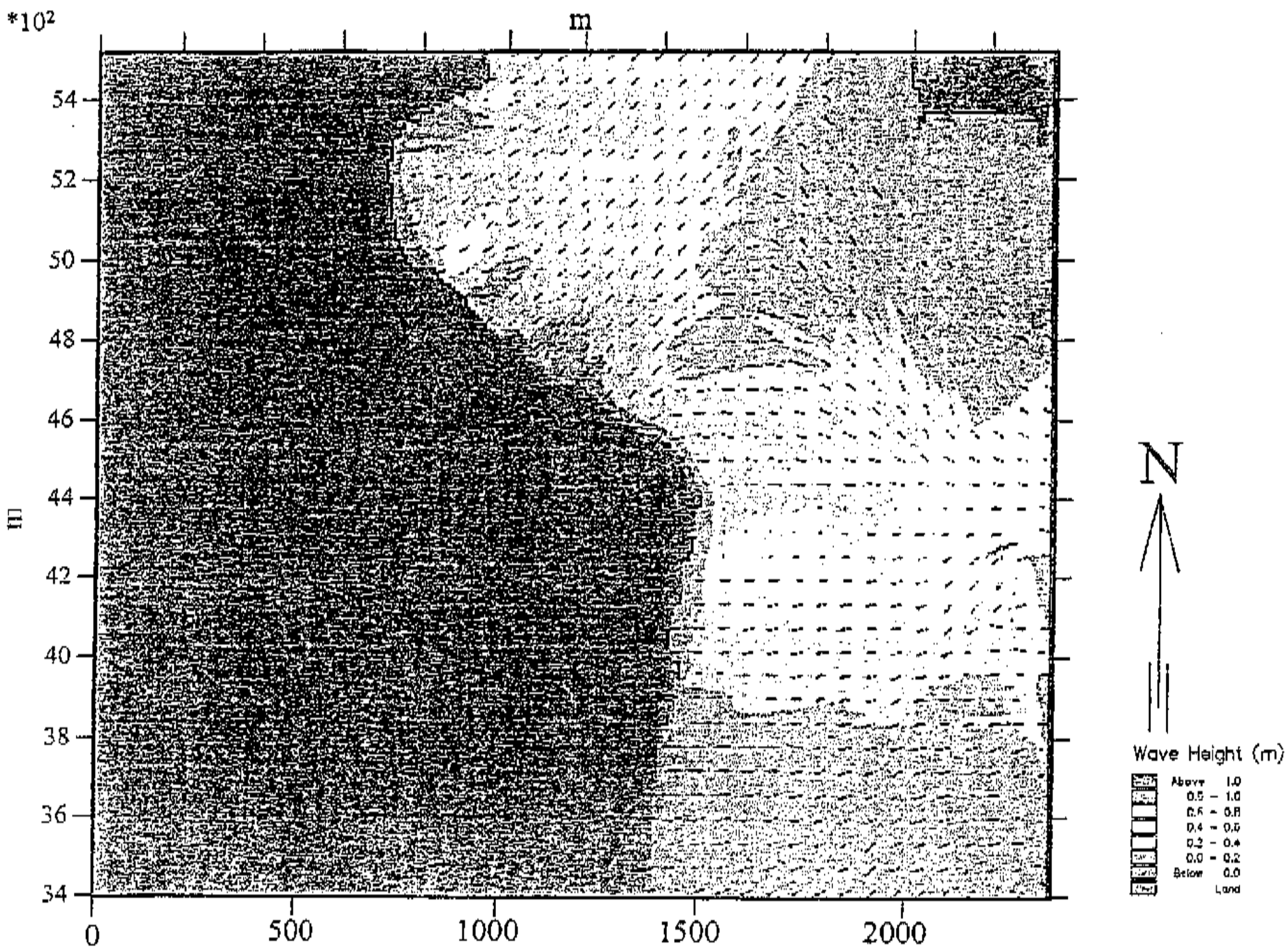


MOFFATT & NICHOL
ENGINEERS

Figure 5.23:
NSW Local Results
1.5 m East Wave - 6 Sec

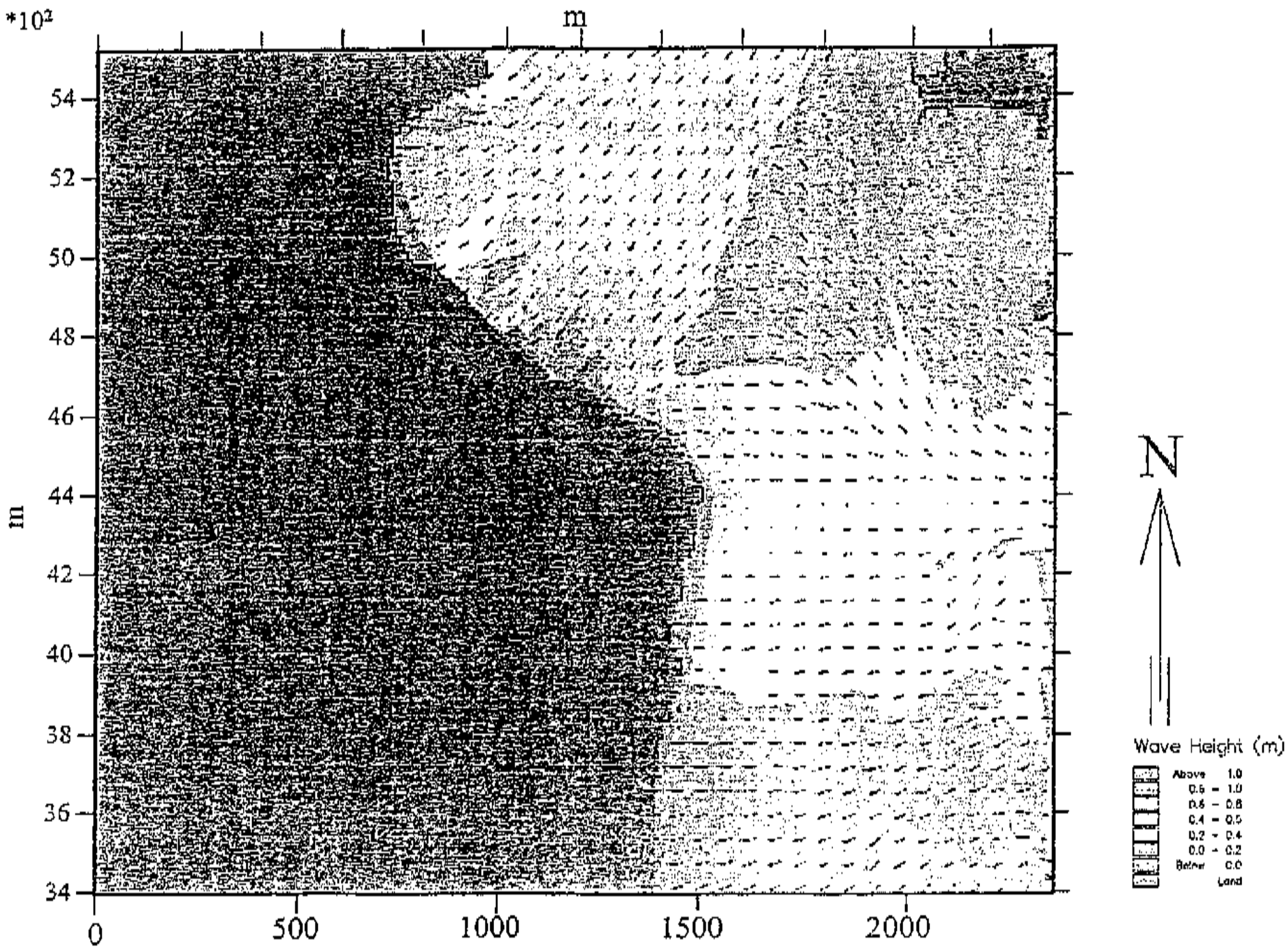


MOFFATT & NICHOL
ENGINEERS

Figure 5.24:
NSW Local Results
1.5 m East Wave - 8 Sec

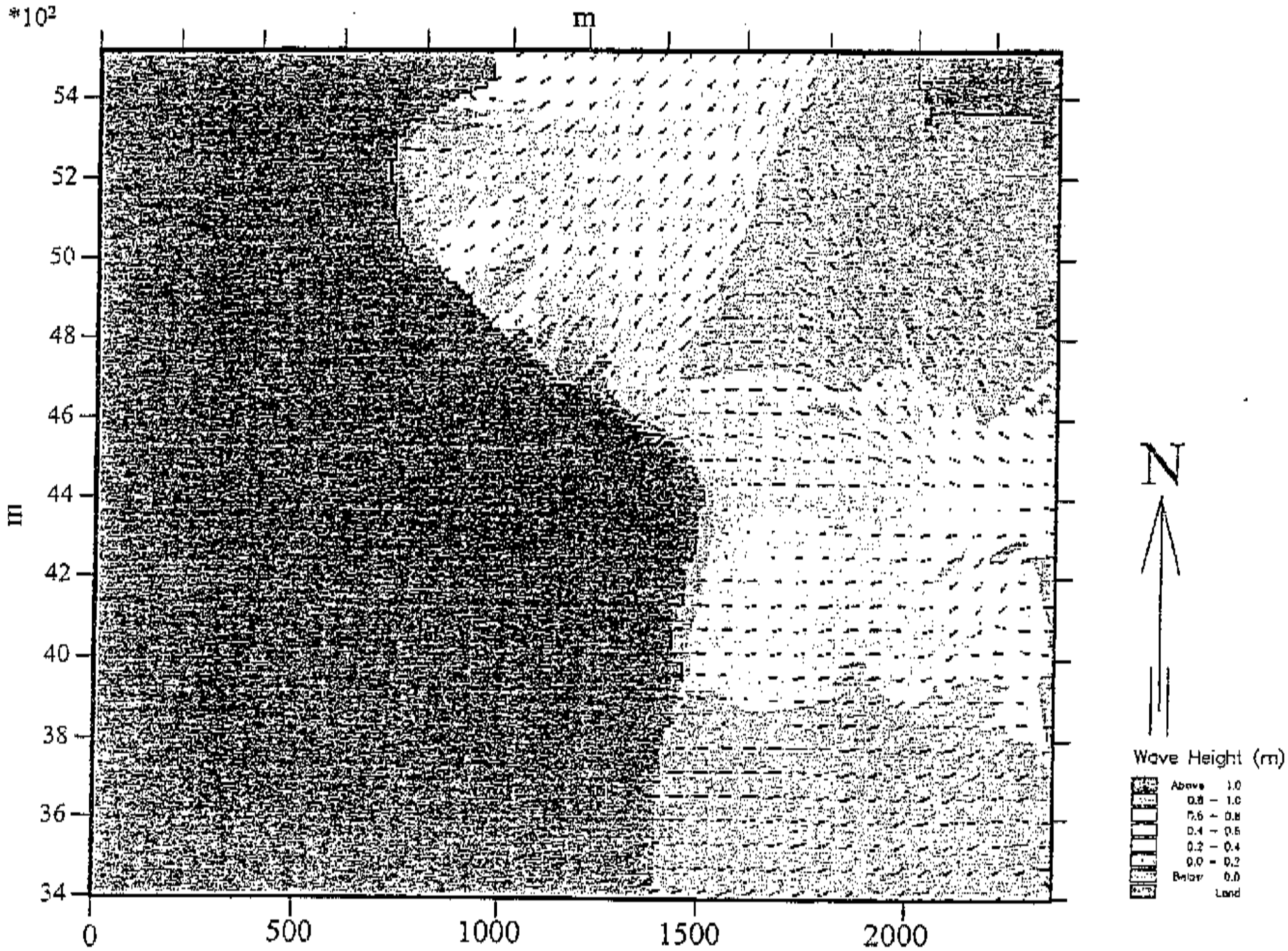


MOFFATT & NICHOL
ENGINEERS

Figure 5.25:
NSW Local Results
1.5 m East Wave - 10 Sec

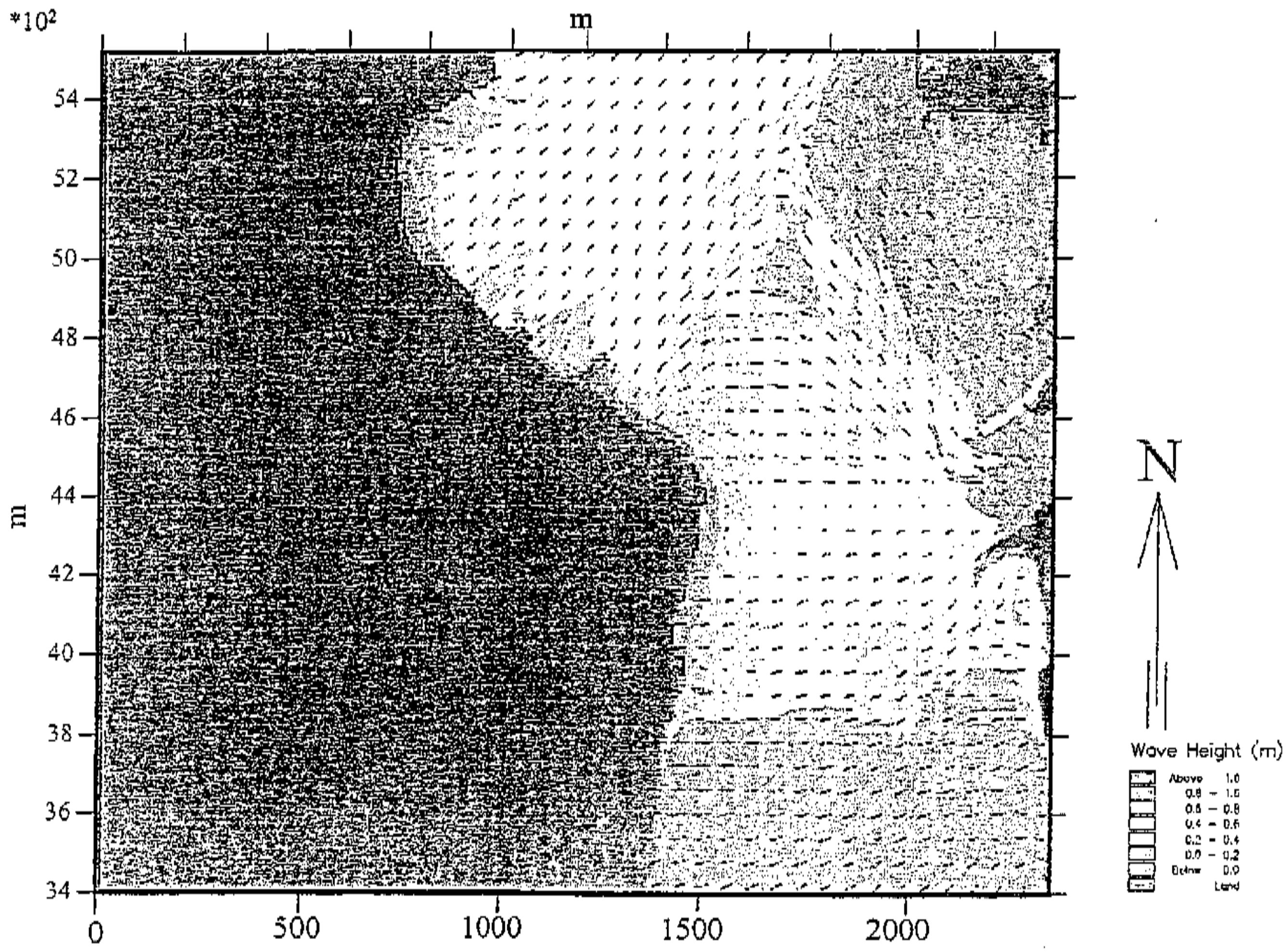


MOFFATT & NICHOL
ENGINEERS

Figure 5.26:
NSW Local Results
2.5 m East Wave - 8 Sec

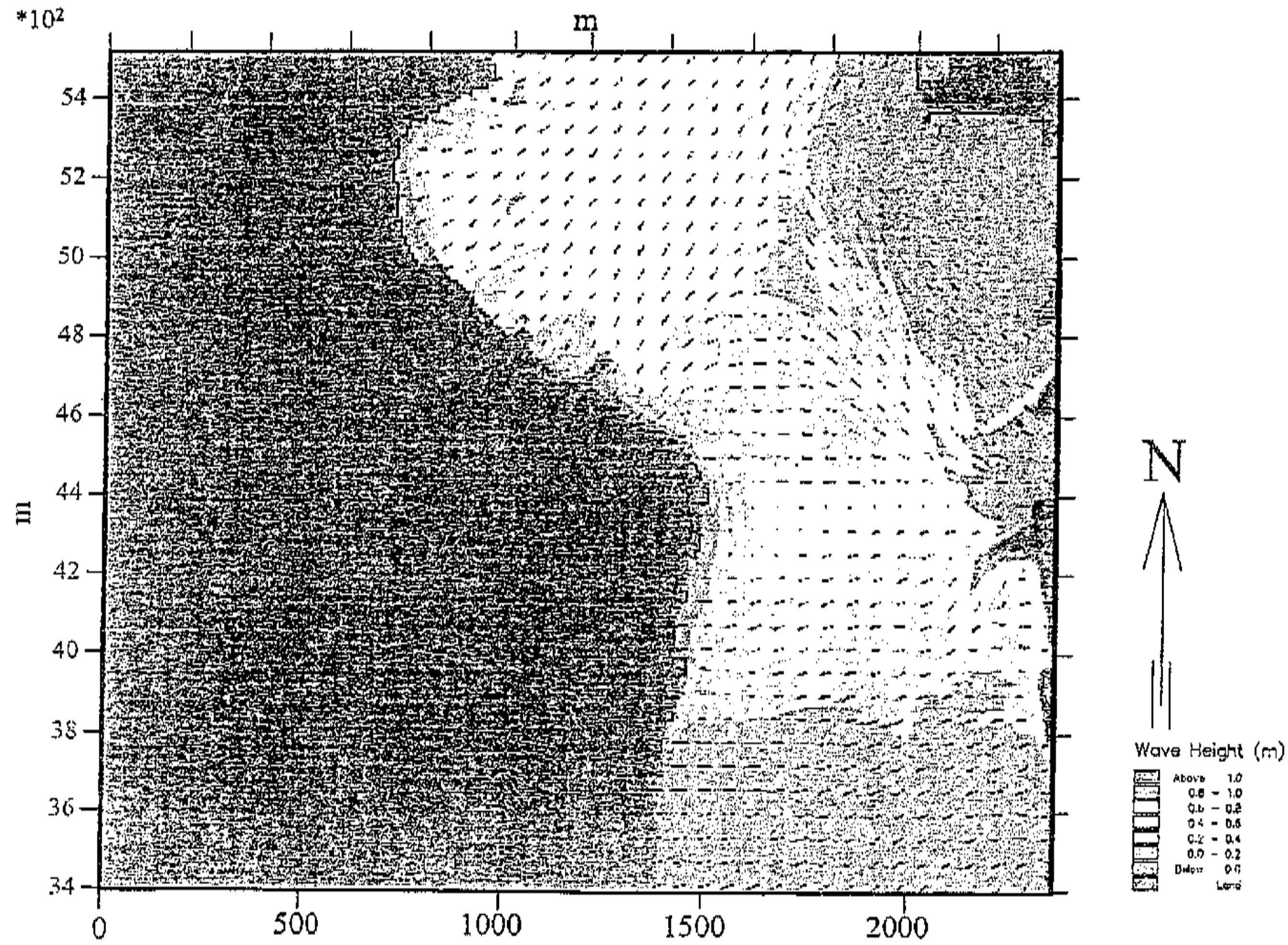


MOFFATT & NICHOL
E N G I N E E R S

Figure 5.27:
NSW Local Results
2.5 m East Wave - 10 Sec

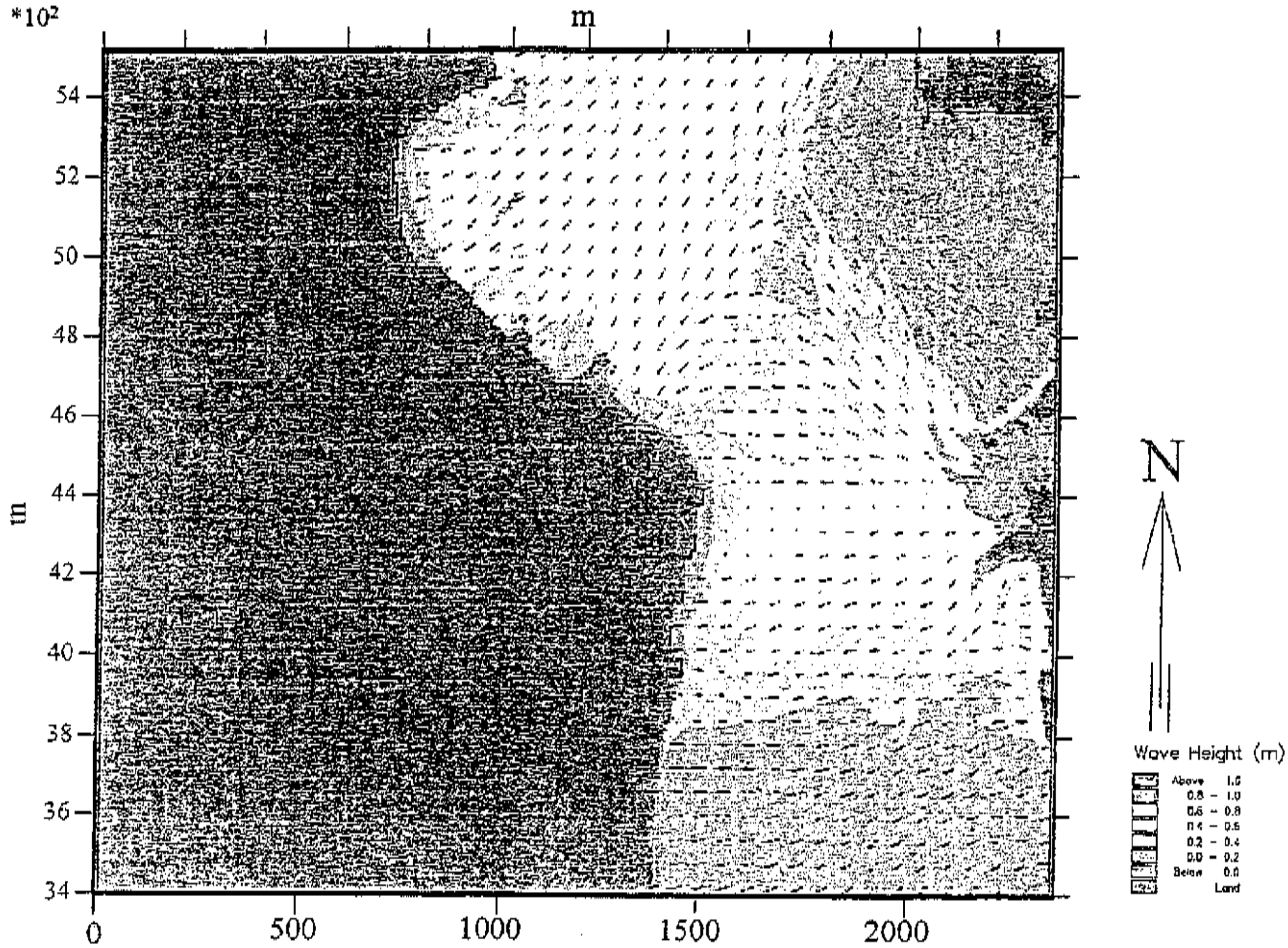


MOFFATT & NICHOL
ENGINEERS

Figure 5.28:
NSW Local Results
2.5 m East Wave - 12 Sec

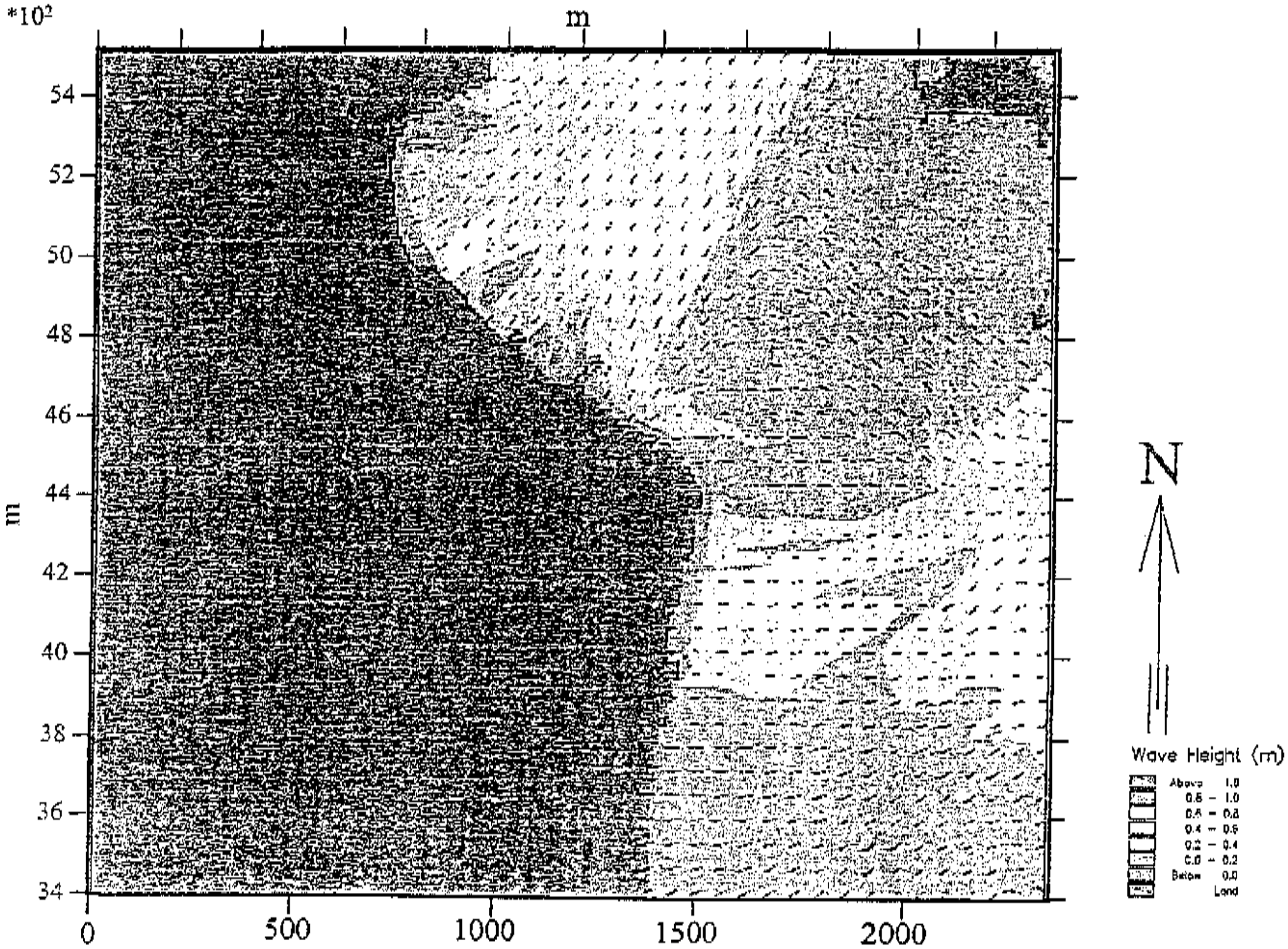


MOFFATT & NICHOL ENGINEERS

Figure 5.29:
NSW Local Results
1.5 m NE Wave - 6 Sec

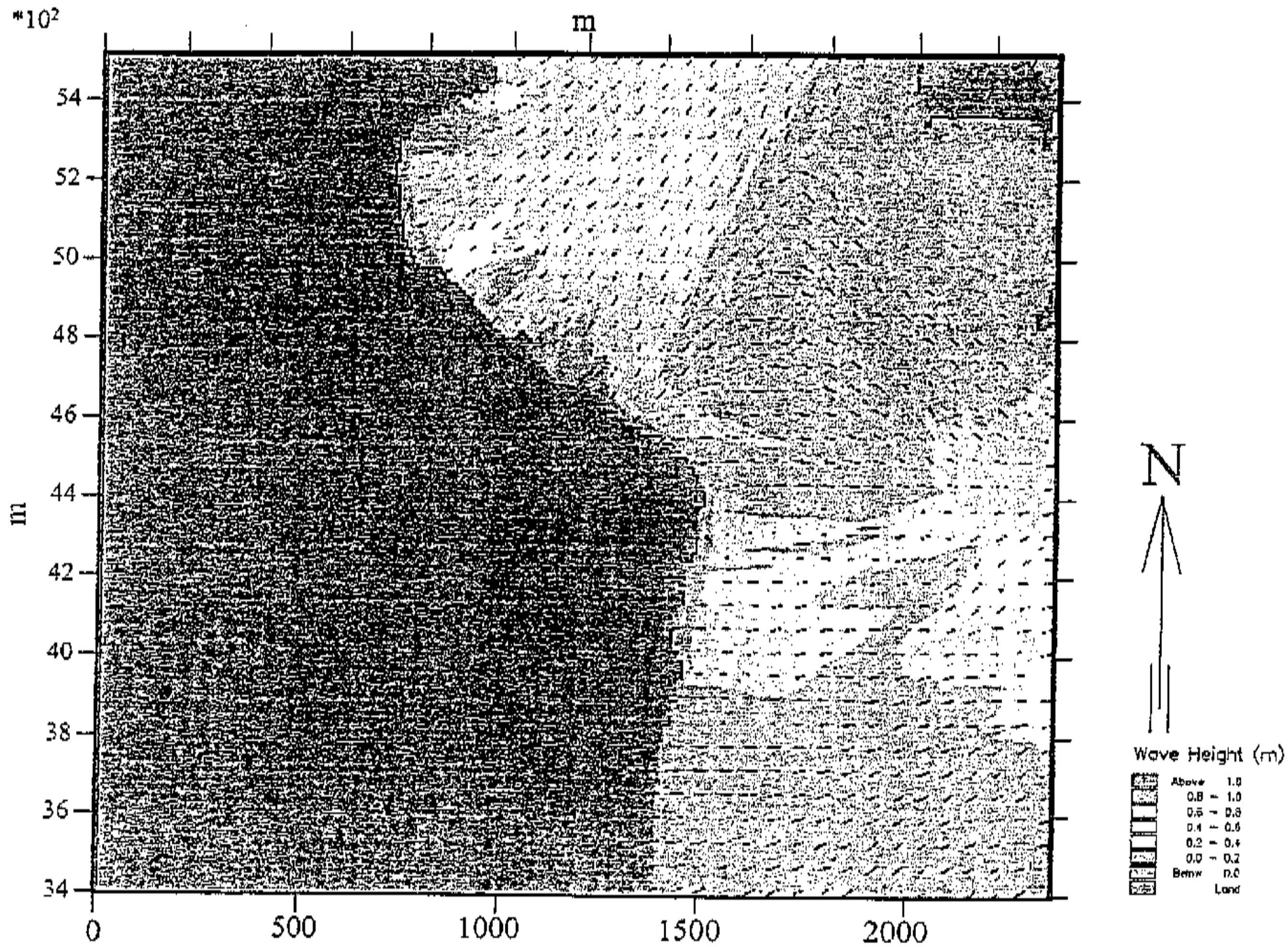


MOFFATT & NICHOL ENGINEERS

Figure 5.30:
NSW Local Results
1.5 m NE Wave - 8 Sec

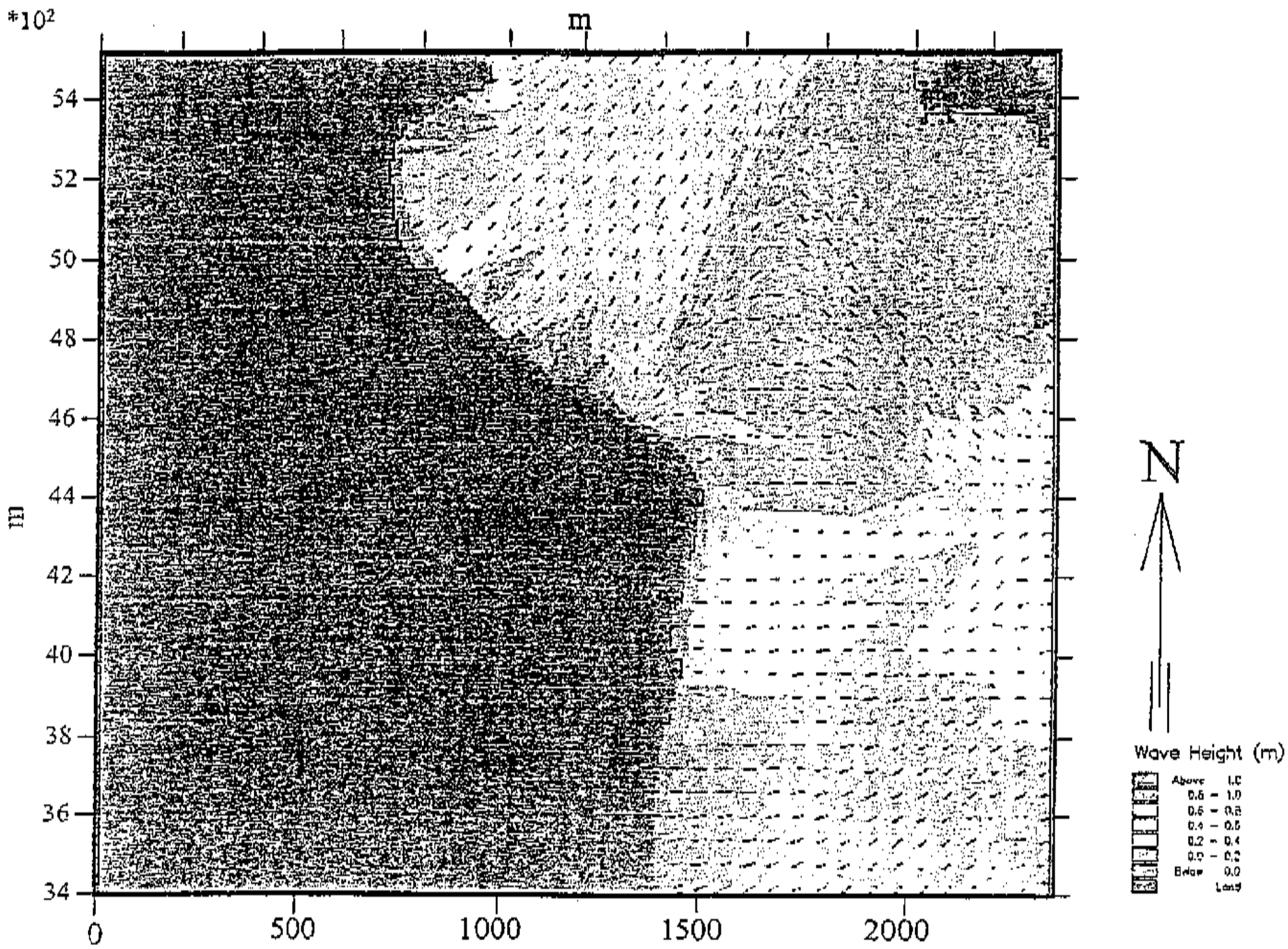


MOFFATT & NICHOL
E N G I N E E R S

Figure 5.31:
NSW Local Results
1.5 m NE Wave - 10 Sec

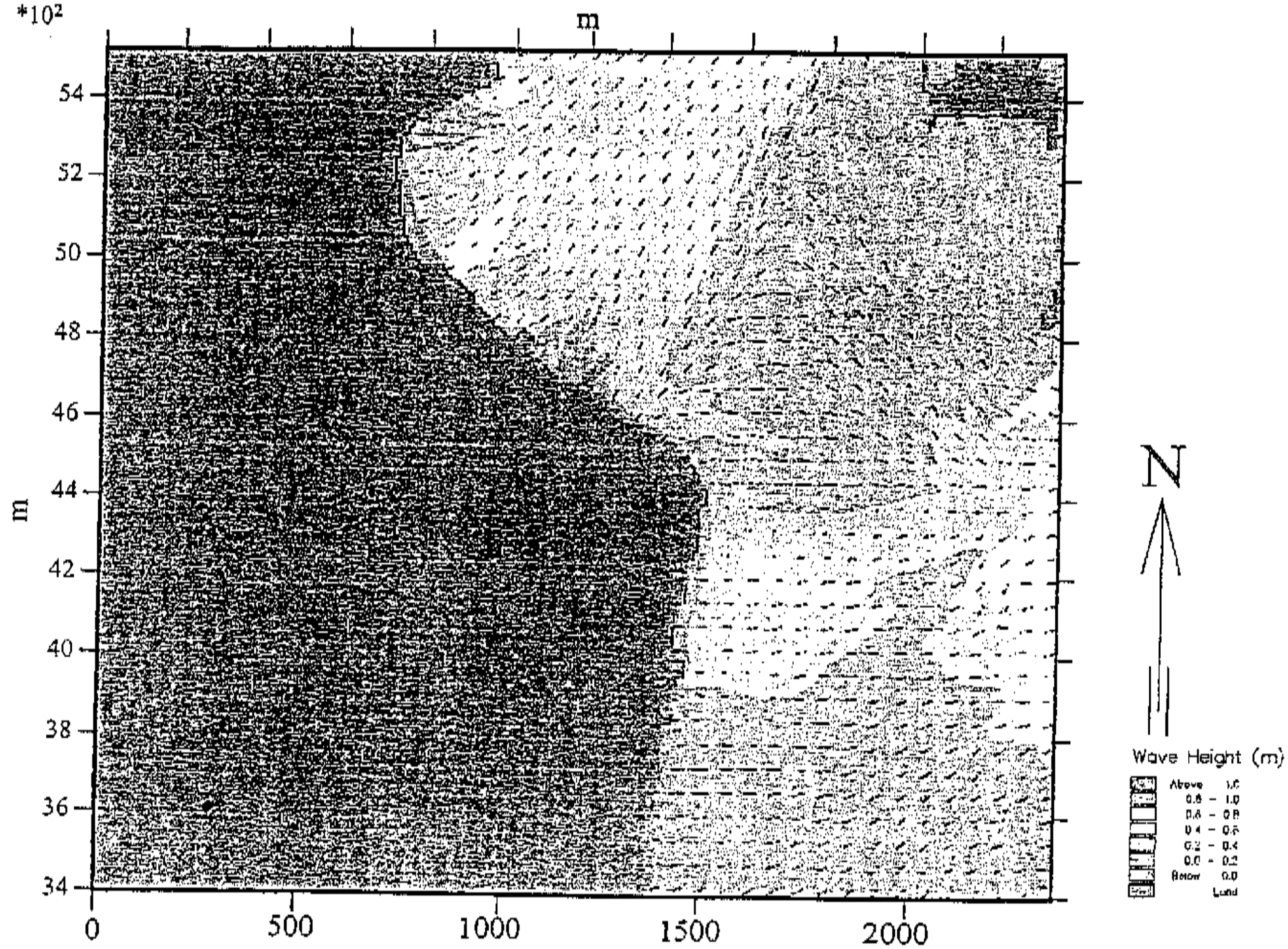


MOFFATT & NICHOL
ENGINEERS

Figure 5.32:
NSW Local Results
1.5 m NE Wave - 12 Sec

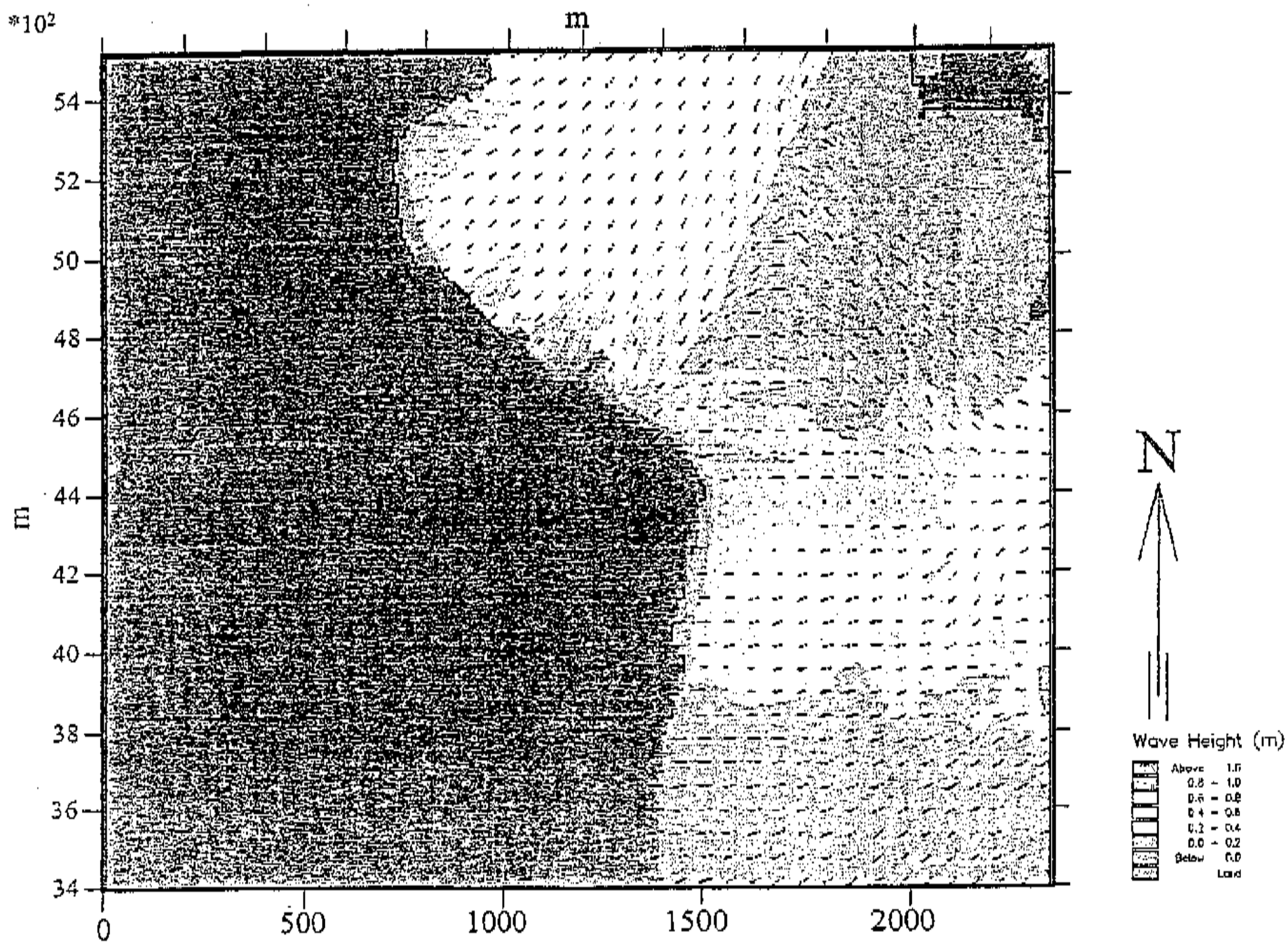


MOFFATT & NICHOL ENGINEERS

Figure 5.33:
NSW Local Results
2.5 m NE Wave - 8 Sec

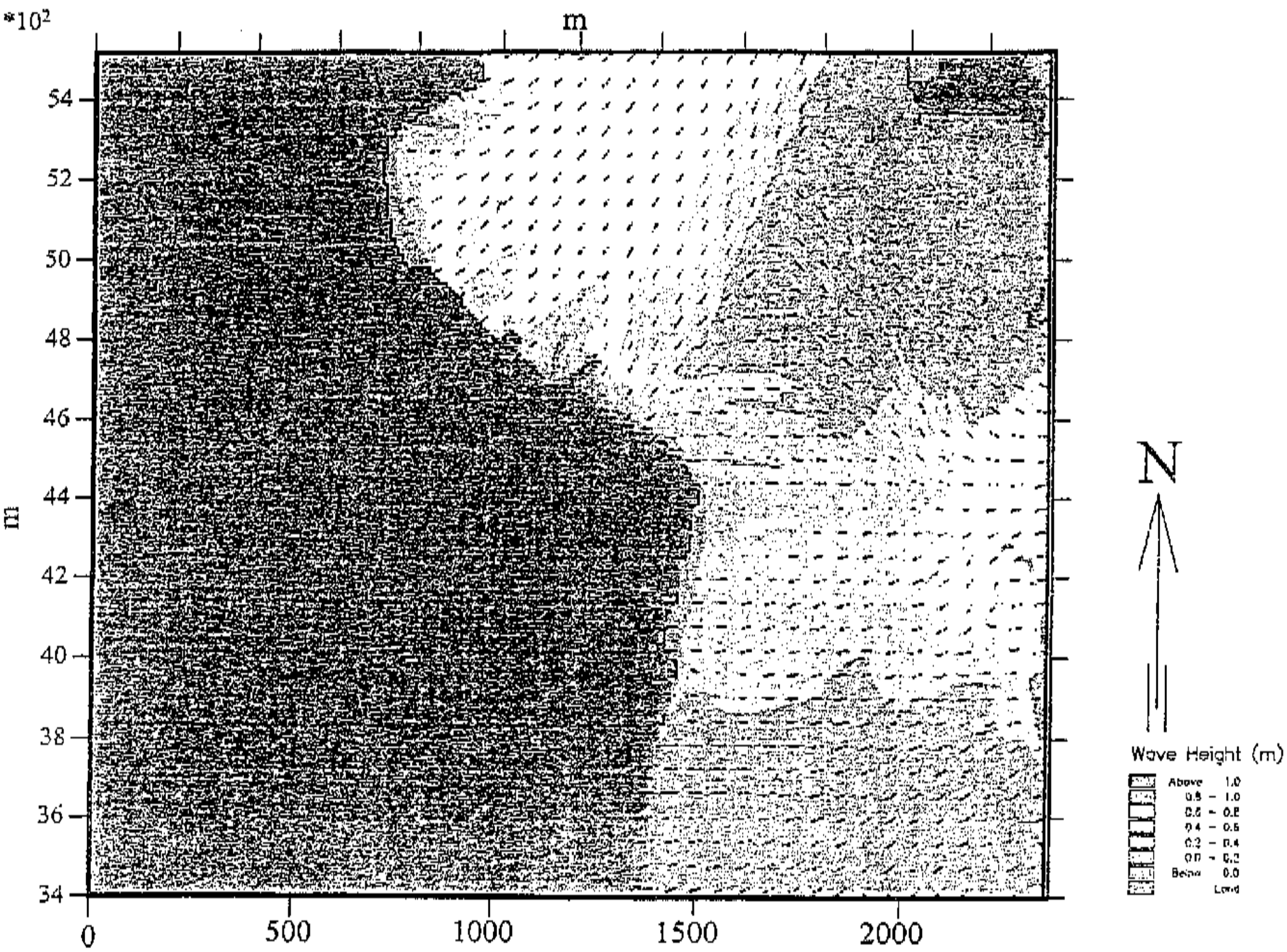


MOFFATT & NICHOL ENGINEERS

Figure 5.34:
NSW Local Results
2.5 m NE Wave - 10 Sec

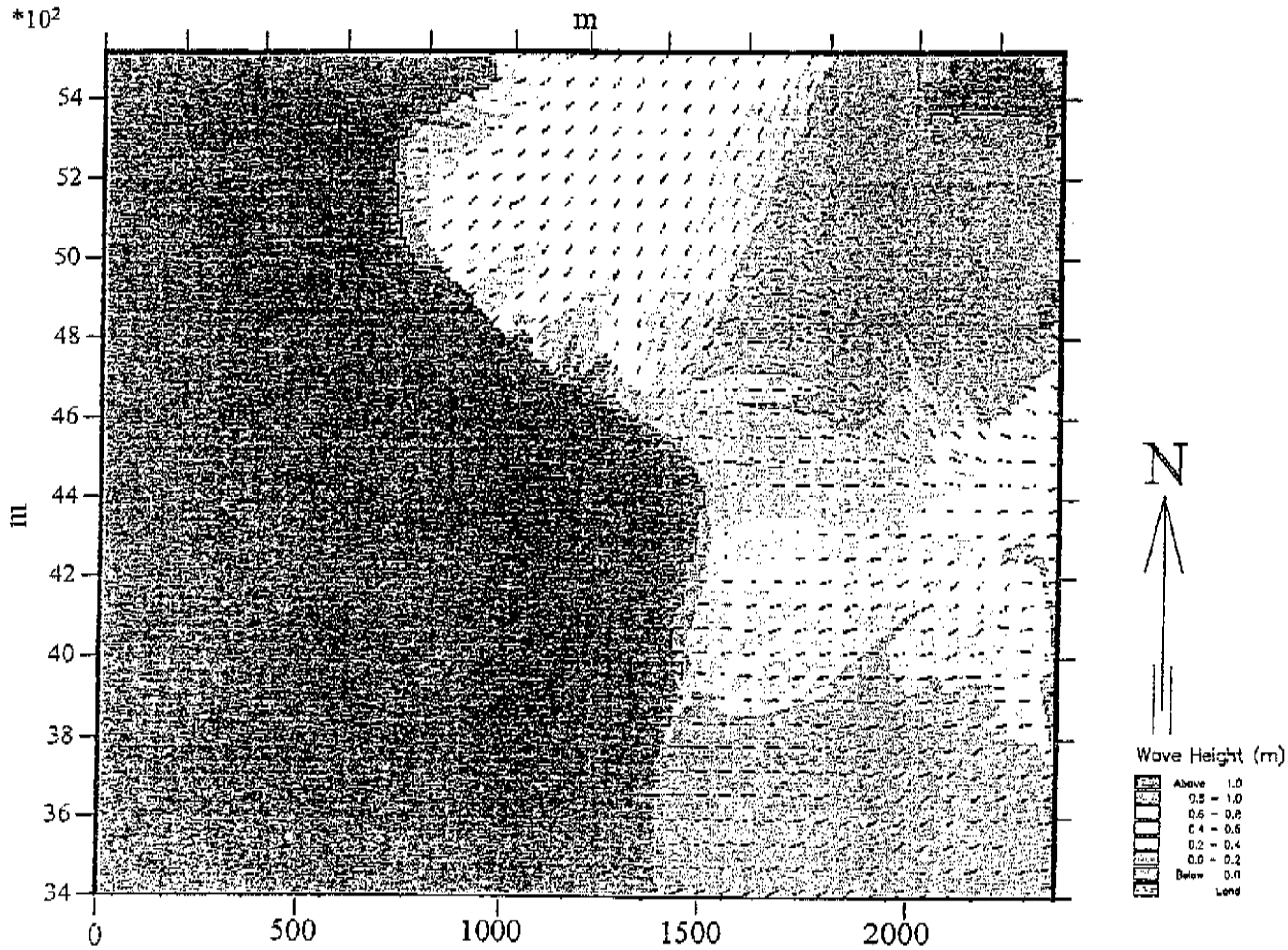


MOFFATT & NICHOL
E N G I N E E R S

Figure 5.35:
NSW Local Results
2.5 m NE Wave -12 Sec

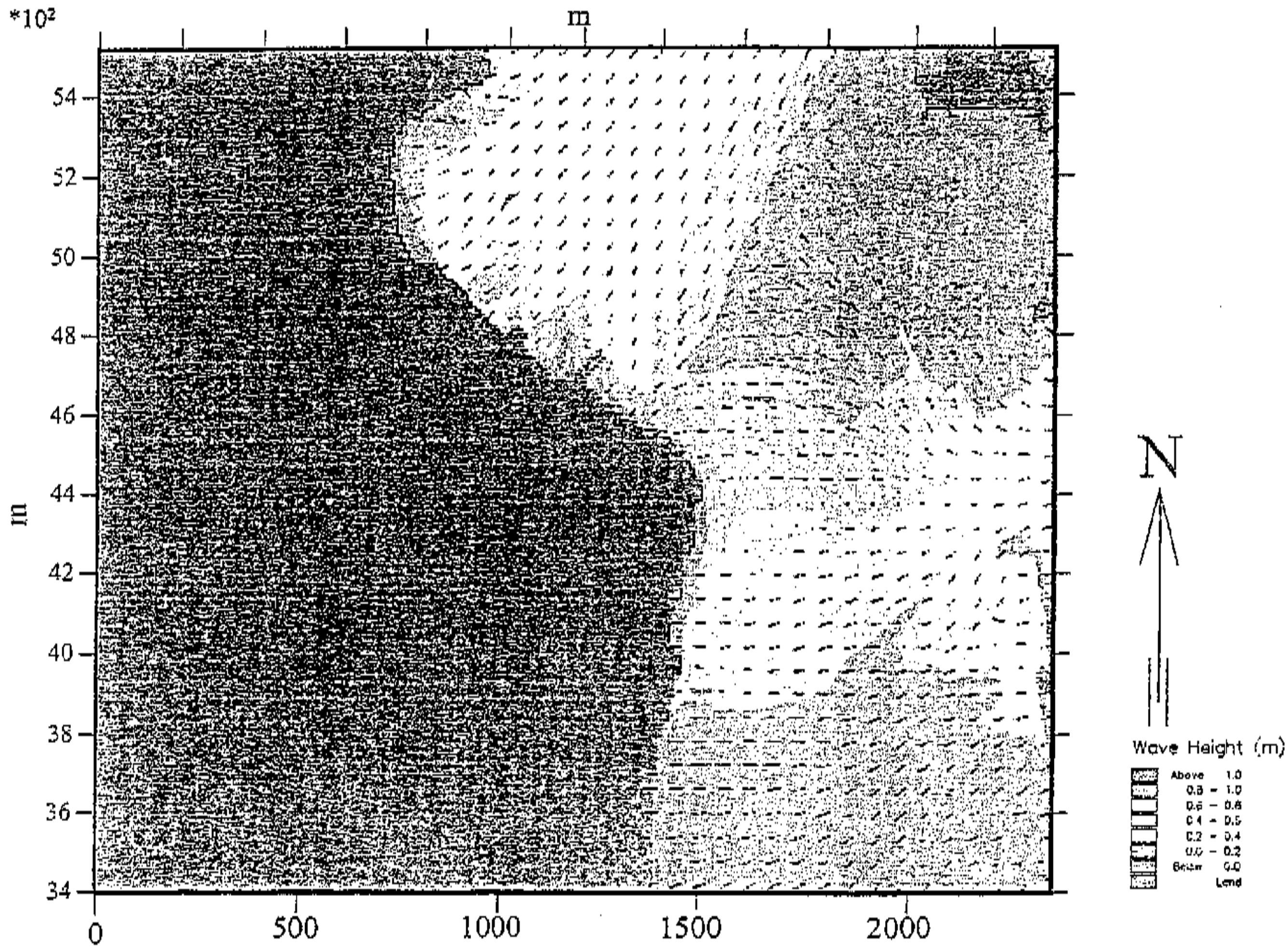




Figure 5.36:
NSW Local Results
2.5 m NE Wave - 14 Sec

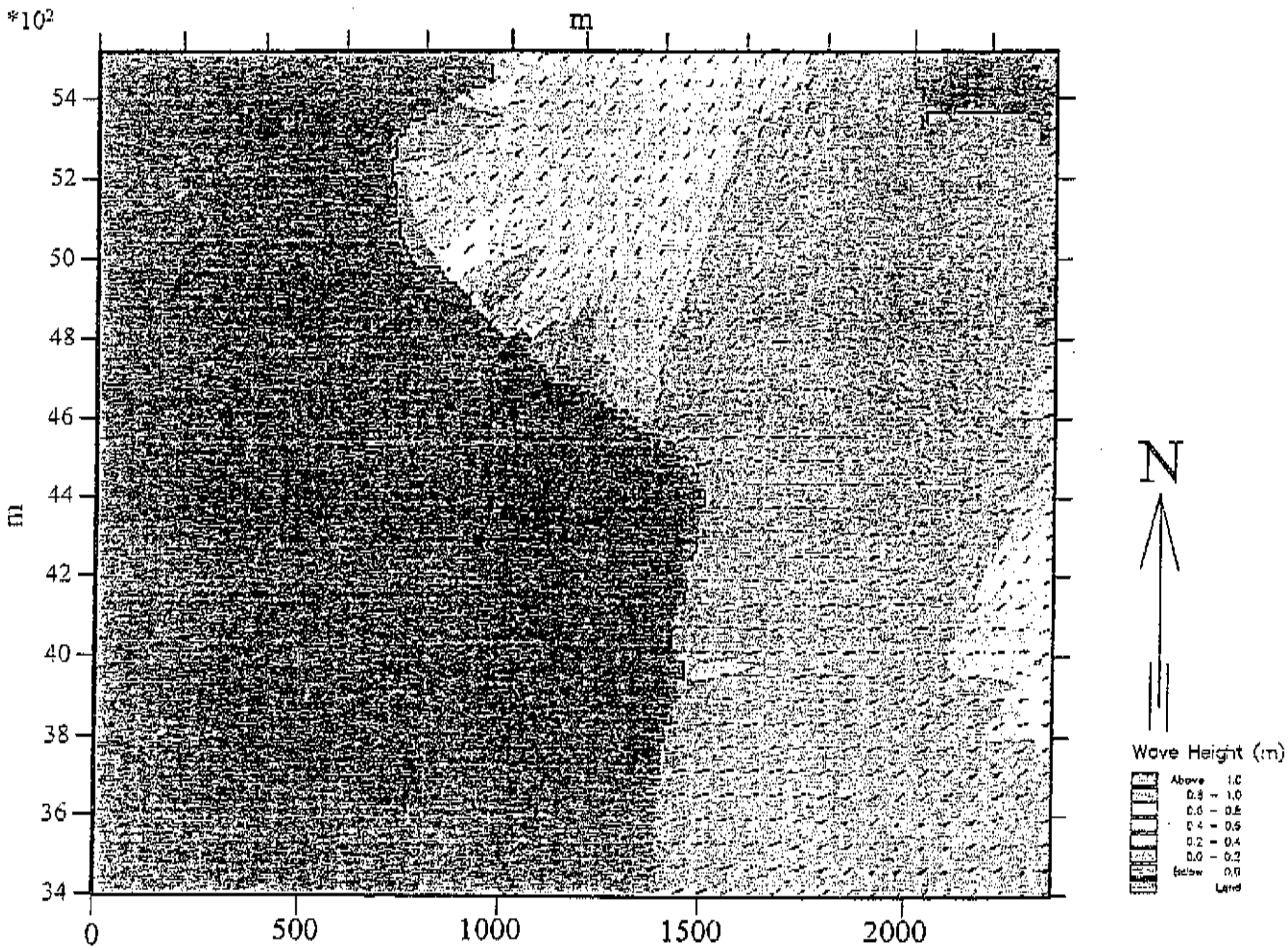


MOFFATT & NICHOL
ENGINEERS

Figure 5.37:
NSW Local Results
1.5 m North Wave - 8 Sec

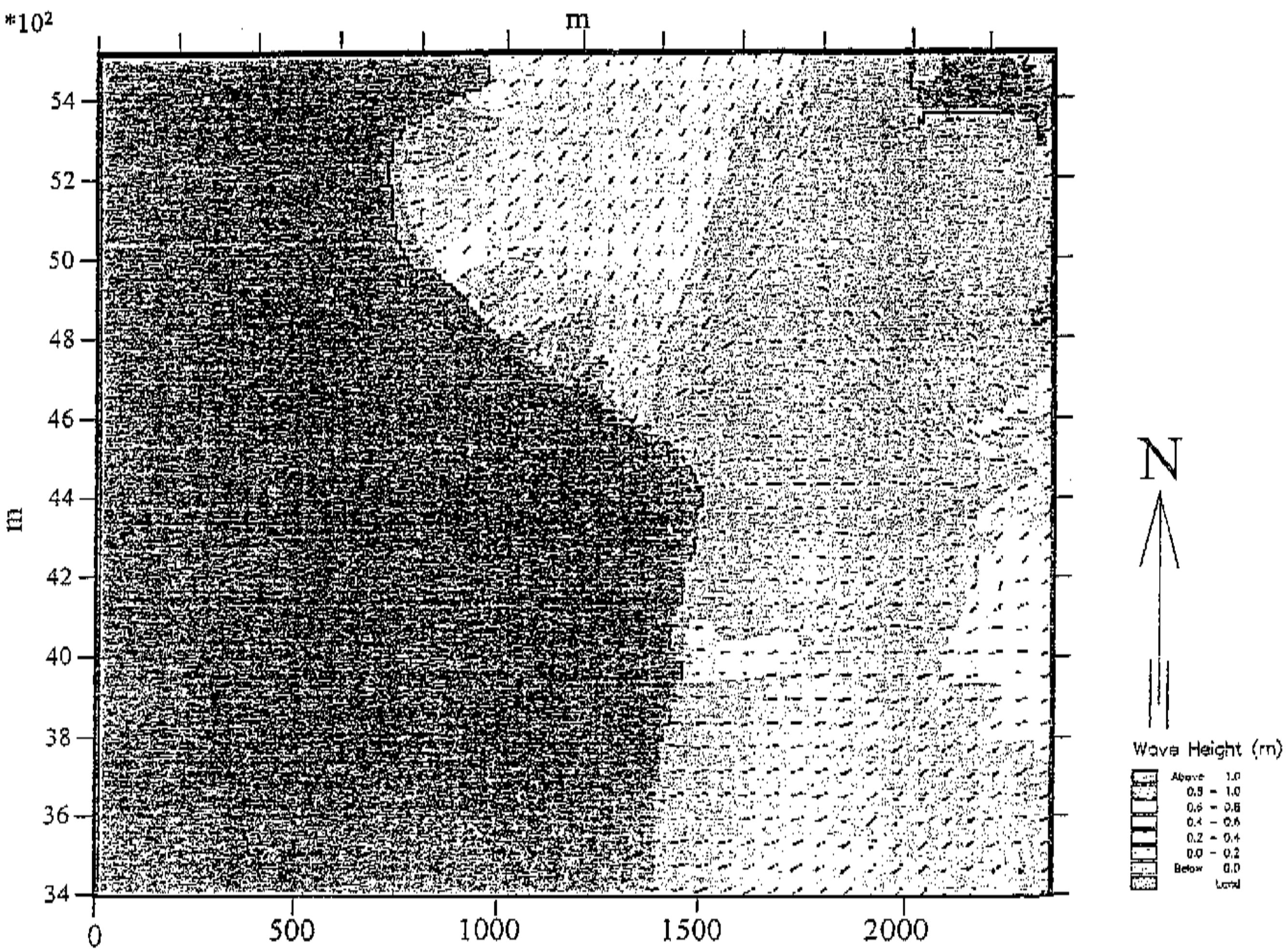


Figure 5.38:
NSW Local Results
1.5 m North Wave - 10 Sec

MOFFATT & NICHOL
E N G I N E E R S

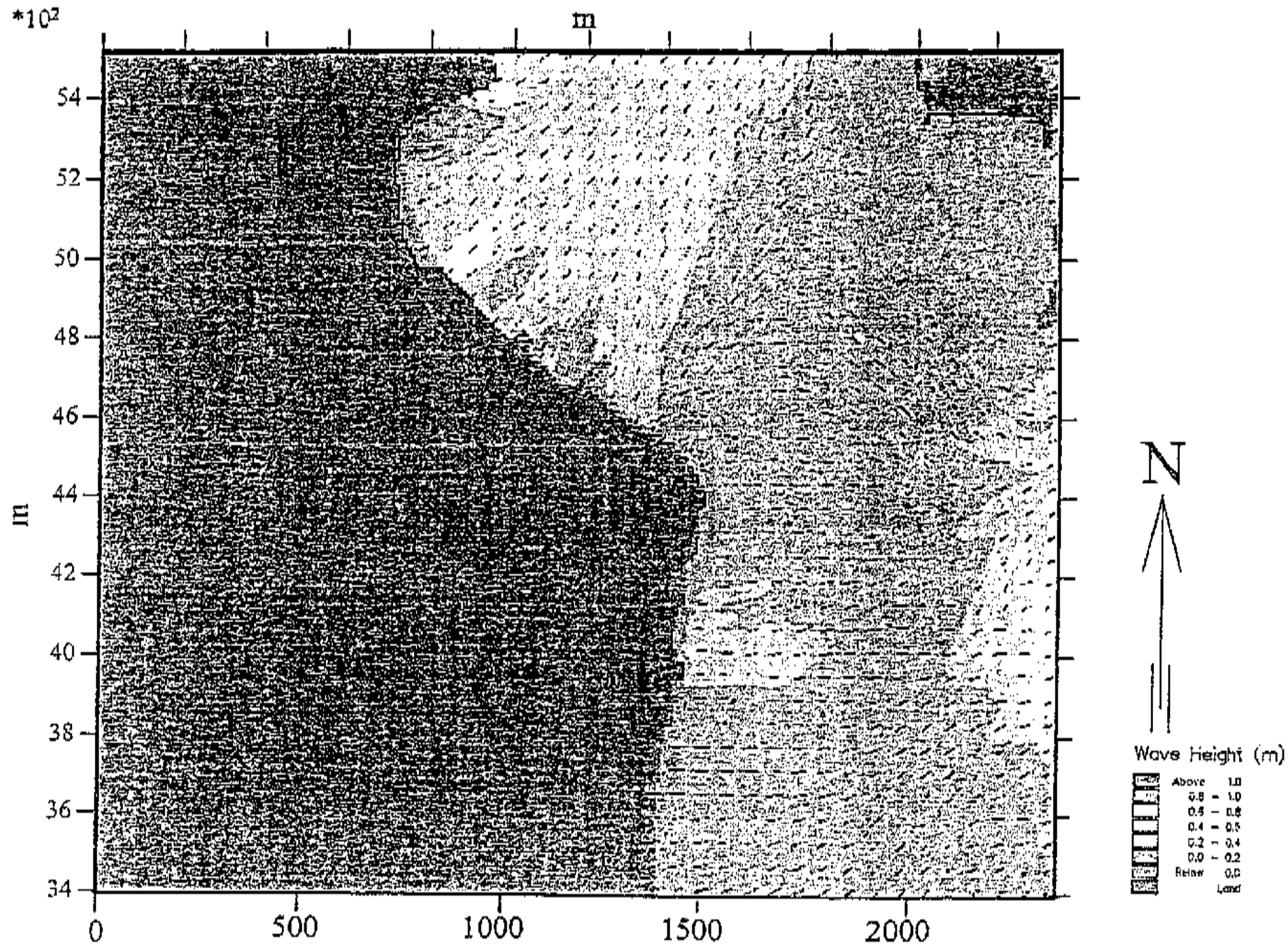


MOFFATT & NICHOL
E N G I N E E R S

Figure 5.39:
NSW Local Results
1.5 m North Wave - 12 Sec

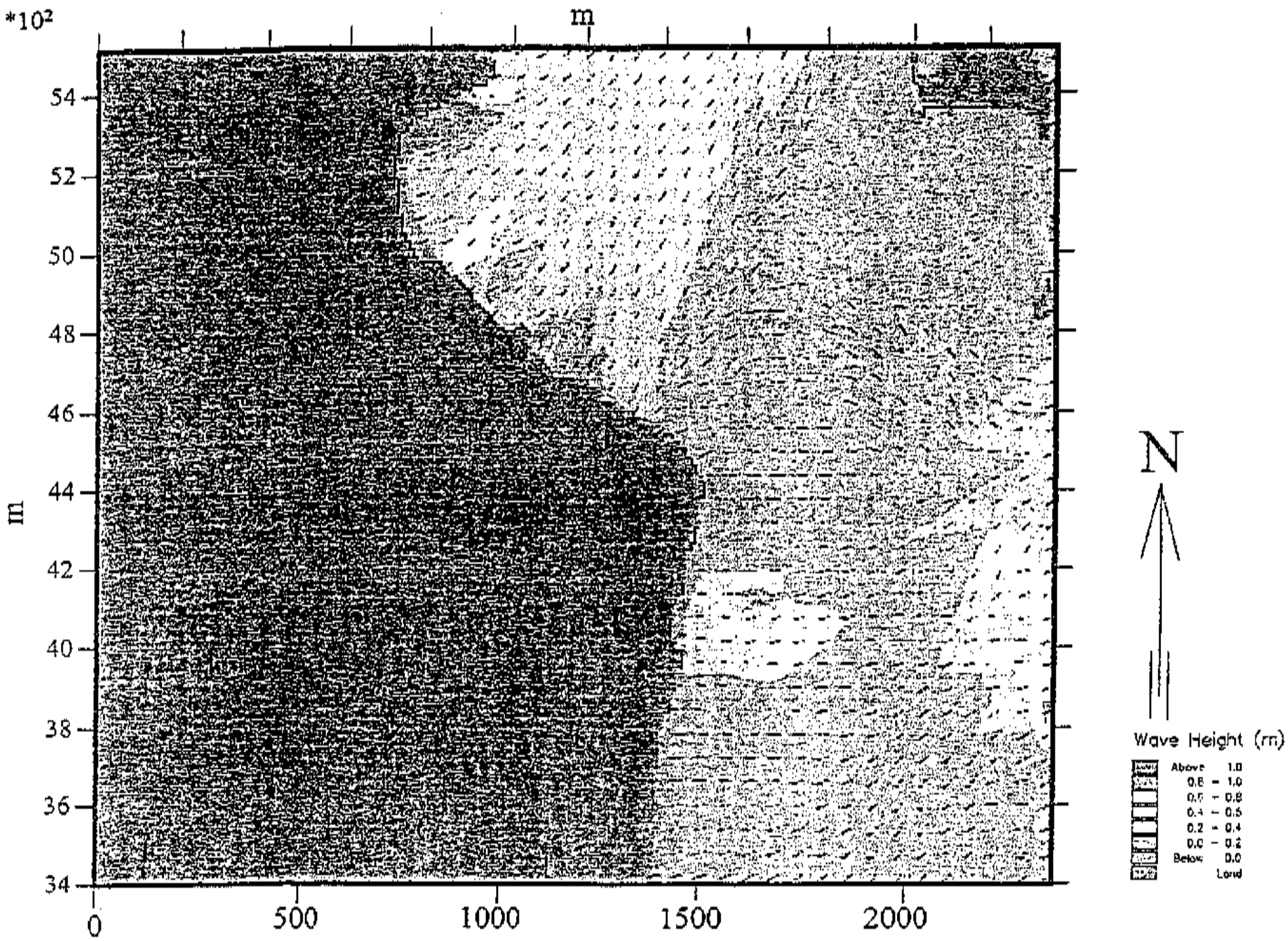


MOFFATT & NICHOL
E N G I N E E R S

Figure 5.40:
NSW Local Results
1.5 m North Wave - 14 Sec

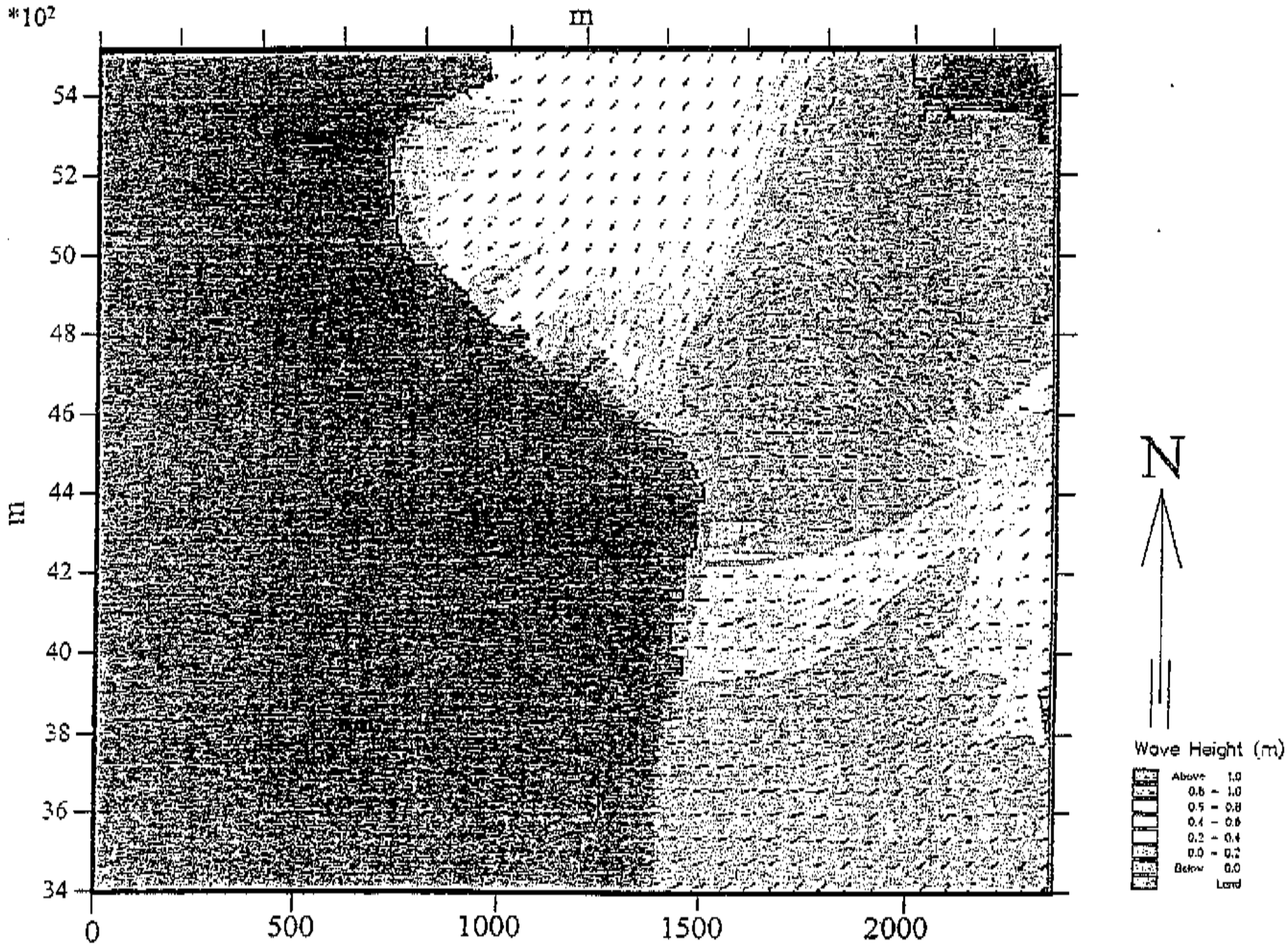


MOFFATT & NICHOL
ENGINEERS

Figure 5.41:
NSW Local Results
2.5 m North Wave - 10 Sec

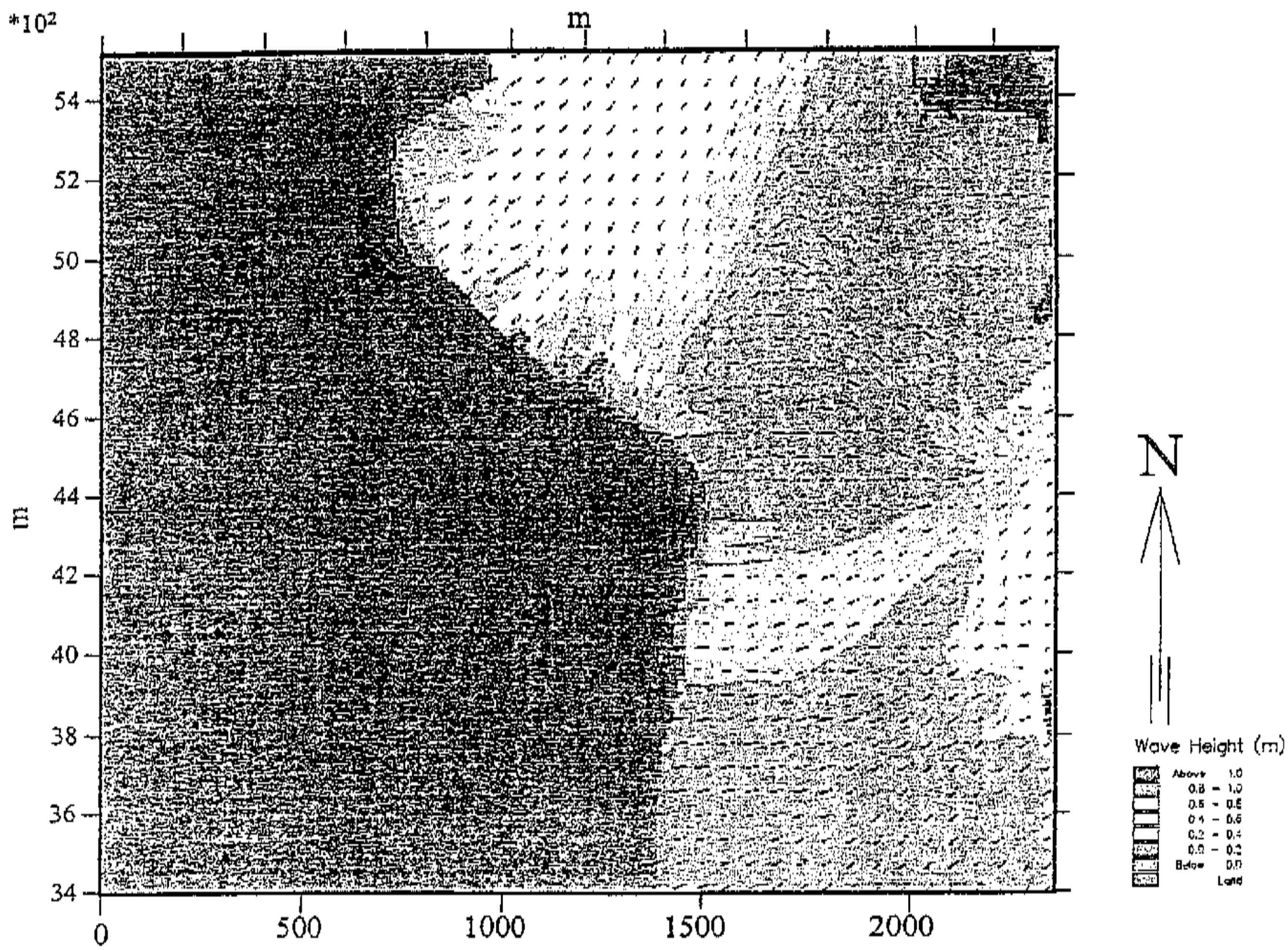


MOFFATT & NICHOL ENGINEERS

Figure 5.42:
NSW Local Results
2.5 m North Wave - 12 Sec

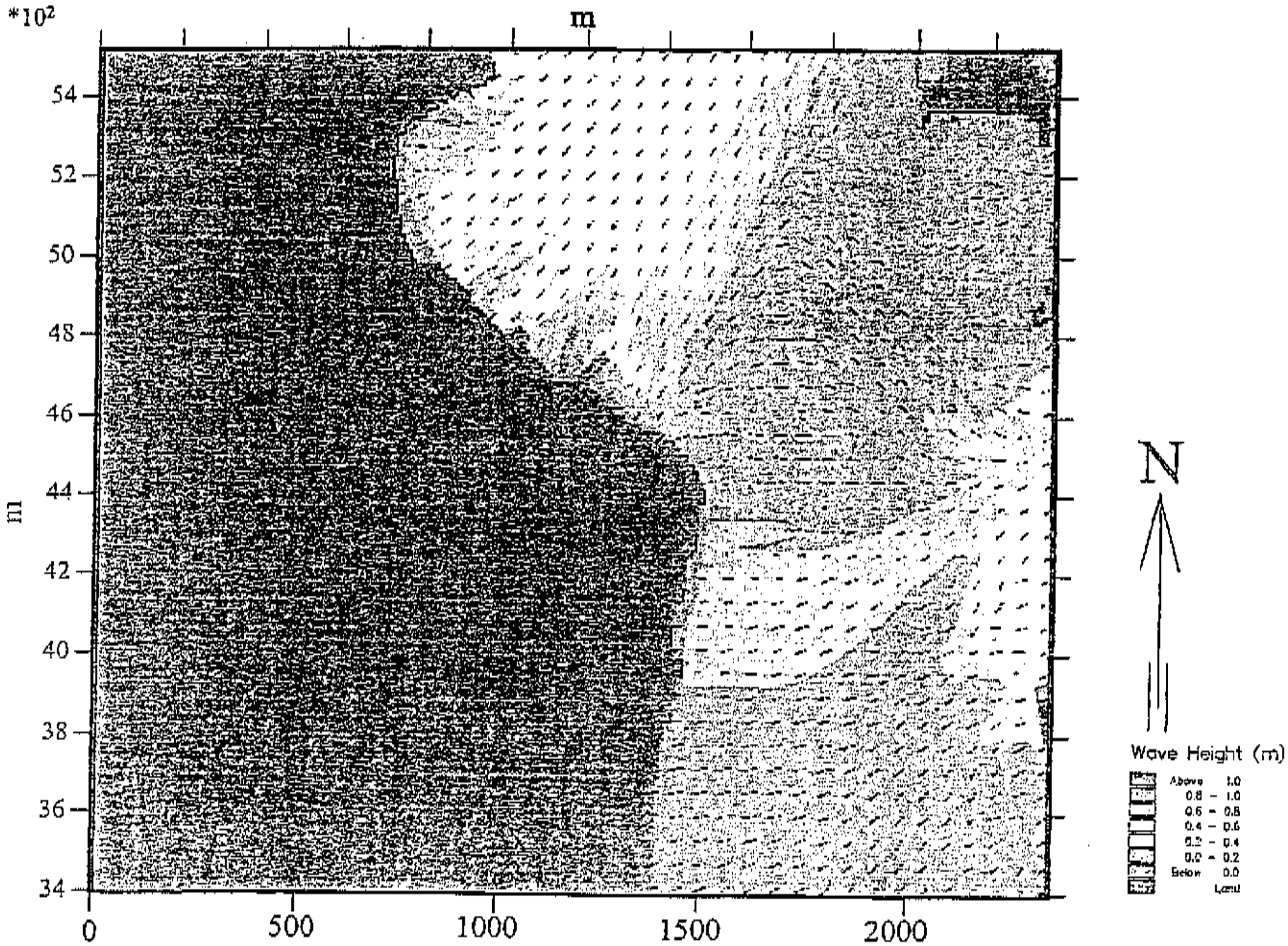


MOFFATT & NICHOL
ENGINEERS

Figure 5.43:
NSW Local Results
2.5 m North Wave - 14 Sec

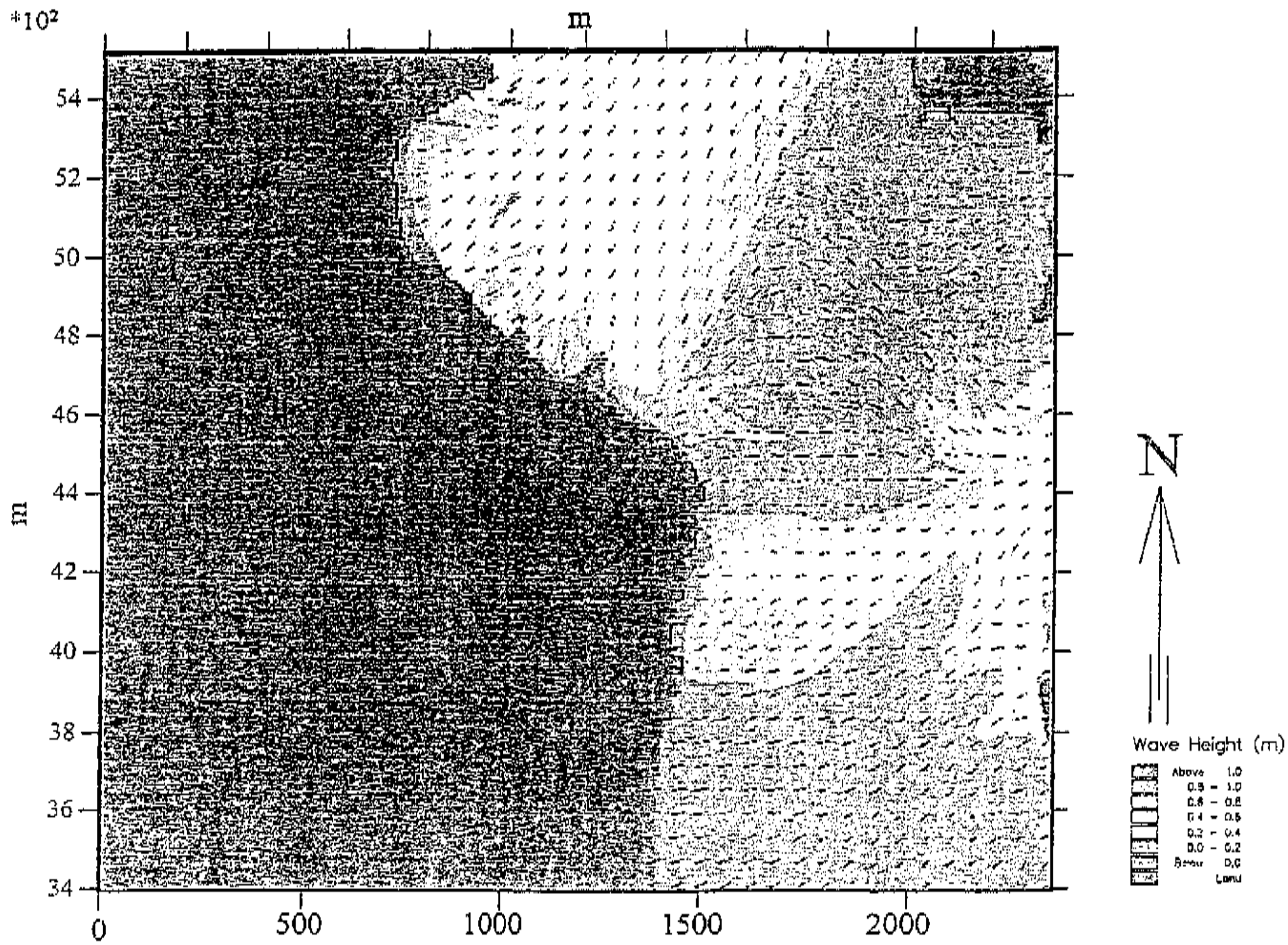


MOFFATT & NICHOL
ENGINEERS

Figure 5.44:
NSW Local Results
3.5 m North Wave - 14 Sec

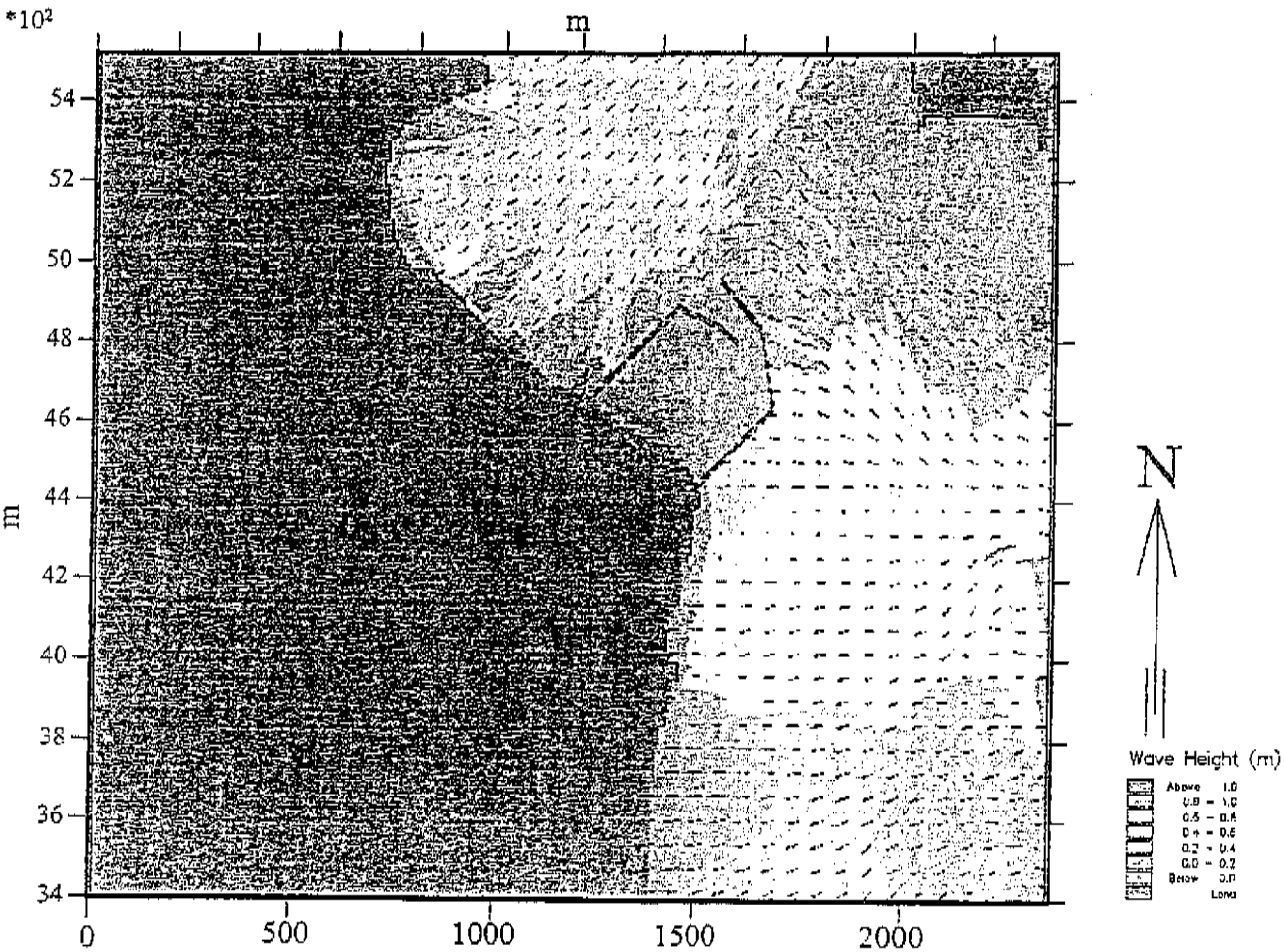


MOFFATT & NICHOL
E N G I N E E R S

Figure 5.45:
NSW Local Results with Breakwater
1.5 m East Wave - 6 Sec

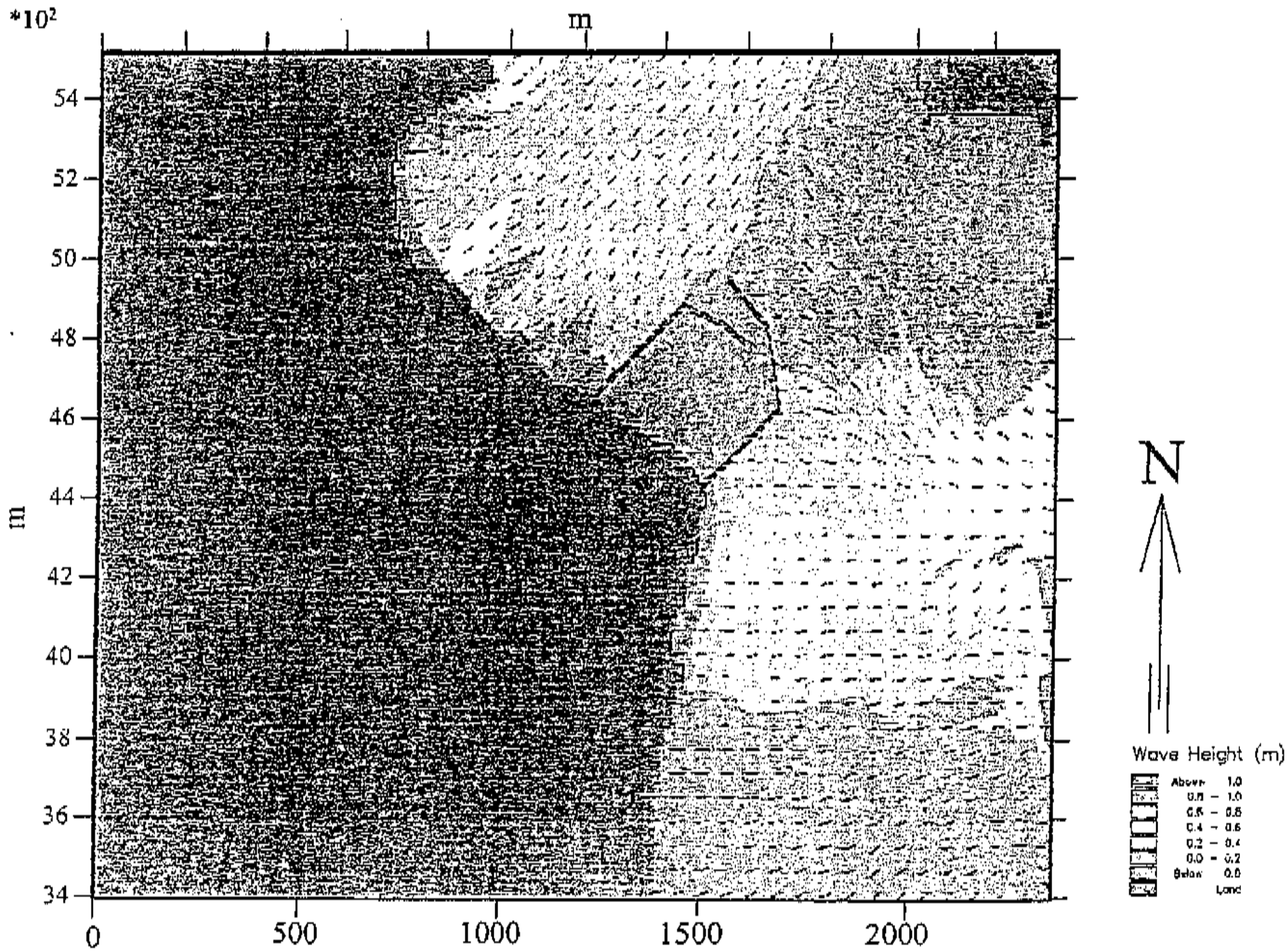


MOFFATT & NICHOL
ENGINEERS

Figure 5.46:
NSW Local Results with Breakwater
1.5 m East Wave - 8 Sec

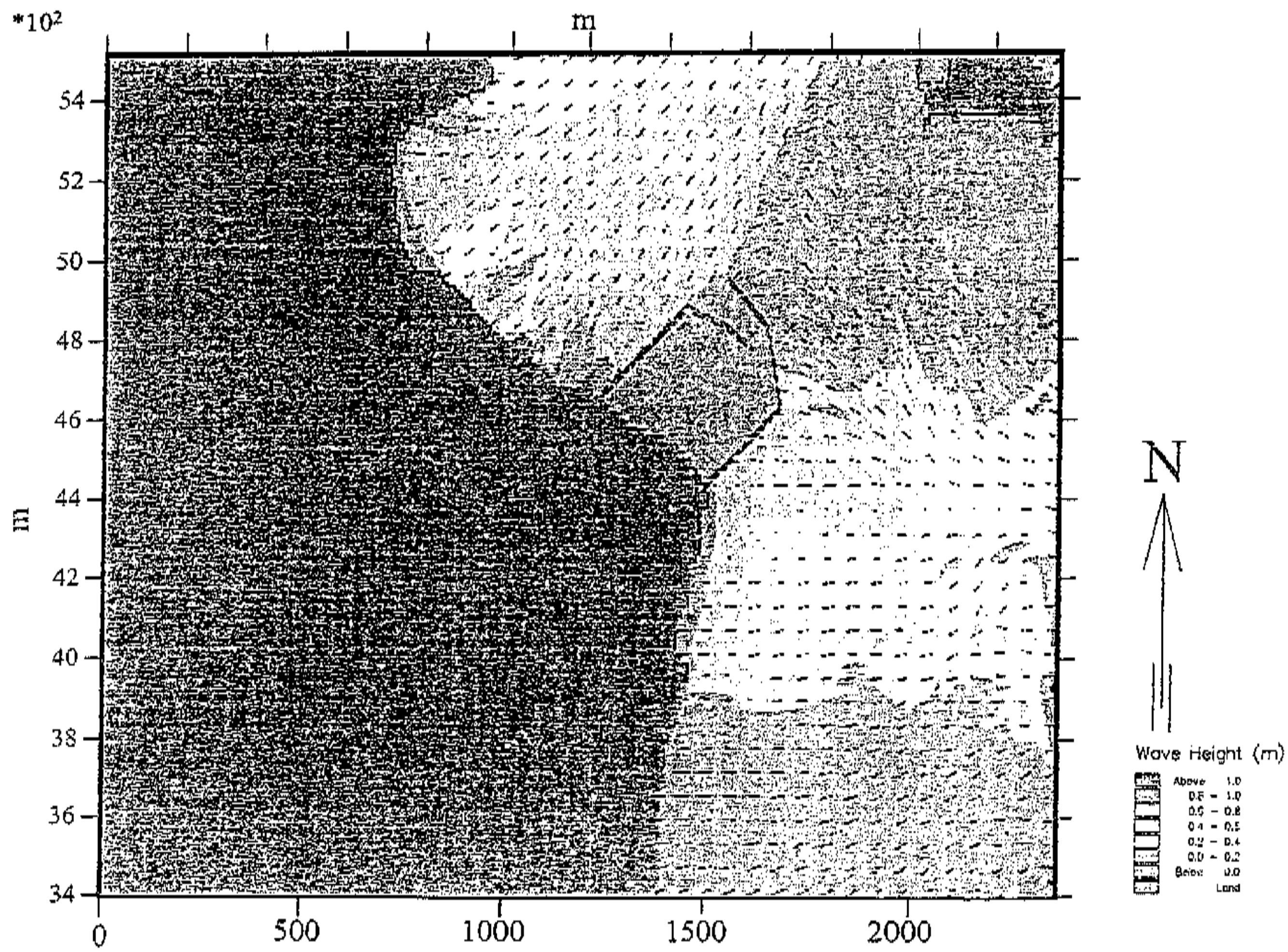


MOFFATT & NICHOL
ENGINEERS

Figure 5.47:
NSW Local Results with Breakwater
1.5 m East Wave - 10 Sec

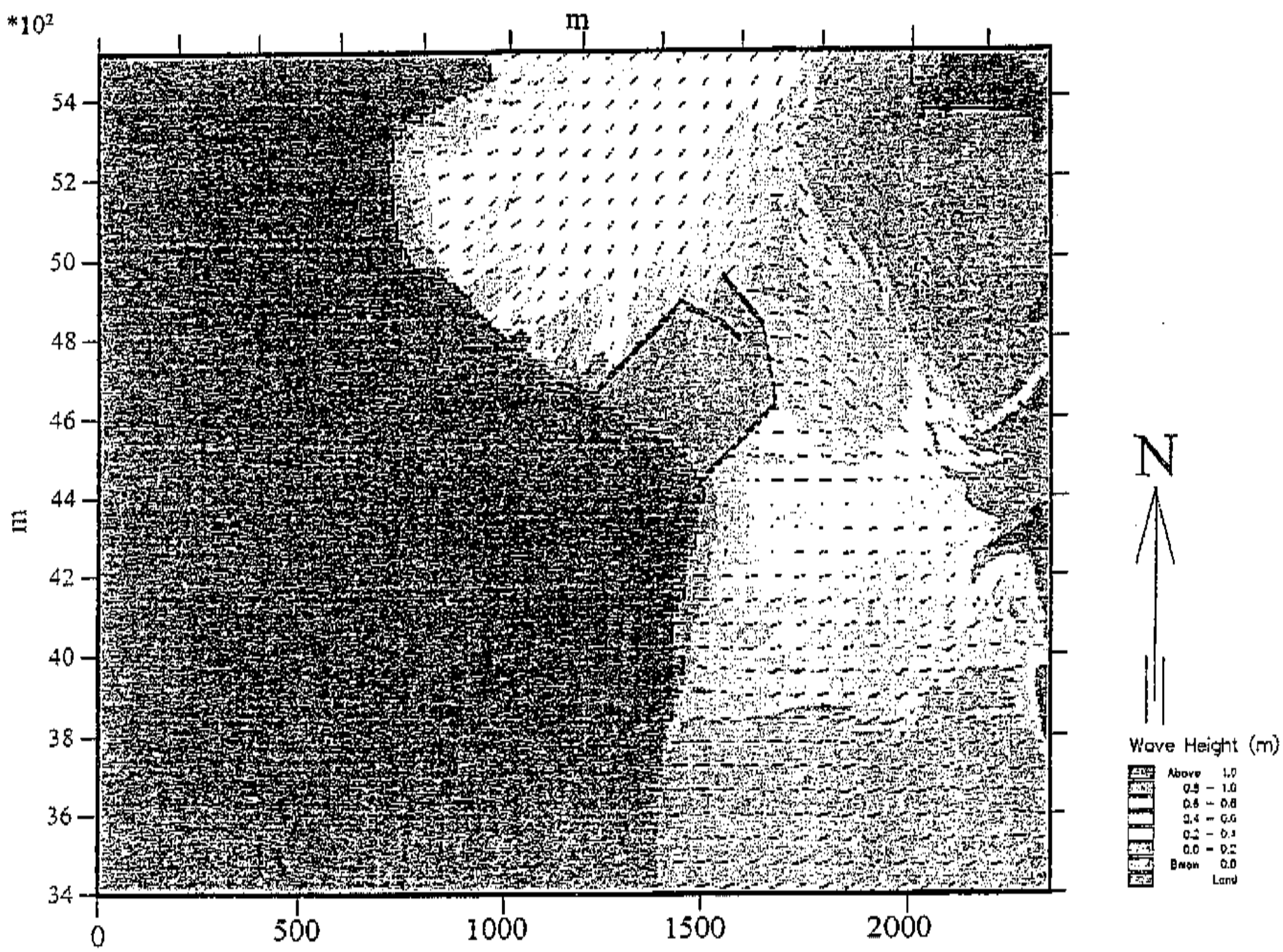


MOFFATT & NICHOL
E N G I N E E R S

Figure 5.48:
NSW Local Results with Breakwater
2.5 m East Wave - 8 Sec

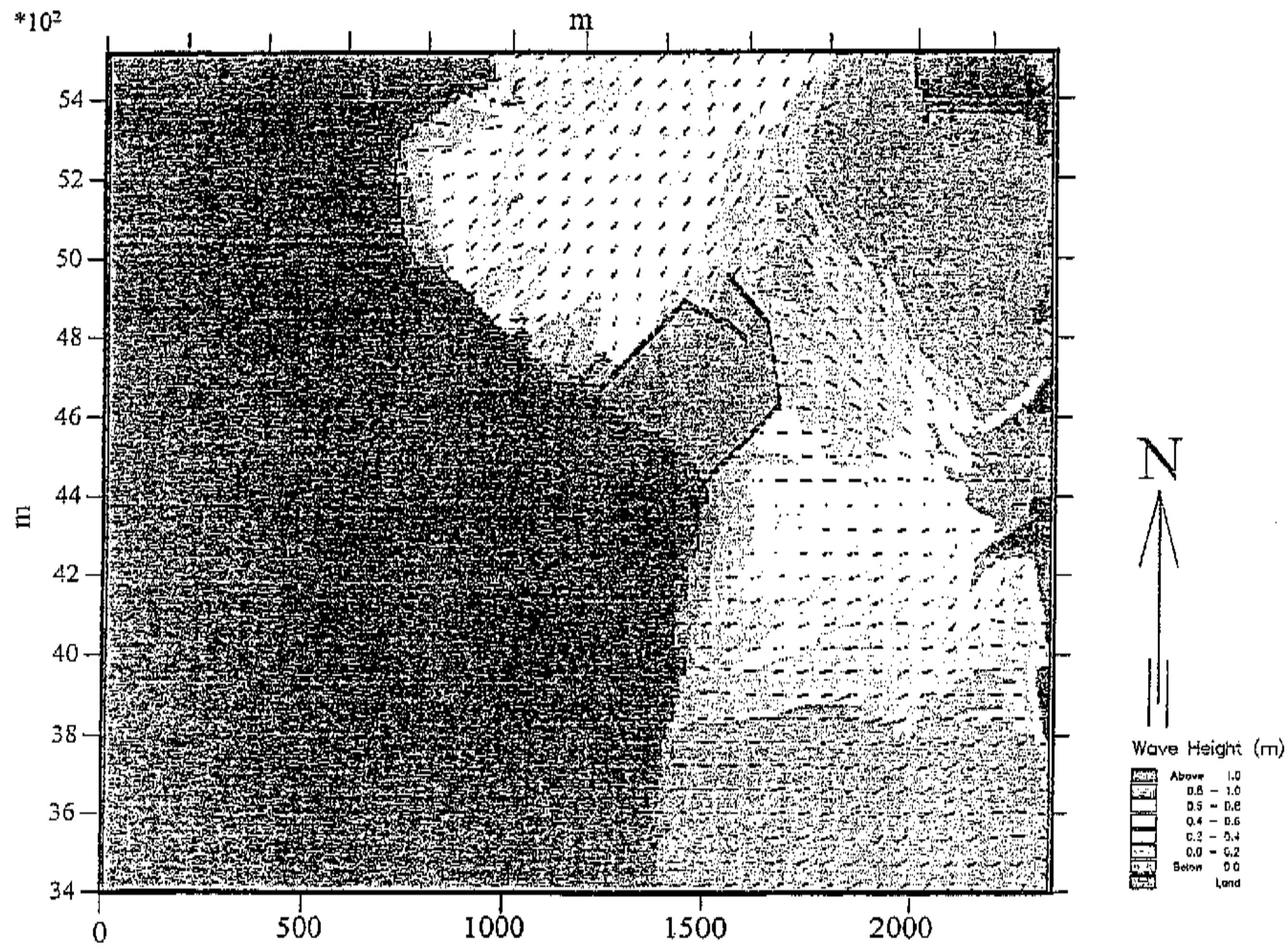


MOFFATT & NICHOL
ENGINEERS

Figure 5.49:
NSW Local Results with Breakwater
2.5 m East Wave - 10 Sec

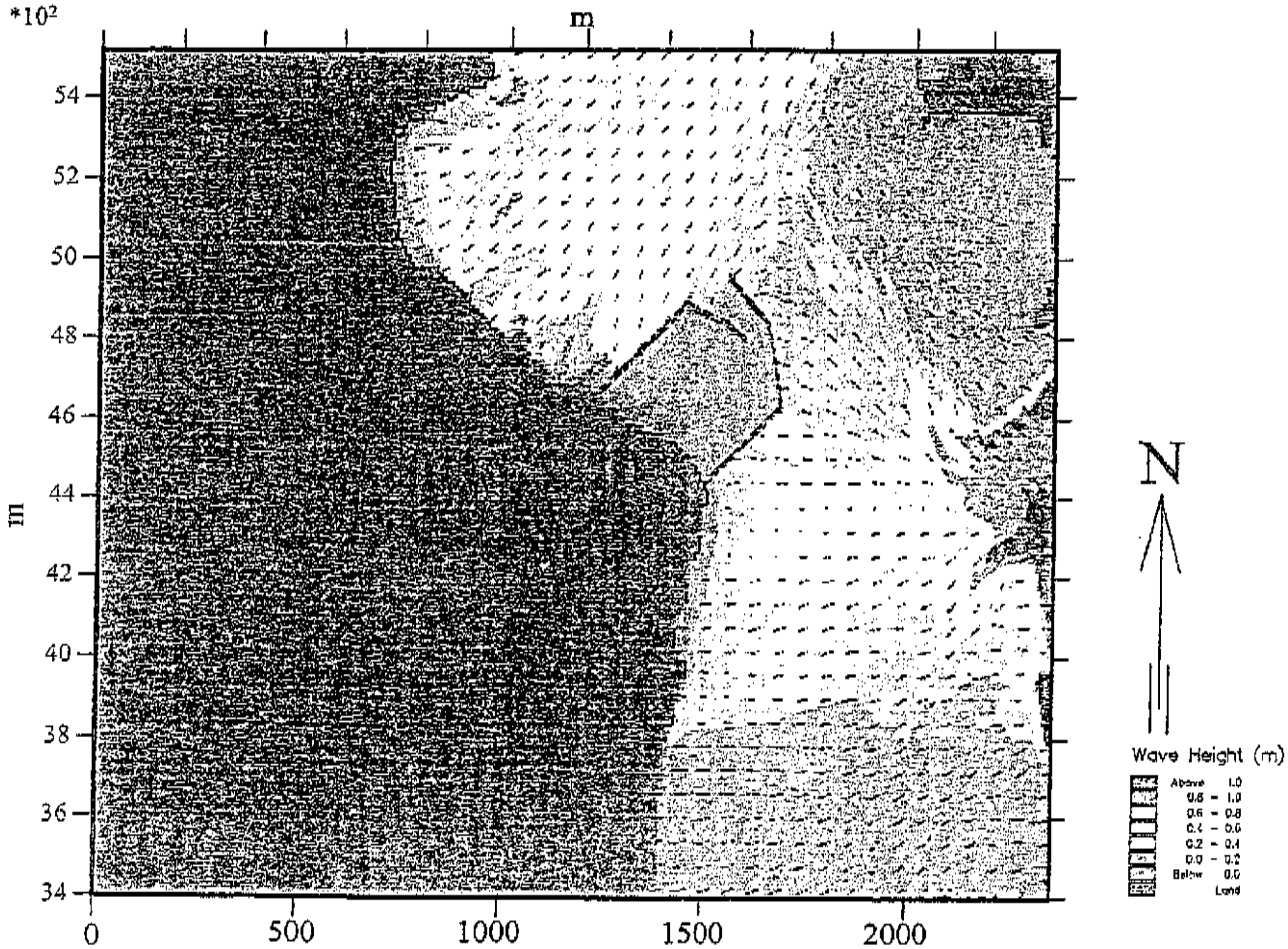


MOFFATT & NICHOL ENGINEERS

Figure 5.50:
NSW Local Results with Breakwater
2.5 m East Wave - 12 Sec

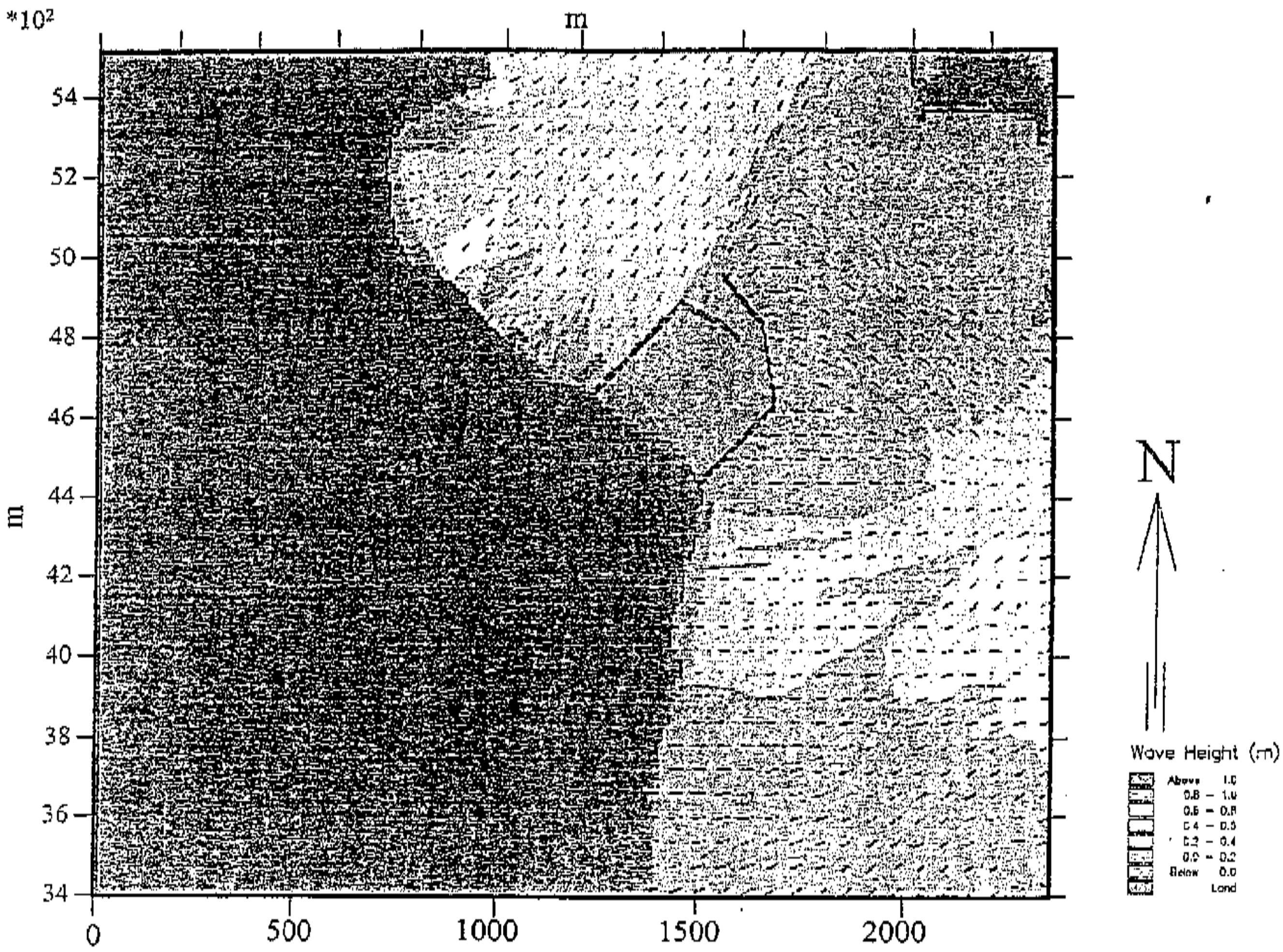


MOFFATT & NICHOL
ENGINEERS

Figure 5.51:
NSW Local Results with Breakwater
1.5 m NE Wave - 6 Sec

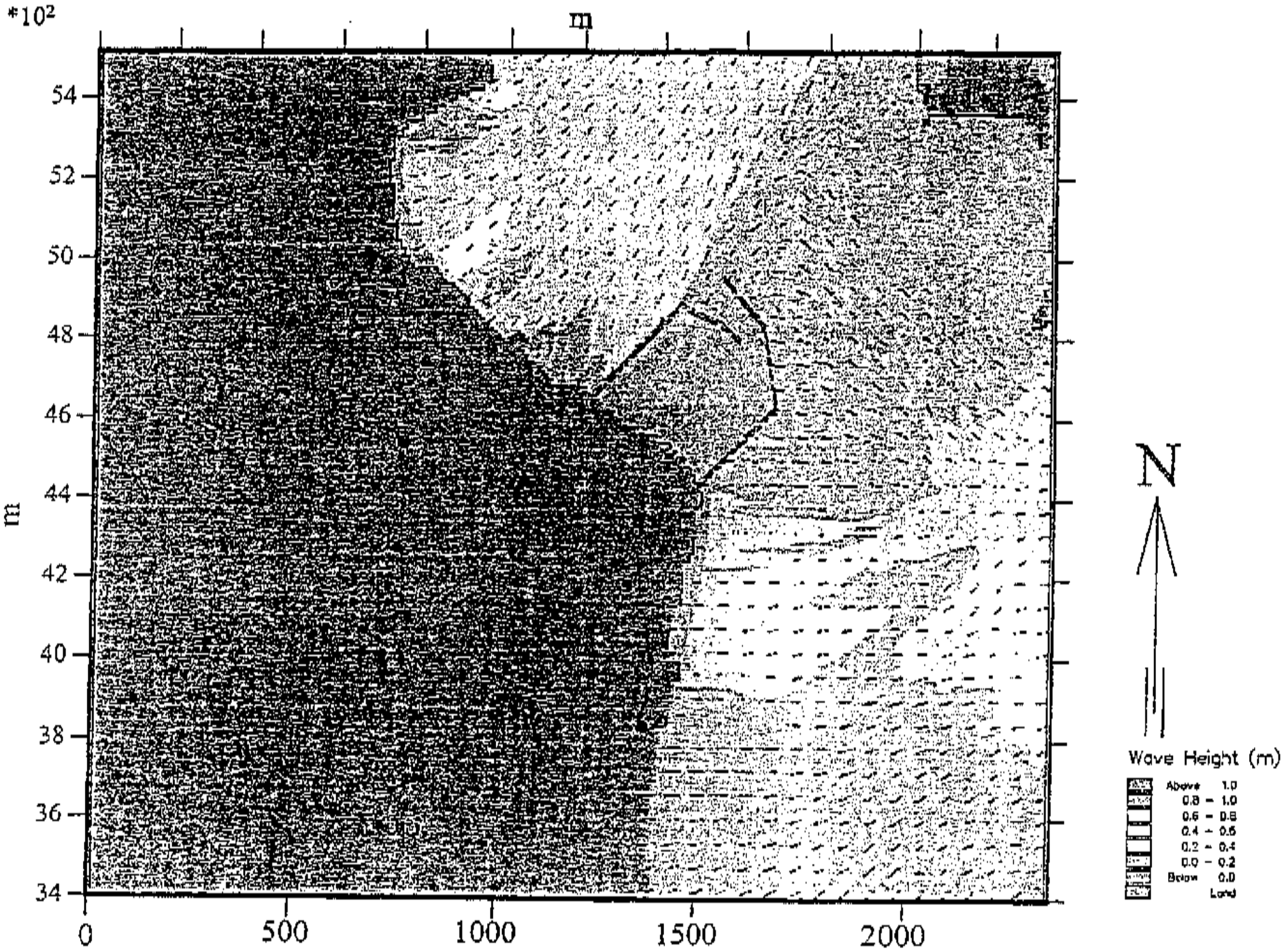


MOFFATT & NICHOL
ENGINEERS

Figure 5.52:
NSW Local Results with Breakwater
1.5 m NE Wave - 8 Sec

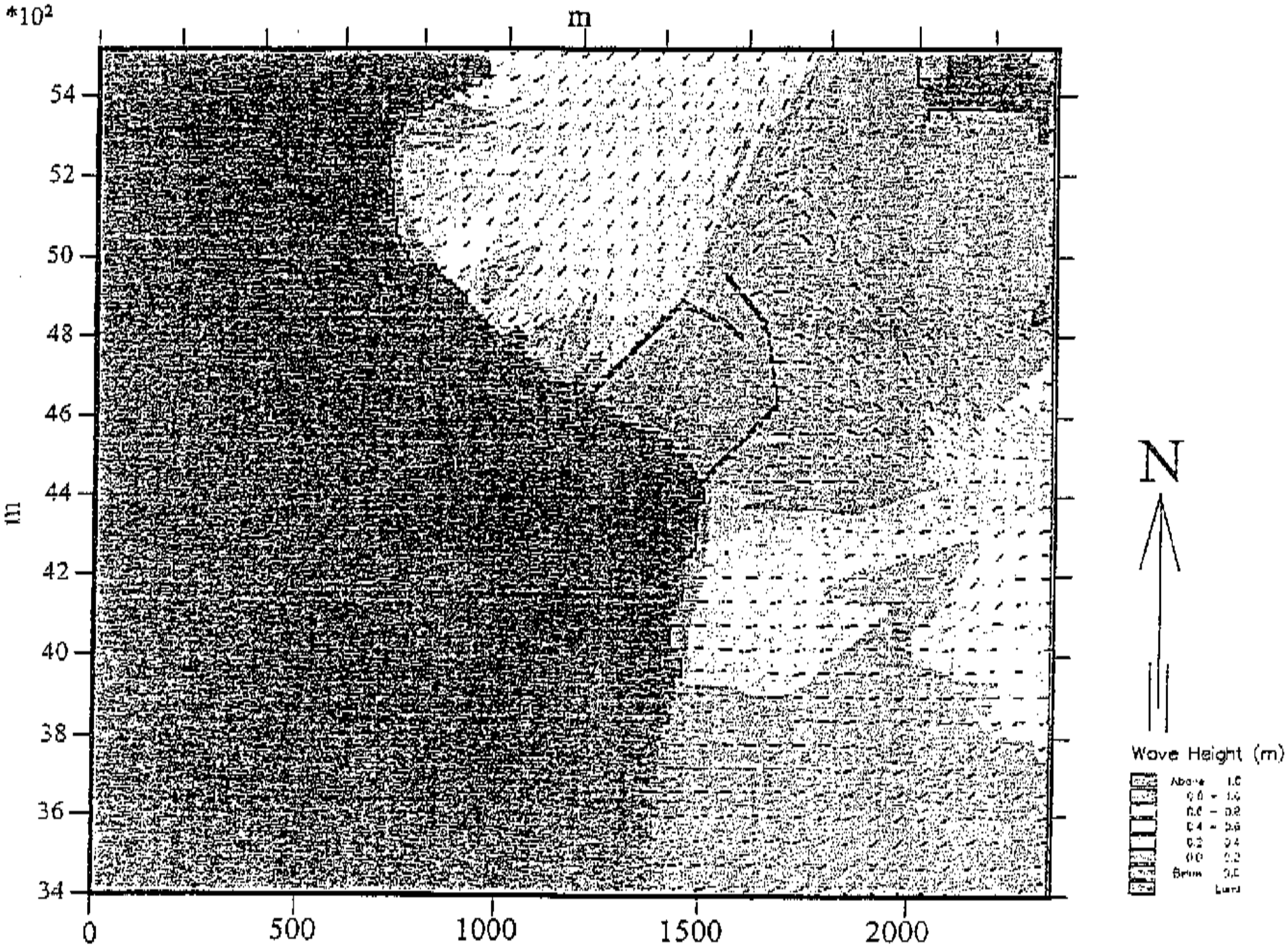




Figure 5.53:
NSW Local Results with Breakwater
1.5 m NE Wave - 10 Sec

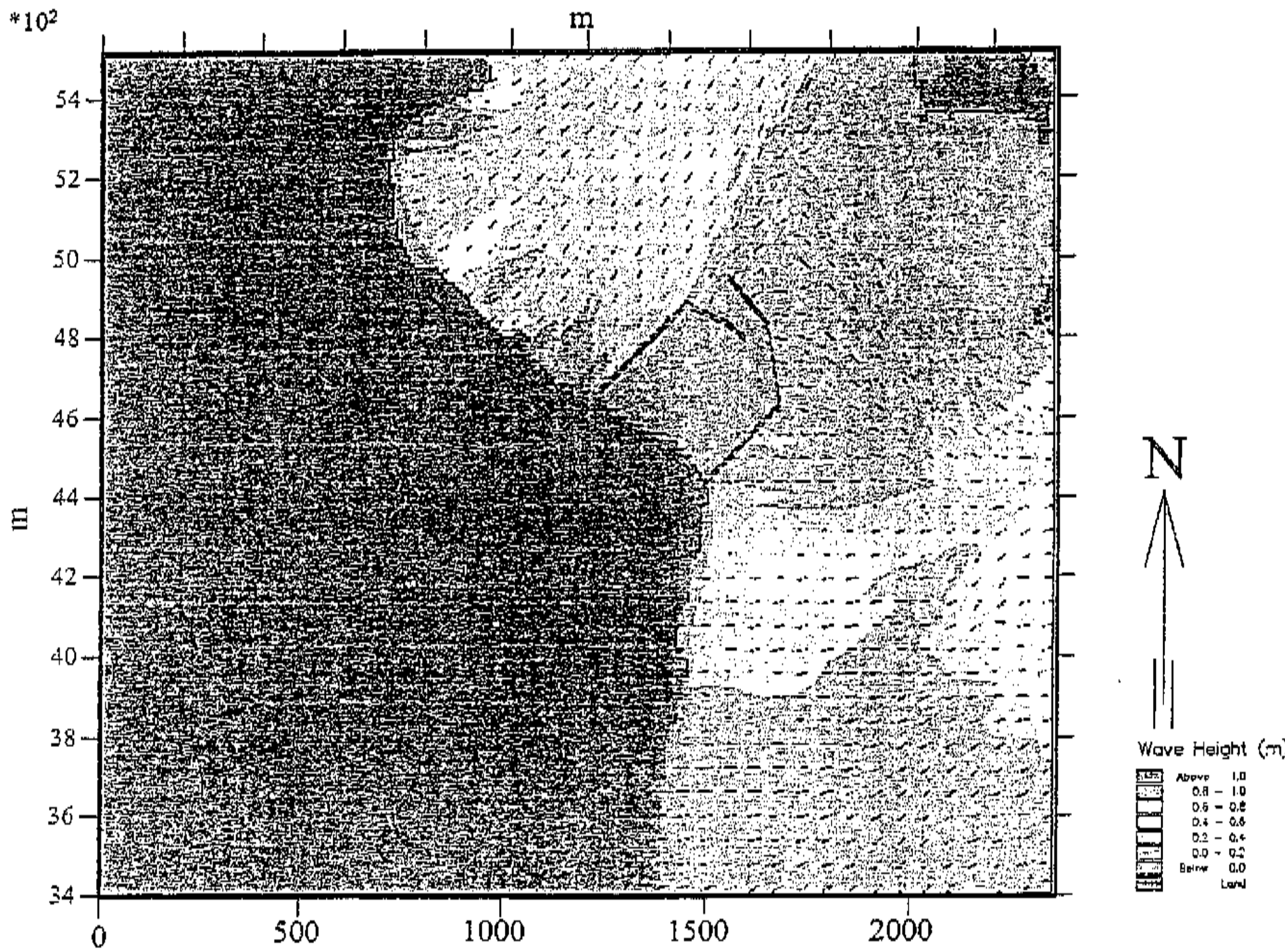


MOFFATT & NICHOL
E N G I N E E R S

Figure 5.54:
NSW Local Results with Breakwater
1.5 m NE Wave - 12 Sec

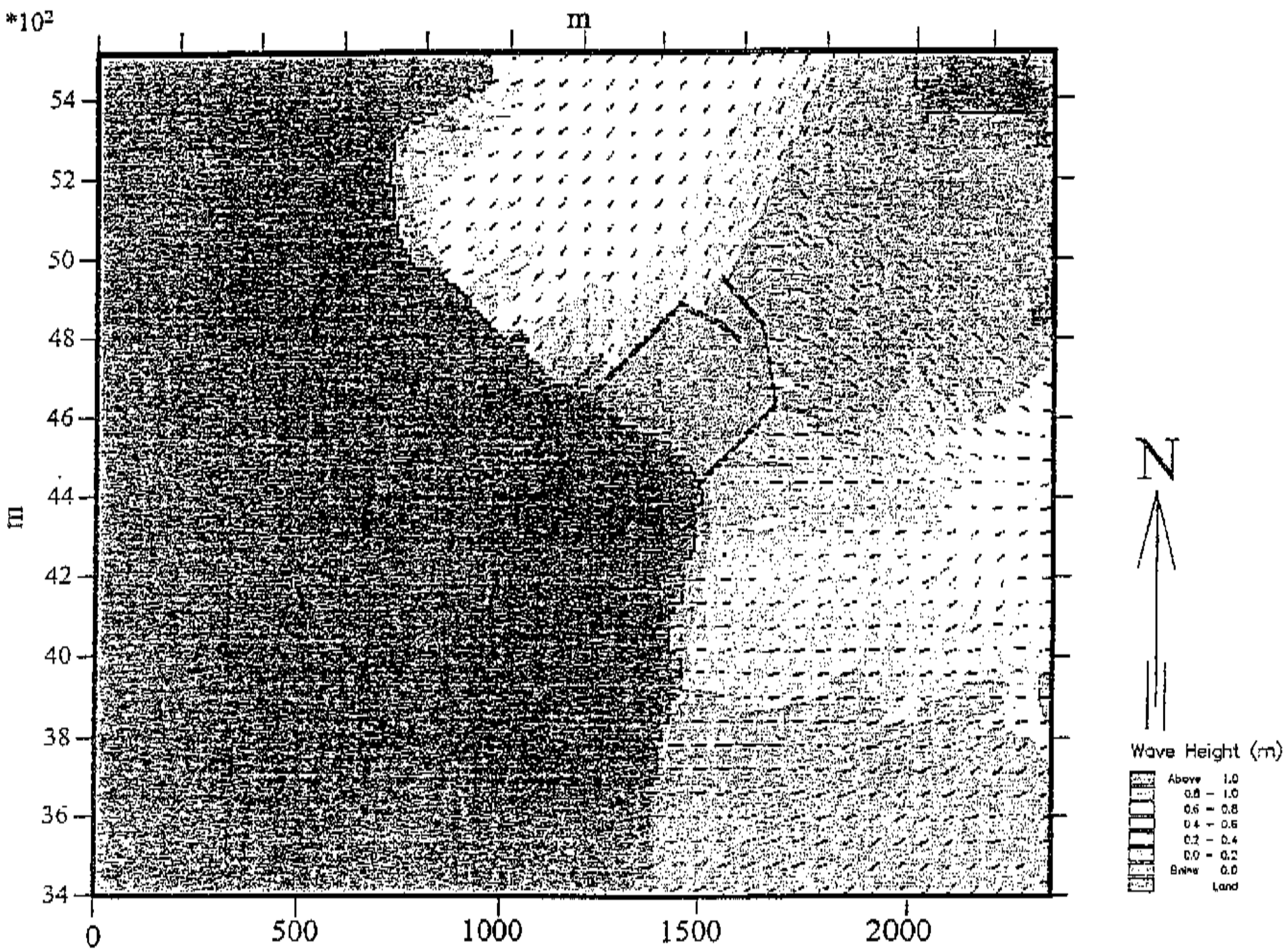


MOFFATT & NICHOL ENGINEERS

Figure 5.55:
NSW Local Results with Breakwater
2.5 m NE Wave - 8 Sec

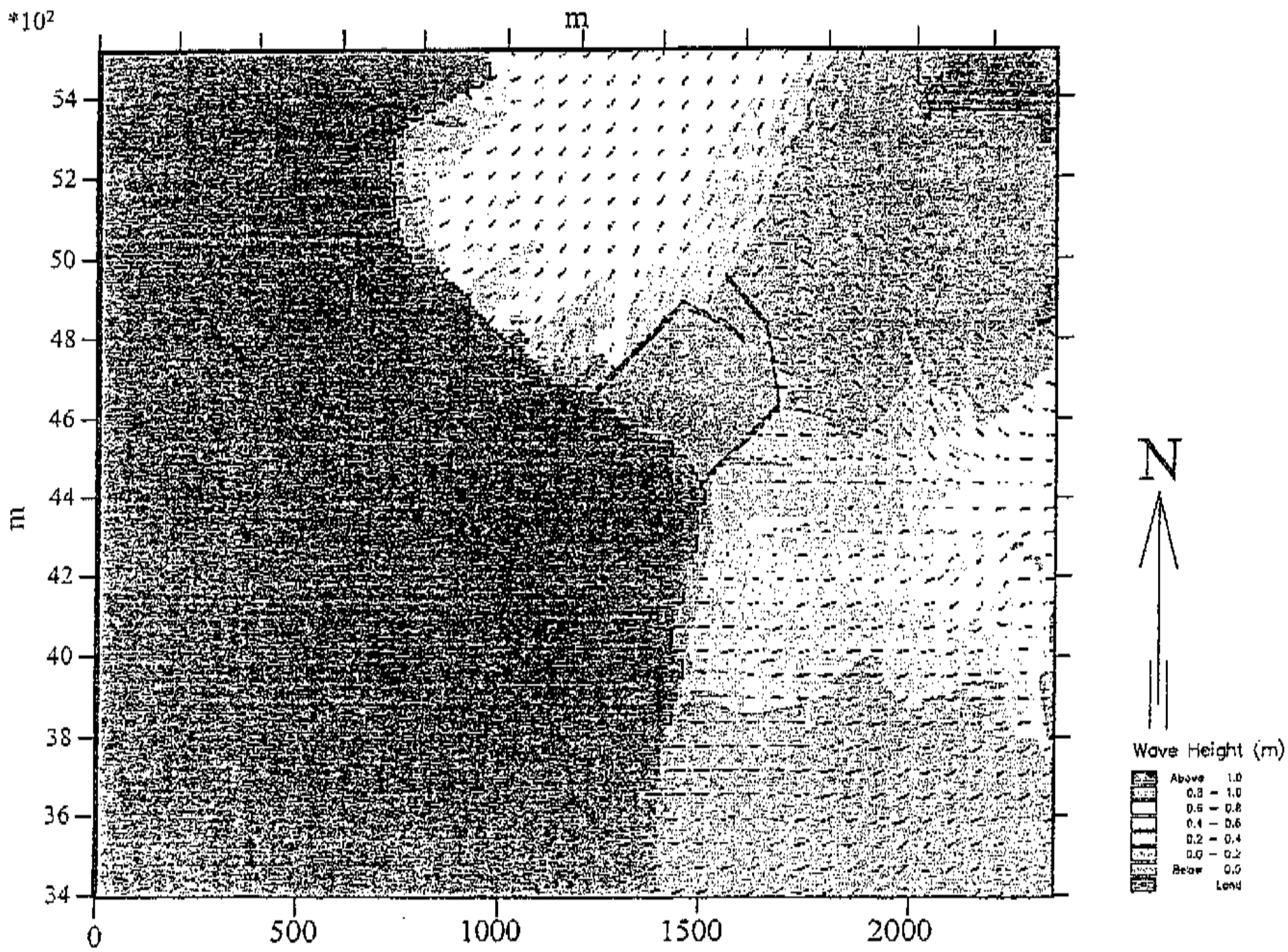


MOFFATT & NICHOL ENGINEERS

Figure 5.56:
NSW Local Results with Breakwater
2.5 m NE Wave - 10 Sec

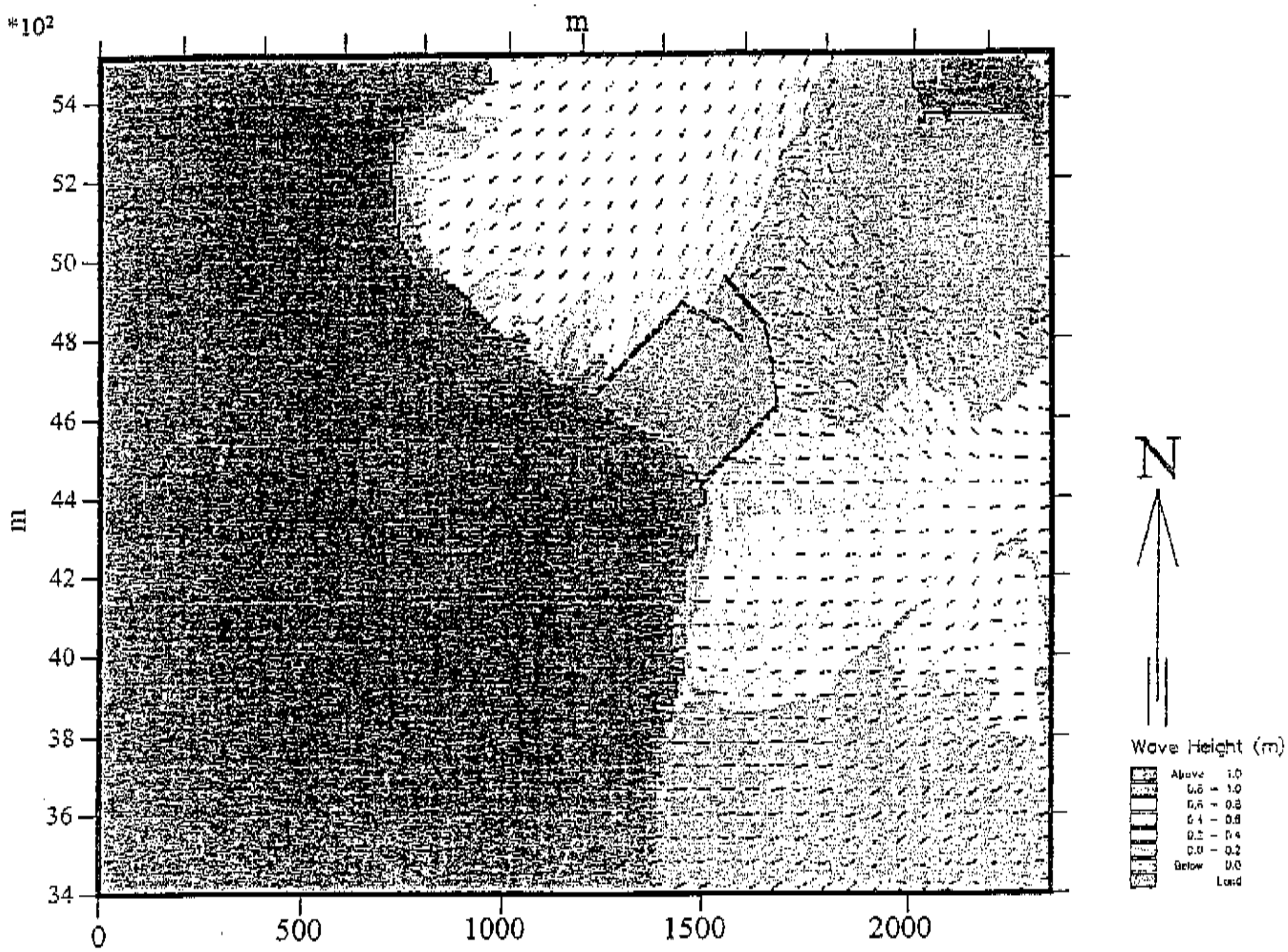


MOFFATT & NICHOL ENGINEERS

Figure 5.57:
NSW Local Results with Breakwater
2.5 m NE Wave -12 Sec

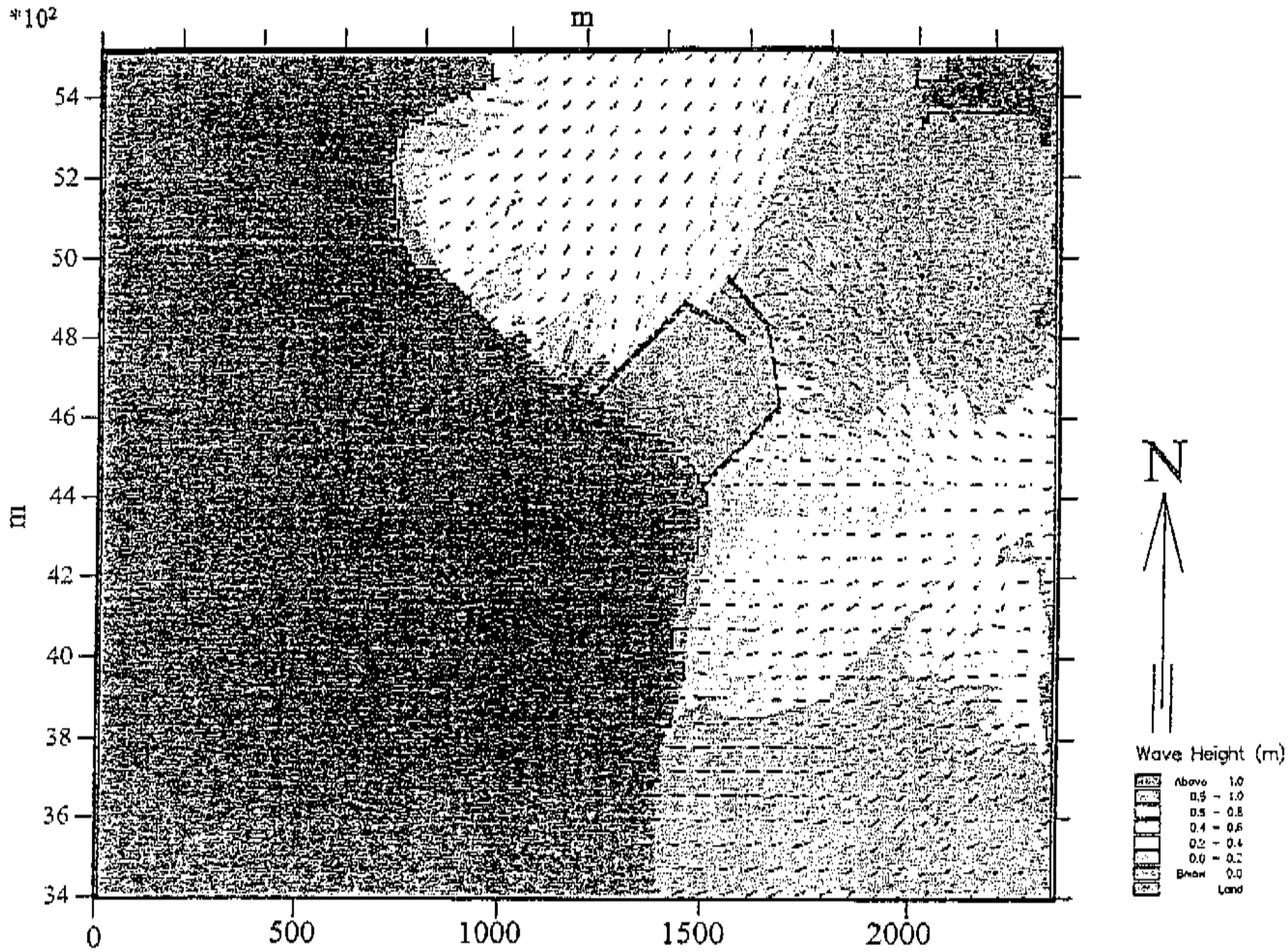


MOFFATT & NICHOL
ENGINEERS

Figure 5.58:
NSW Local Results with Breakwater
2.5 m NE Wave - 14 Sec

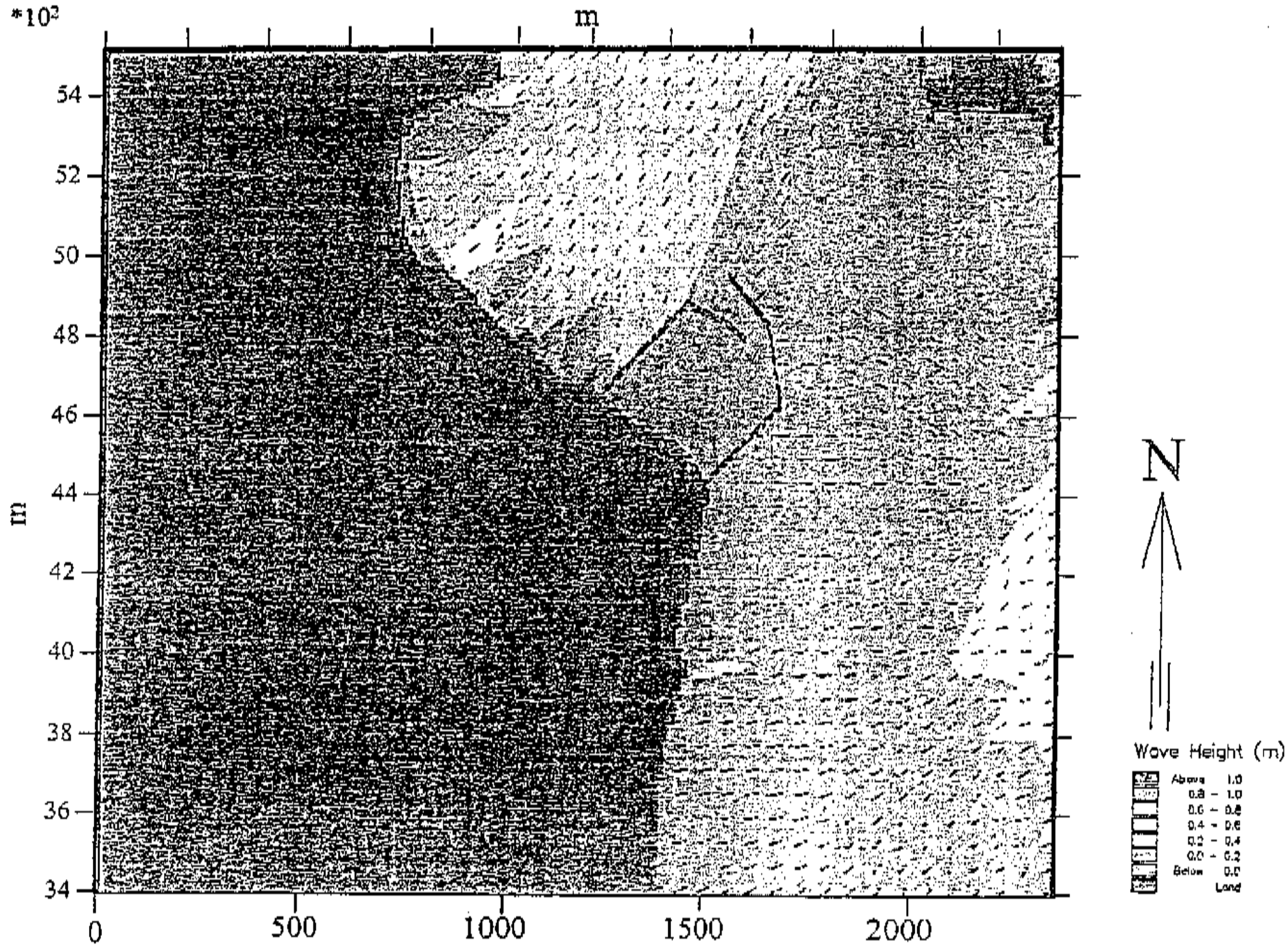


MOFFATT & NICHOL
ENGINEERS

Figure 5.59:
NSW Local Results with Breakwater
1.5 m North Wave - 8 Sec

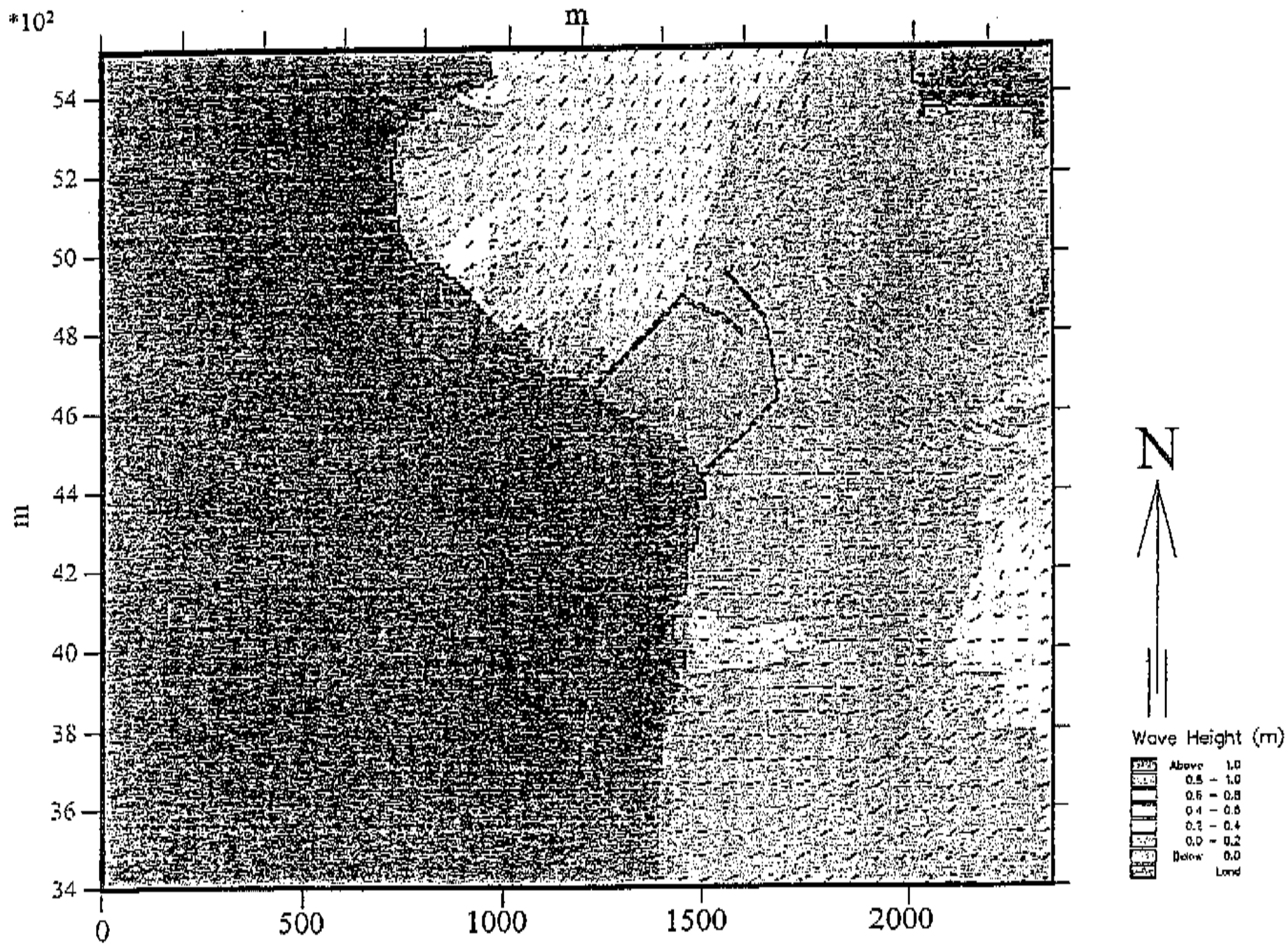


MOFFATT & NICHOL
ENGINEERS

Figure 5.60:
NSW Local Results with Breakwater
1.5 m North Wave - 10 Sec

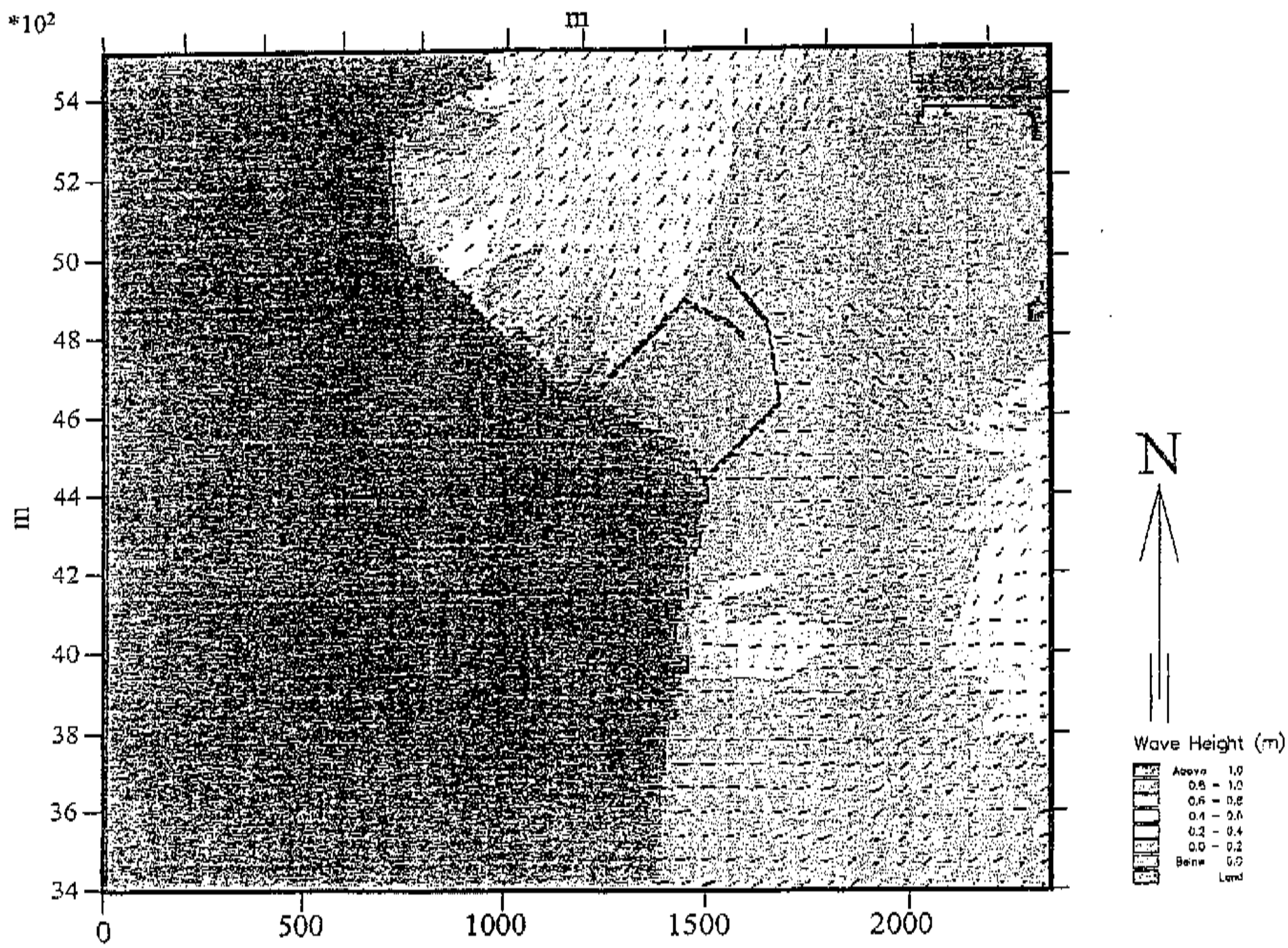


MOFFATT & NICHOL
E N G I N E E R S

Figure 5.61:
NSW Local Results with Breakwater
1.5 m North Wave - 12 Sec

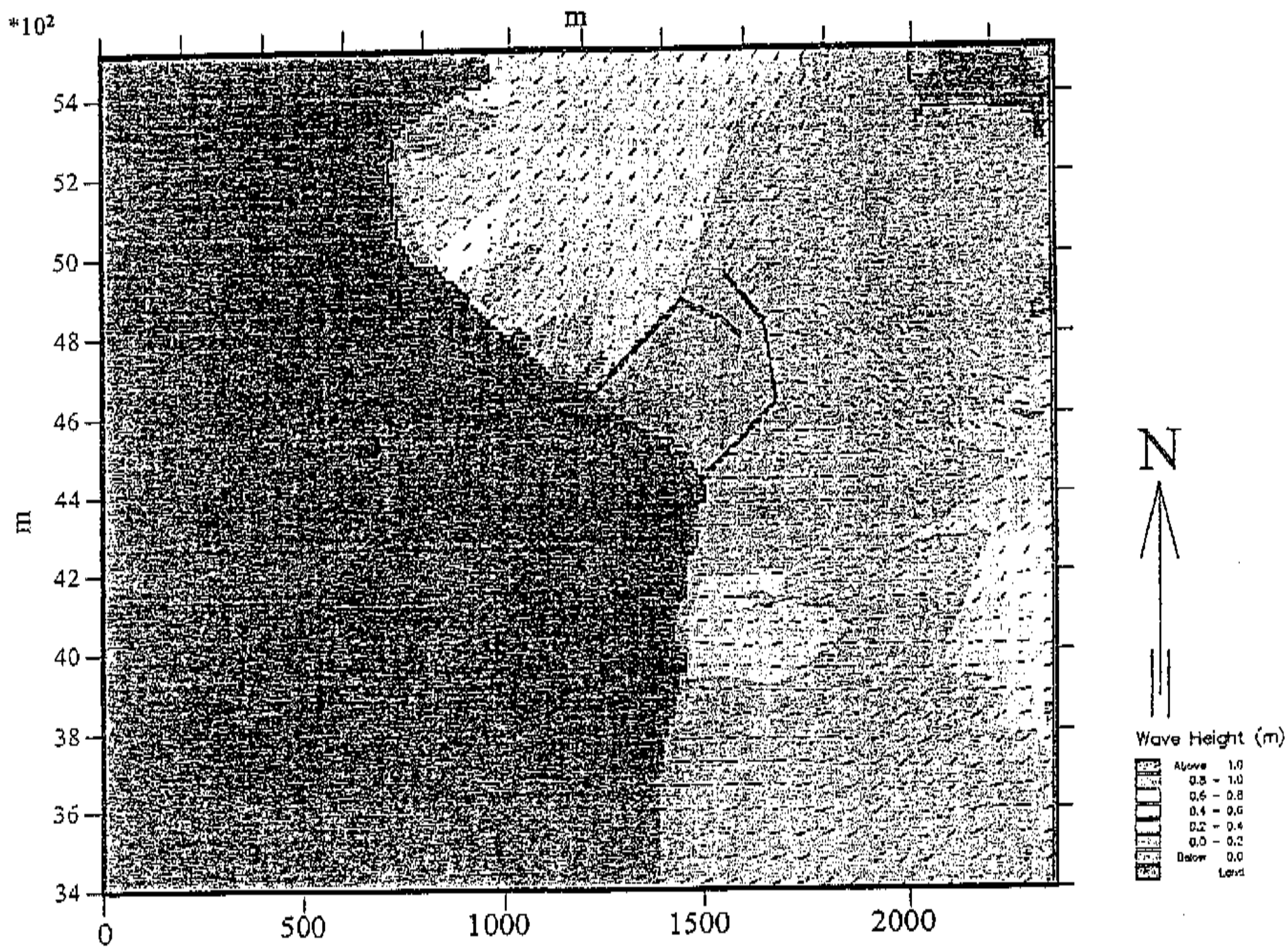


MOFFATT & NICHOL ENGINEERS

Figure 5.62:
NSW Local Results with Breakwater
1.5 m North Wave - 14 Sec

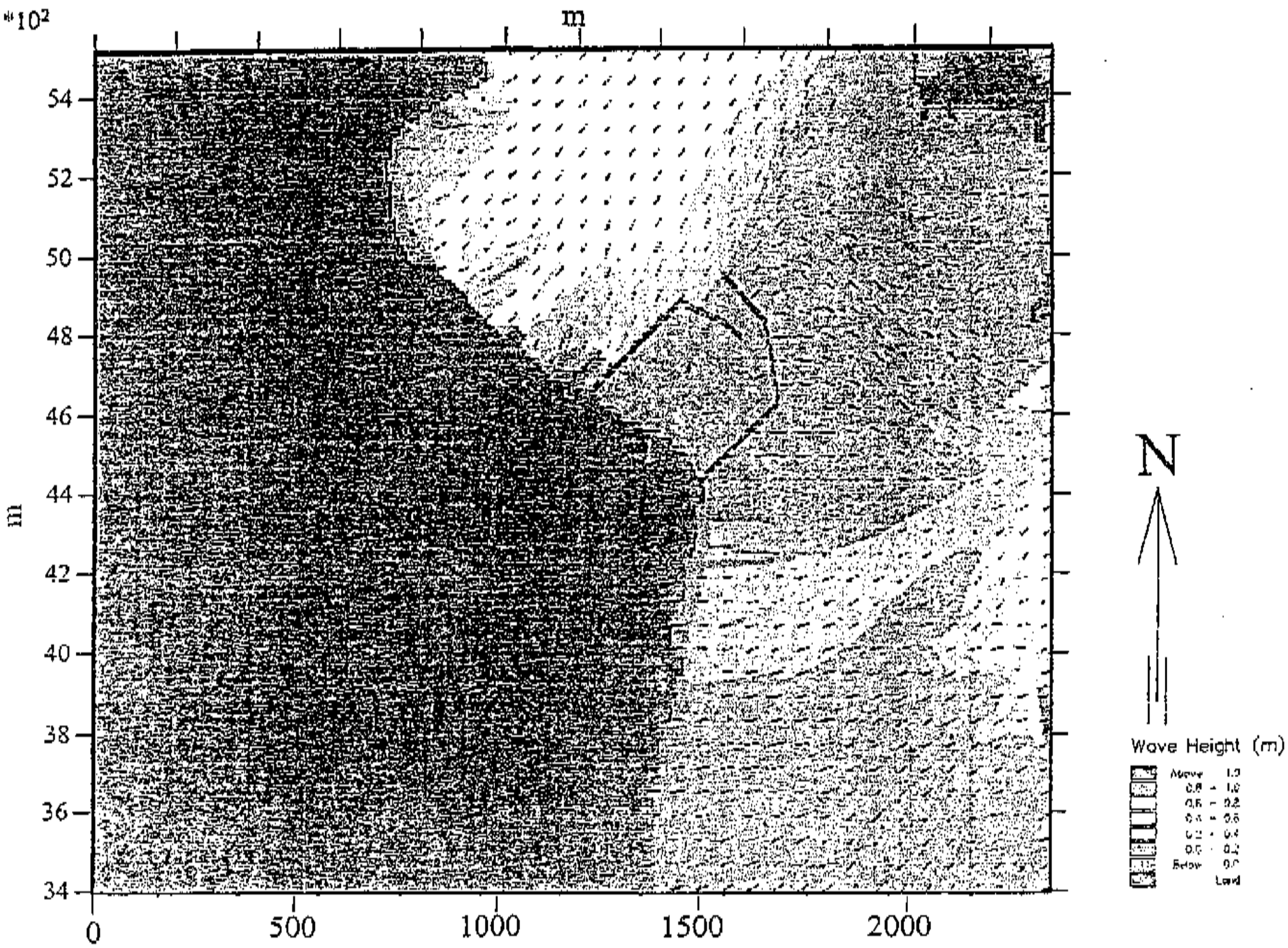


MOFFATT & NICHOL
E N G I N E E R S

Figure 5.63:
NSW Local Results with Breakwater
2.5 m North Wave - 10 Sec

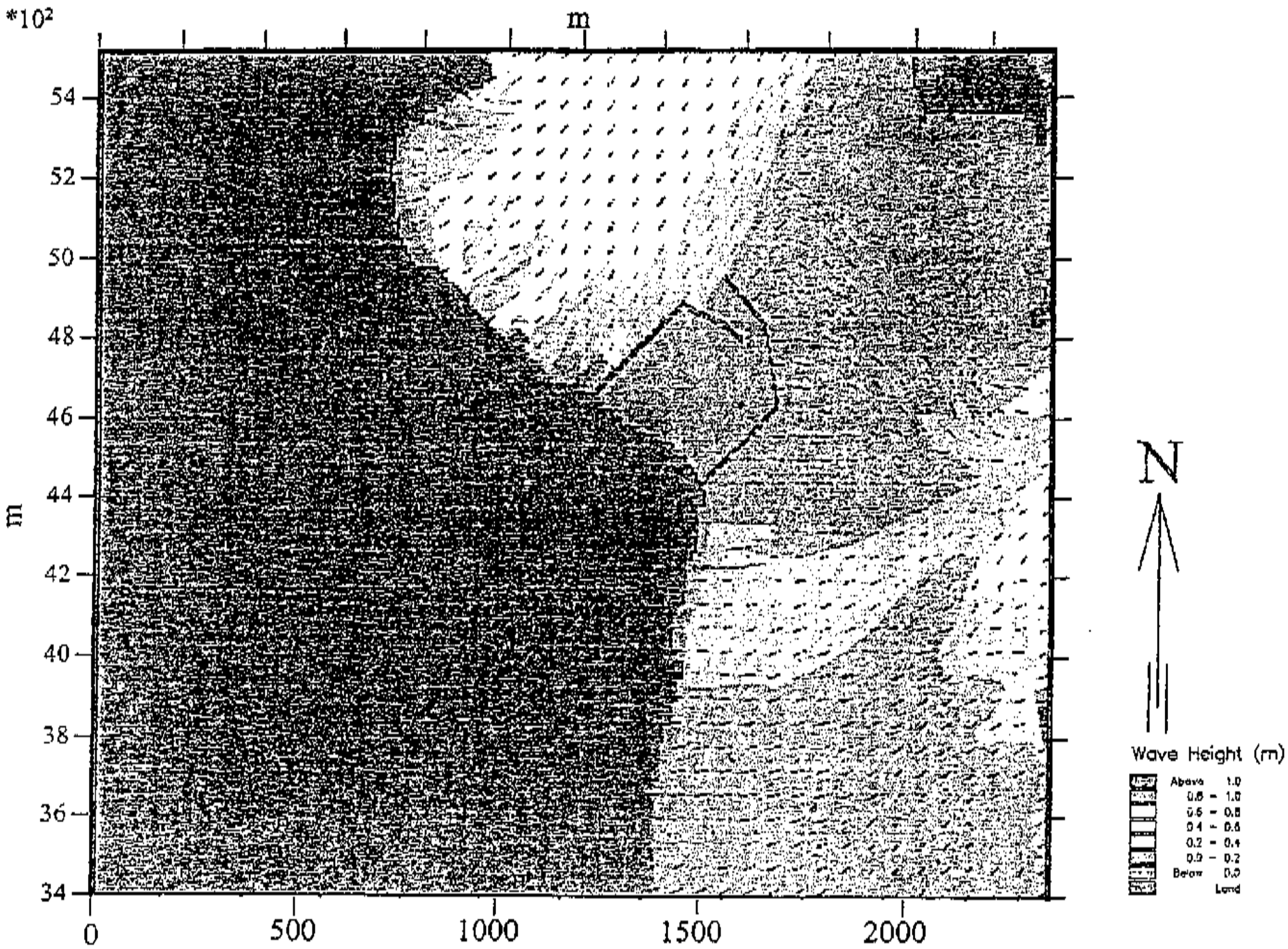




Figure 5.64:
NSW Local Results with Breakwater
2.5 m North Wave - 12 Sec

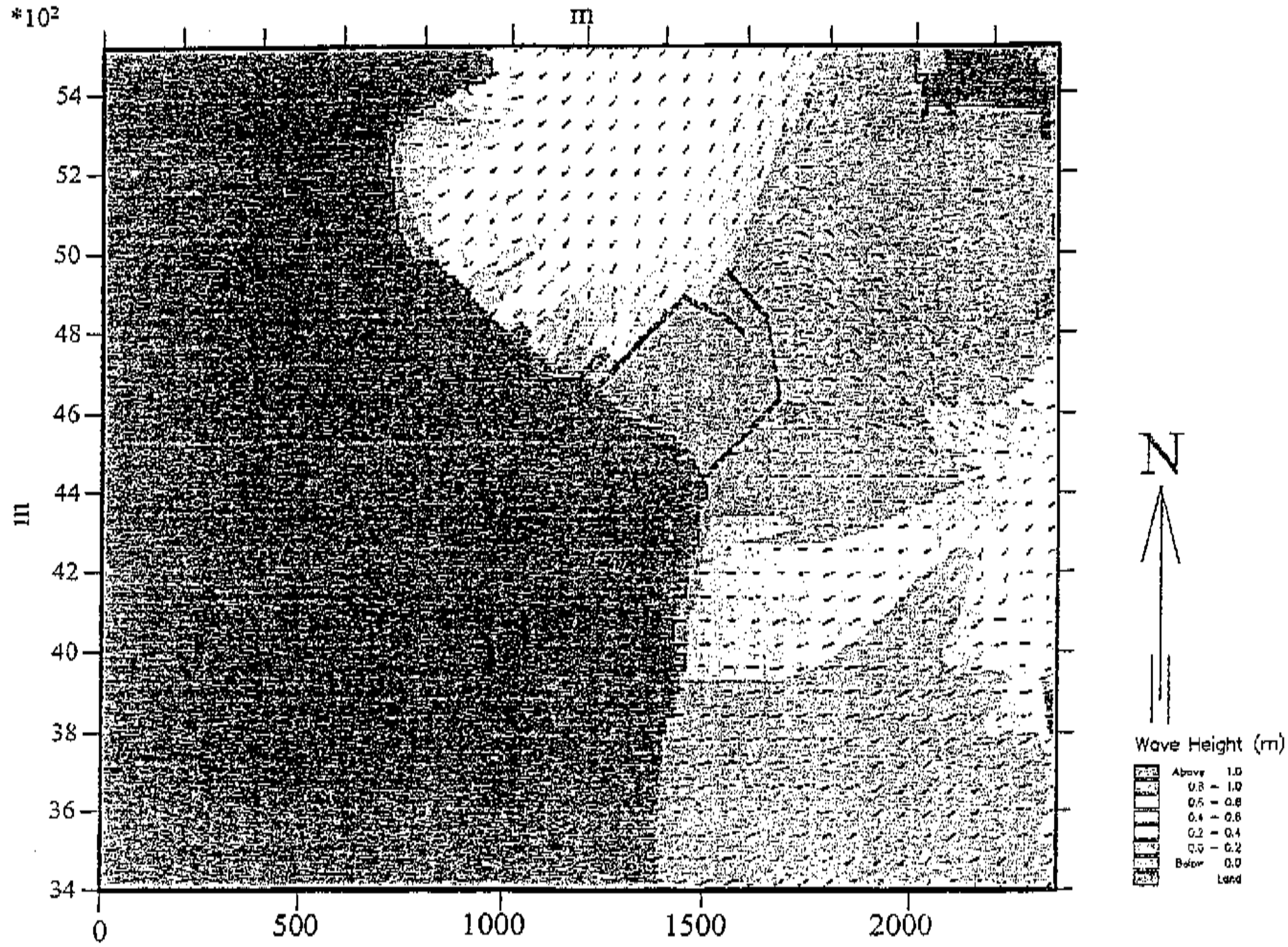


MOFFATT & NICHOL ENGINEERS

Figure 5.65:
NSW Local Results with Breakwater
2.5 m North Wave - 14 Sec

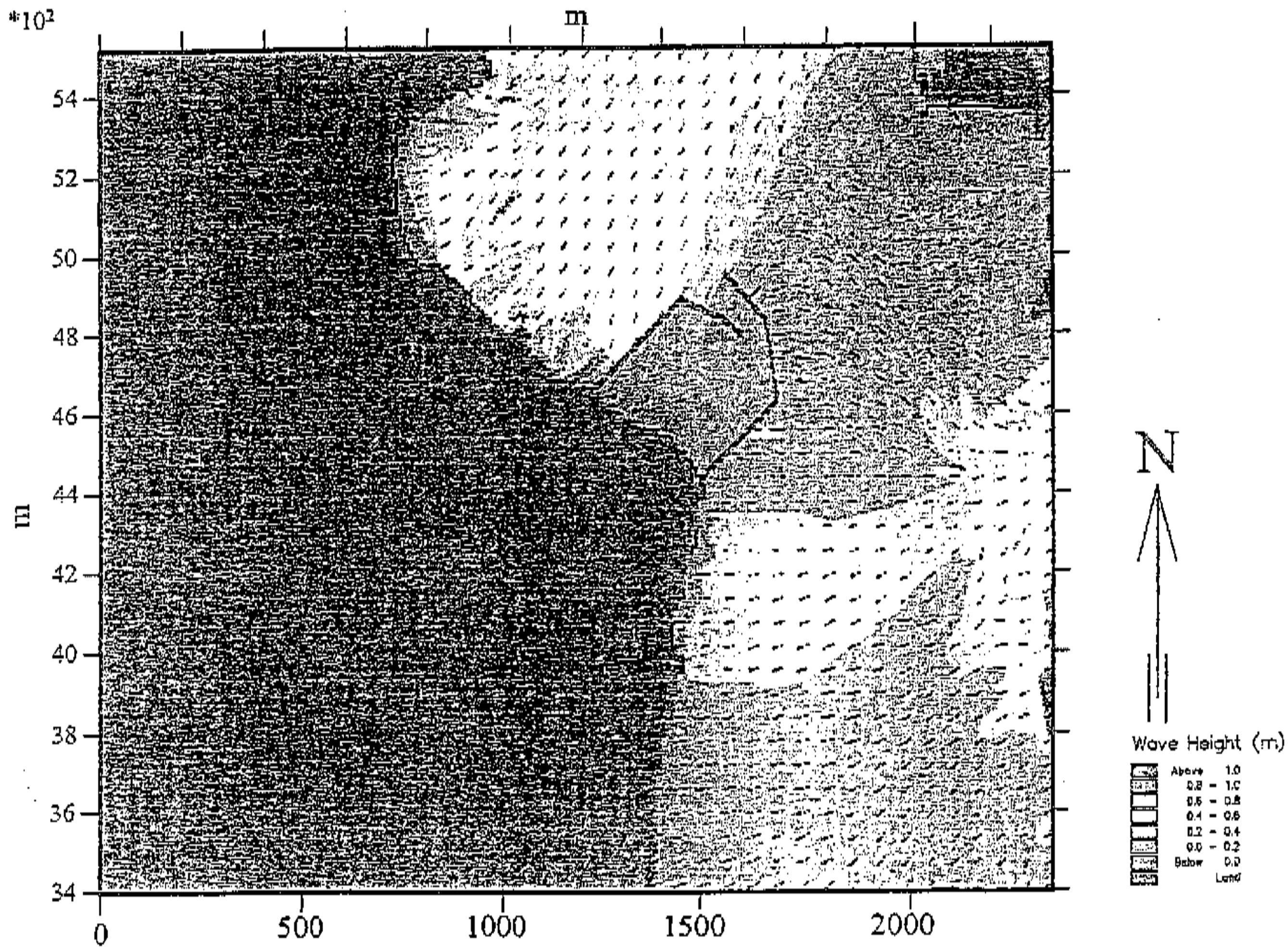


MOFFATT & NICHOL ENGINEERS

Figure 5.66:
NSW Local Results with Breakwater
3.5 m North Wave - 14 Sec

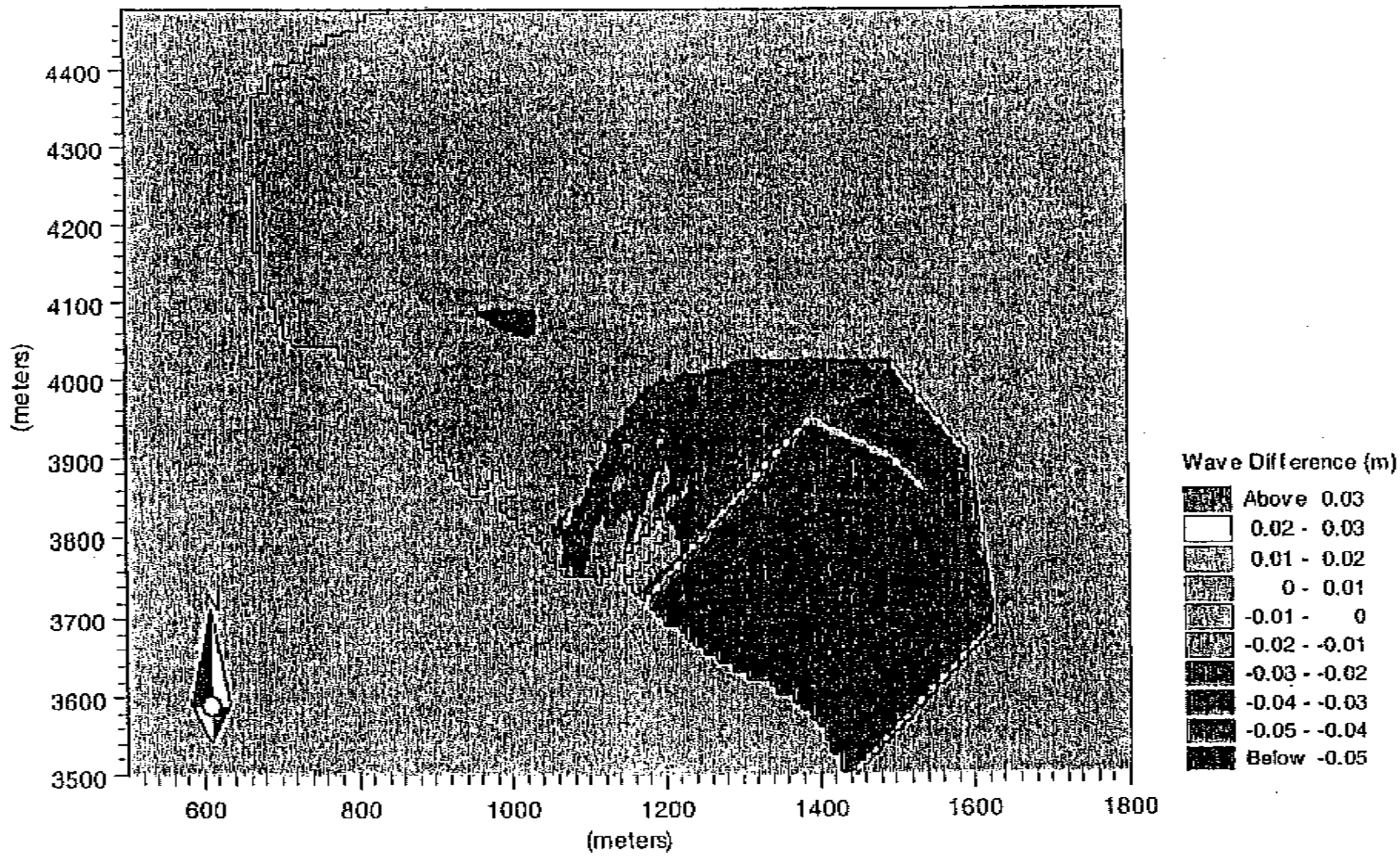


MOFFATT & NICHOL ENGINEERS

Figure 5.67: Wave Height Difference
(Offshore 1.5 m, 8 s waves from the east)

MIKE21 HD is the basic model of the entire MIKE 21 system. It provides the hydrodynamic basis for the computations performed in the models for sediment processes and environmental hydraulics. The HD model simulates the water level variations and flows in response to a variety of forcing functions in lakes, estuaries, and coastal areas. The water levels and flows are resolved on a rectangular grid covering the area of interest when provided the bathymetry, bed resistance coefficients, wind field, hydrographic boundary conditions, etc.

The system solves the full-time dependent nonlinear equations of continuity and conservation of momentum. The solution is obtained using an implicit ADI finite difference scheme of second order accuracy. The following effects are included in the equations (as applicable):

- Convective and cross momentum
- Bottom shear stress
- Wind shear stress at the surface
- Barometric pressure gradients
- Coriolis forces
- Momentum dispersion
- Wave-induced currents
- Sources and sinks (e.g. outfalls, intakes)
- Evaporation
- Flooding and drying.

The outcome of a simulation is the water level and fluxes (velocities) in the computational domain. (Danish Hydraulic Institute, MIKE21 Hydrodynamic Module - User Guide and Reference Manual.)

Tides were input as boundary conditions along the open boundaries of the hydrodynamic model grid. Tidal water levels for the predicted tides at Playa de Fajardo based on the NOAA station at San Juan, Puerto Rico were used (Tides & Currents, Nautical Software Inc.). The modeled water levels and approximate depth averaged current velocities were then calibrated based on available local tidal and current measurements by varying the time lag of tidal water surface elevations across the model gird. A typical daily tidal cycle from 9:20 a.m. on May 24, 2001 to May 25, 2001 at 9:20 a.m. was calibrated and used as the model period over which calculations were performed.

All HD model runs were then completed based on the calibrated tides and the results of the representative wave cases modeled during the NSW model runs. Wave current stresses (radiation stresses) were input from the wave transformations (NSW) over the model area. Both of these parameters were used as input files for the hydrodynamic simulation. This resulted in a complete picture of the velocity field for each wave condition.

MIKE21 ST is the sand transport model of the system for the assessment of the sediment transport rates and of the initial rates of bed level change in coastal areas subject to the combined action of waves and current. The initial rates of bed level change at the end of the design period are determined based on the mean transport conditions during the mentioned period.

The sediments are assumed to be non-cohesive, i.e. sand, but the grain size and gradation may vary throughout the model area. Furthermore, uniform or graded sediments may be chosen. The currents may be tidal, wind-driven, wave-driven, or a combination of the three.

The transport capacity at each node of a rectangular grid covering the area of interest is determined using the bathymetry, the water depth, the sediment size and gradation, and the current and wave characteristics as input data. Erosion and deposition rates in the model area are estimated from the computed sand transport. (Danish Hydraulic Institute, MIKE21 Sand Transport Module - User Guide and Reference Manual.)

The objective of the sediment transport calculations was to determine potential areas of increased deposition due to the presence of the proposed marina breakwater. This was done by assessing the initial rate of bed level change due to the changes in sediment transport rates resulting from differences in local waves and currents. The sedimentation rates assume an unlimited supply of sediment. As such, the results present the worst-case scenario for potential sediment deposition.

Bijker's total-load transport method was used. The method includes the effects of both waves and currents on sediment transport. Sediment transport is calculated as the sum of the bed-load and suspended load. It accounts for the effect of waves in increasing both the bed shear stress and the amount of turbulence. Sediment transport rates are calculated at every grid point for each time step. The rate of bed level change from this transport is averaged over the simulation period.

Based on the limited geotechnical data that is available, a silt (very fine sand) grain size of 0.06 mm was assumed for the analysis. The sediment transport was calculated for each wave case over a typical daily tide using the results of the hydrodynamic model (which included wave radiation stresses) and the local wave transformation model.

To determine the actual combined sedimentation due to the various events, each event was weighted by its percent occurrence per year. These weighted transport rates were summed to determine the total average daily sediment deposition as a rate of bed level change in millimeters per day (mm/day). This was performed once for the existing conditions and once with the proposed breakwater. The change in deposition due to the addition of the breakwater could then be obtained. The average sediment deposition was calculated in seven sub-areas of interest. These areas represent six existing berthing areas and the dredged navigational channel. The seven sediment deposition calculation areas are shown in Figure 7.1. The summary of net increase in sediment deposition rates is given in Table 7.1.

**Table 7.1 Initial Rates of Increased Deposition**

| Region as Shown in Figure 7.1 | Increased Rate of Sediment Deposition (mm/day) |
|---|---|
| Berth Area 1 | 0.13 |
| Berth Area 2 | 0.68 |
| Berth Area 3 | 0.11 |
| Berth Area 4 | -0.24 |
| Berth Area 5 | -0.05 |
| Berth Area 6 | 0.30 |
| Dredged Channel Area 7 | -0.19 |

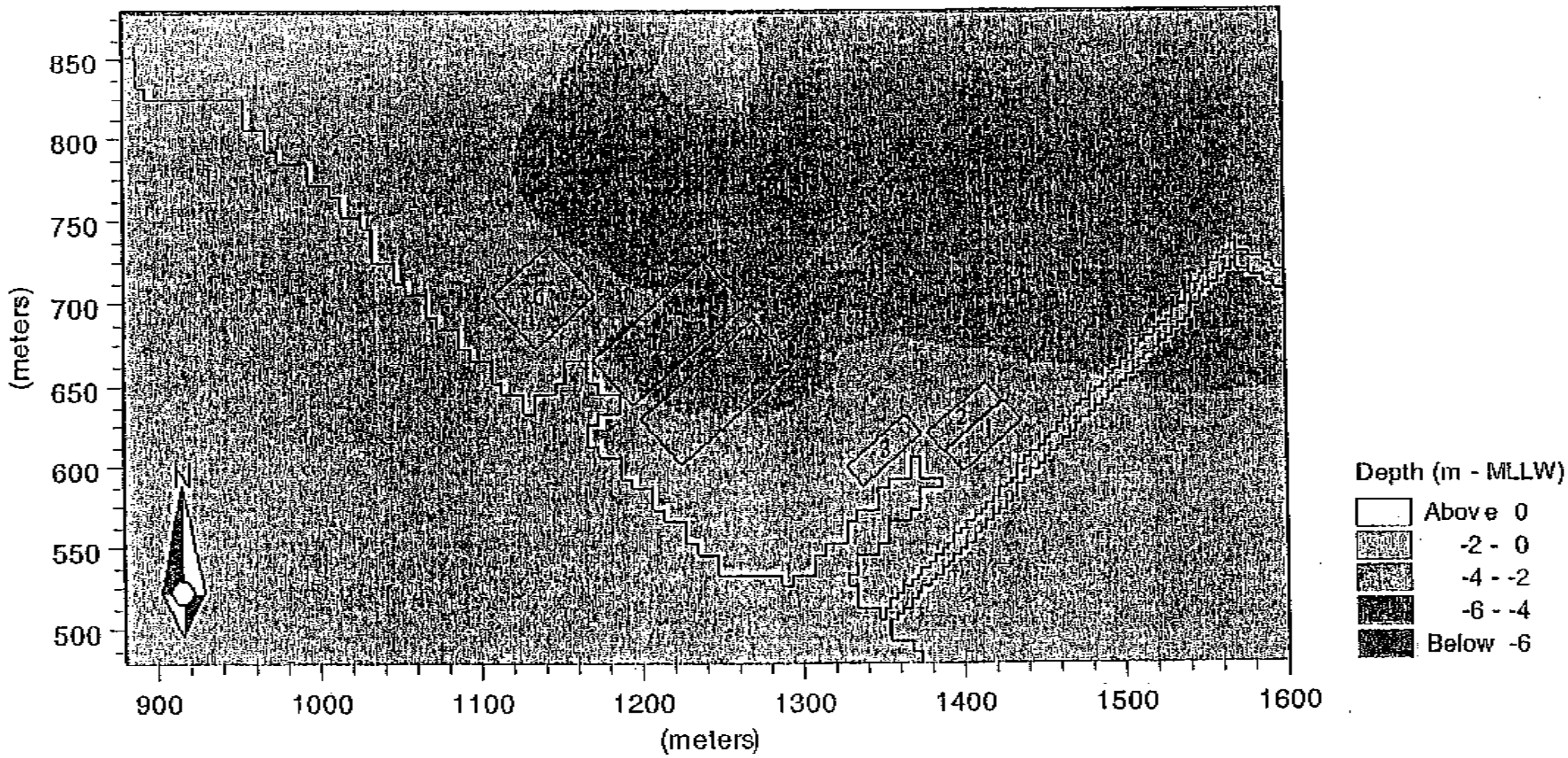


MOFFATT & NICHOL
ENGINEERS

Figure 7.1: Sediment Calculation Areas

## 7.1 Sedimentation Discussion

The sedimentation analysis indicates the potential for slight increases in sediment deposition in Areas 1, 2, 3 and 6 and decreased rates of deposition in Areas 4, 5 and 7. The largest potential increase in the rate of sedimentation, 0.68mm/day, is predicted in Area 2 off the tip of the existing ferry pier. These changes are the result of changes in wave heights due to the construction of the breakwater. The impact of construction on tidal currents alone does not cause any changes in deposition / erosion patterns at these areas.

However, these predicted rates should be considered a worst case scenario for the following reasons:

- This is a predicted initial rate of deposition. As the bottom bathymetry changes, the sediment transport patterns will also change. Thus, it can be expected that this rate will decrease over time as the bottom adjusts to a new equilibrium condition that smoothes out the high and low points in the bathymetry. Therefore, simply multiplying this rate by 365 days to determine the amount of material expected to be deposited in this area over the course of 1 year over-predicts the amount of deposition.
- The actual water depths in these areas of concern are typically deeper than those shown on navigation charts of the area and used for the numerical modeling analysis. It appears these berths are dredged or propeller scoured to provide sufficient water depths for the vessels using them. If the water depths are deeper than those modeled, then the waves will have less influence on the bottom, thereby reducing the sediment transport and the amount of material predicted to be deposited in these areas.
- The numerical model used requires the input of various parameters to calculate the sediment transport rates. Typically, these parameters are adjusted to calibrate the model against measured conditions. Since this was not possible in this case due to the lack of deposition and erosion data at the berths in question, a conservative estimate of the primary transport parameter was used. This value could be reduced by as much as 2/3, and still be within the acceptable range. Thus, the predicted deposition rate for Area 2 (worst location) could easily be as small as 0.23 mm/day based on this adjustment alone.

- The propeller wash from the vessels using these berths will have a much greater impact on the movement of sediment than the relatively mild wave climate at the site. Thus, the movement of these vessels and their transit speeds will likely be a more important parameter than the changes in wave heights due to the construction of the breakwater. Site observations indicate that there is a significant amount of silt that is suspended by the local ferries during their arrivals and departures.
- Presently, there is sediment deposition due to the suspended sediments from the river, as evidenced by the nature of the bottom material (silts and clays) in the area and the required maintenance dredging at the berths. This analysis did not consider the effects of suspended sediments from the river being transported and deposited in these areas. Clearly, the construction of the breakwater will eliminate this transport path, and would reduce, if not eliminate deposition due to these suspended sediments at the areas in question.

The main objective of this study was to determine the impact of the proposed marina breakwaters on sedimentation in the existing shipping region adjacent to the site. The following is a summary of the findings of this report:

- The project site is protected by a chain of islands that dissipates a large majority of the incident wave energy. This reduction in wave energy corresponds to lower values of sediment transport along the shoreline of the bay.
- The WIS Wave Hindcast Data was separated into 22 representative cases based on wave height, period, incidence direction, and frequency of occurrence.
- The most frequently occurring wave group was Case 18 at 20.4%, where waves originated from the east with $H_s$ = 1.5 m and T = 8 s. The second most frequent occurrence was Case 17 at 16.7% (from the east with $H_s$ = 1.5 m, T = 6 s). All other cases had a frequency of occurrence less than 9%.
- The presence of the breakwaters caused little change to the existing wave climate.
- The total net increase in sediment deposition rates within the current ship berth areas and the dredged navigation channel ranged from –0.2 mm/day to 0.7 mm/day. However because of the conservative nature of the analysis (as presented in Section 7.1) these values represent the worst-case scenario.
- Based on the results of the modeling, it is our opinion that the construction of the breakwaters will not have a significant impact on the adjacent properties.